NOVEL CELLULOSE ESTERS

by

James Edward Sealey II

Thesis submitted to the Faculty of

Virginia Polytechnic Institute and State University

in partial fulfillment of the requirements for the degree of

MASTERS OF SCIENCE

in

Wood Science and Forest Products

APPROVED:

_____

W. G. Glasser; Chairman

_____ _____

R. Helm J. Riffle

January 24, 1994

Blacksburg, Virginia

NOVEL CELLULOSE ESTERS

by

James E. Sealey II

W. G. Glasser chairman

Wood Science & Forest Products

ABSTRACT

Research in cellulose esters in recent years has concentrated on creating a variety of novel esters with a wide range of thermal and mechanical properties. These cellulose derivatives can be used for membranes, coatings, polymer blends, and other products. Novel cellulose solvent systems (DMAc/LiCl) introduced within the last twenty years have allowed the use of several esterification techniques that could not be used effectively in the past. The combination of the new cellulose solvent systems and esterification chemistry has enabled a large variety of novel cellulose esters to be produced.

Four groups of novel cellulose esters were produced in this study, cellulose trifluoroethoxy acetate (CT), cellulose acetate trifluoroethoxy acetate (CATA), cellulose esters of long chain linear aliphatic acids, and cellulose acetate laurate (CAL). The derivatives were synthesized in a homogeneous reaction medium of DMAc/LiCl. Several esterification chemistries were used including one based on reactions with TsCl (para-tolulene sulphonyl chloride). A wide range of degree of substitutions (DS) were produced without degradation to the starting polymer using a range of stoichiometric ratios. The fully substituted mixed cellulose esters were synthesized by consecutive reactions (work-up between reactions) and by "single pot" reactions. "Single" cellulose esters, with free hydroxyls, were produced by single pot reactions.

Structure property relationships were examined by several thermal and mechanical analyses. Mechanical response was studied with dynamic mechanical thermal analysis (DMTA) and thermal mechanical analysis (TMA). Thermal response was recorded by differential scanning calorimetry (DSC) and visual analysis. The CT

derivatives revealed a linear relationship between T_g and DS between a DS range of 0.6 and 3.0, but no T_m was apparent. All the products with DS > 0.6 flowed without discoloration, therefore the materials were assumed to be mainly amorphous. The CATA derivatives revealed sharp T_gs and T_ms. Surprisingly, the T_gs did not change between the CT and CATA derivatives, and the CATA's T_ms decreased linearly with increasing DS of fluoro-ester. Substituent and main chain T_gs were observed for both CT and CATA derivatives, but the substituent T_g remaining constant throughout the DS range of the flouro-esters. Surprising solubilities were also observed for both CT and CATA derivatives.

The long linear aliphatic cellulose esters (with C_{12} to C_{20} alkyl substituents) revealed a wide range of thermal and mechanical responses. Side chain and main chain T_gs and T_ms were observed for C_{12} and C_{14} derivatives. Only one broad T_m with no T_g was observed for C_{18} and C_{20} derivatives by DSC analysis. After annealing, multiple crystalline responses were seen for all the highly substituted C_{12} to C_{20} cellulose esters. CAL derivatives revealed sharp T_ms with no T_g. The crystallization rate proved to be much faster for the CAL derivatives than any other derivative in this study.

ACKNOWLEDGEMENTS

I would like to express my thanks to the staff, students, and faculty in Forest Products for their encouragement and assistance over the years. I would like to personally thank Jody Jervis and Jason Todd for their assistance, and also thank Chip Frazier and Gamini Samaranayake for their skillful guidance and support over the years.

I would especially like to thank my research committee for their time and assistance, and the financial support of AKZO Research American Incorporated. I would also like to thank my parents and friends for their encouragement.

Finally, a special dept is owed to Dr. Wolfgang Glasser for giving me the chance and challenge of being a member of his research group, and for his support and patience over the years. I dedicate this work to him.

TABLE OF CONTENTS

LIST OF TABLES

LIST OF FIGURES

recorded. This test was performed with an expansion probe with 1 g/ 10.7 mm^2 of force placed on the sample.

14. DSC scans of DS 1.5 CT derivative. Each heating scan was performed at 10°C per minute, and each cooling scan was performed at 5°C per minuet. The T_g was easily isolated after the first heat.
15. CT derivatives T_g vs DS from TMA analysis (--+--) and DSC analysis (-O-). A strong linear relationship between DS and T_g was observed for both techniques.
16. CT derivative DMTA transitions vs DS (O) α- transition (+) β- transition. The α- transition temperature decline linearly with increasing DS while the β- transitions temperatures stay about the same.
17. CATA molecular structure. This structure represents a DS_f 2.0 and a DS_a 1.0. All CATA structures were fully substituted.
18. ^1H NMR of CATA derivative DS_f 1.7 and DS_a 1.3. The fluoro substituent's protons overlap with cellulose's backbone protons but they can still be identified. The acetate protons were seen at 2.0 ppm δ.
19. FTIR of CATA derivative DS_f 2.1 and DS_a 0.9. A strong ester response was seen at 1735 wavenumber while also no OH response was detected.
20. DSC scans of 1.7 DS_F CATA derivative. Each heating scan was performed at 10°C per minute while each cooling scan was performed at 5°C per minute. The fourth heating scan was produced after annealing at 10°C above the T_g for over four hours.
21. CATA and CT derivatives T_g vs DS_F. CATA (O); CT (+). Almost no difference was detected between the T_gs of the CT and CATA. The strong linear relationship between DS and transition temperature remain.
22. CATA derivatives T_m vs DS_F. A linear relationship between T_m and DS was observed for DS_f 1.1 and above derivatives.
23. Comparison of Homo and Heterogeneous reaction systems (TsCl).
24. long linear aliphatic cellulose ester molecular structure. This structure represents a fully substituted cellulose laurate. The structures studied range between the substituent length of C_{12} (laurate) to C_{20}.
25. ^1H NMR of cellulose laurate DS 2.9. The long linear substituent's protons produced four separate regions of response.
26. FTIR of DS 2.9 C_{20} ester. The strong ester response was seen with a small OH response.
27. Bulky esters DMTA thermal transition temperatures α- transition (+); β- transitions (◆). The long linear aliphatic cellulose ester T_gs decline with increasing substituent length, but the β- transitions increases and seem to merge at C_{20}.
28. Bulky esters T_m vs substituent #C length main chain T_m (+); side chain T_m (◆). Assuming that the T_ms of C_{18} and C_{20} were from side chain melting only, The side chain T_m increases linearly with side chain length.
29. DSC scans of C_{14} mixed ester DS_M 2.8. The side chain and main chain crystals

could be annealed separately.

30. TMA penetration mode flow temperatures for bulky esters. The onset of flow decreased in temperature with increasing substituent length.
31. TMA expansion mode T_g for bulky esters. An increase in expansion rate was detected for C_{12} to C_{18} derivative, but C_{20} did not.
32. CAL molecular structure. This structure represents a DS_L 2.0 and DS_H 1.0 derivative. All CAL derivatives are fully substituted.
33. Stoichiometric reactivity of cellulose laurate with the TsCl esterification reagent system.
34. DMTA (−) and TMA (O) (expansion mode) transition temperatures of CL. Both techniques detected a trend of decreasing T_g with increasing DS of lauric acid.
35. DSC scans of CAL derivatives. Sharp crystallization responses were detected for even quench cooling scans. The T_m detected on the heating scan remained constant regardless of cooling rate.
36. T_m vs DS_L for CAL derivatives. A linear decrease in T_m was detected with increasing DS_L between DS_L 0.6 and 2.9.
37. T_m vs DS_H and DS_L for CAH and CAL derivatives. The CAL T_ms compare closely with the CAH T_ms.

GLOSSARY

α-transition-	The first transition going from high to low on the temperature scale.
β-transition-	The second transition going from high to low on the temperature scale.
Bulky esters-	Large ester substituents with more than eight carbons.
CAL-	Cellulose acetate laurate.
CATA-	Cellulose acetate trifluoroethoxy acetate.
CL-	Cellulose laurate.
CT-	Cellulose trifluoroethoxy acetate. A fluoro-ester of cellulose.
DMTA-	Dynamic mechanical thermal analysis.
DP_n-	Degree of polymerization, number average.
DP_w-	Degree of polymerization, weight average.
DS-	Degree of substitution. The statistical average of substituted hydroxyl groups per anhydroglucose unit. Range is 0 to 3.0. DS of 0 is pure cellulose and DS of 3 is fully substituted cellulose with no free hydroxyls.
DSC-	Differential scanning calorimetry
DSF-	Degree of substitution of flouro-ester.
FTIR-	Fourier transform infrared spectroscopy.

GC-	Gas chromatography.
Heterogeneous reaction-	A reaction in which the reagents are not in solution.
Homogeneous reaction-	A reaction in which reagents are in solution.
MW-	Molecular weight.
Main chain-	The repeat unit chain. Main polymer chain.
Mixed anhydride-	The anhydride between two different acids.
Mixed ester-	A cellulose ester substituted with more than one ester type.
NMR-	Nuclear magnetic resonance.
Side chain-	The long linear substituent. branch unit.
T_c-	Crystallization temperature.
T_g-	Glass transition temperature.
T_m-	Melting point temperature.
TMA-	Thermal mechanical analysis.
TsCl-	para-toluene sulphonyl chloride. Esterification reagent.

1.0 INTRODUCTION

Cellulose acetate, which has been produced on an industrial scale for over 60 years, was derived from reacting cellulose with acetic anhydride, acetic acid, and sulfuric acid (Eicher 1988). Because of the long history of cellulose esters, it was the first material used in many polymer science fields. Membranes, fiber spinning and melt processing are just a few. The demand for cellulose esters has been inversely proportional to the growth in synthetic polymers. New synthetic polymers have replaced cellulose esters in many applications as the polymer field grew into the multi-billion dollar business that it is today. The high cost of the raw materials, of production, and limited properties were the main reasons why cellulose esters have gradually lost competitiveness. Most cellulose acetate that is produced today is used as cigarette filter material for its complex adsorptive properties.

Even after many years, the industrial process used to make cellulose acetate has not changed significantly. This heterogeneous reagent system has remained the most cost effective method of production although the reaction affords significant depolymerization. The interest in a non-degradative esterification system, and the production of a wide variety of cellulose esters has been published as early as the 1950's (Ott et al. 1954). The few non-degradative esterification systems that have

been reported have been very limited in reactivity or acyl group size (Ott et al. 1954). For example, acid anhydrides in pyridine have a high reactivity, but it can only be used effectively for acetic to butyric anhydride.

The introduction of new homogeneous solvent systems in the early 1980's along with the increased interest in renewable materials has sparked research in cellulose derivatives (McCormick, Callais 1987). A large portion of recent cellulose derivative research as been performed in homogeneous reaction media. The homogeneous reaction systems have several advantages over the heterogeneous systems. An evenly substituted polymer can be produced throughout the entire DS range without the need for saponification, and less reagents are needed to react the dissolved form of cellulose (Samaranayake,Glasser 1993a). Novel derivatives with large bulky substituents or highly polar sites that can't be produced by conventional heterogeneous methods can also be synthesized (Shimizu,Hayashi 1989).

Novel derivatives offer a much wider range of thermal and mechanical properties for cellulose esters. For example, DS 0.7 cellulose acetate with a DP_n of 120 or less which is water soluble (Buchanan, Edger et al.1991), or C_{18} cellulose ester which has a low modulus at room temperature, and have softening points at 35°C (Morooka et al. 1984). These more versatile processing ranges promote polymer blend studies between cellulose derivatives and a wide variety of synthetic and biodegradable polymers.

2.0 LITERATURE REVIEW

2.1 HISTORICAL REVIEW OF CELLULOSE ESTERS

2.1.1 CELLULOSE ACETATE AND TRIACETATE

Cellulose acetate, which is the second oldest man-made fiber, continues to have a significant impact on several industries. Over 300,000 metric tons of cellulose acetate fiber and 200,000 metric tons of filter tow are produced every year (Serad,Sanders 1988). While several cellulose acetate markets have declined in recent years, the overall production aspects are still good. Most cellulose acetate, degree of substitution (DS) 2.4, and triacetate, DS 2.9, fibers are used for textile products like blouses, lingerie, dresses and draperies. Non-fiber usages are films, sheets and lacquers. Specialty products are dialysis and hollow fiber membranes.

Commercial cellulose acetate is a polymer with a degree of polymerization (DP) of around 300. This is generated from pure cellulose of 1000-1500 DP. Intensive search has been done on thermal characteristics in the past (Scandola,Ceccorulli 1985) (Kamide,Saito 1979) (Malm et al. 1957). The T_m is 305 and 270°C for DS 3.0 and 2.4 cellulose acetate respectively,and the T_g is reported between 190 and 205°C depending on the DS of acetate and the moisture content of the product (Eicher 1988).

Cellulose triacetate, which was introduced in 1954, has ease-of-care properties

like lower water uptake, higher brightness and greater thermal stability than cellulose acetate. It is particularly important in velour and suede-like fabrics for robes and dresses (Serad,Sanders 1988) (Astheimer 1988).

Disadvantages to cellulose acetate and triacetate are lower strength and abrasion resistance than most other man-made polymers. This is why cellulose acetate fibers are combined with nylon and polyester fibers in yarns. Moisture uptake can also be a disadvantage especially for stain resistant materials.

Cellulose acetate and triacetate's main advantages are their complex absorptive properties and their toughness. It is also a glossy product with good print and dye qualities. It is more resistant to decay compared to other cellulose derivatives, and it produces no harmful reaction, due to ingestion or skin contact. It can also be plasticized to generate a wide variety of thermal properties. Moisture adsorption can be beneficial in certain applications. The plasticizing effect induced by adsorbed moisture can soften the feel of the fibers.

2.1.2 MIXED ESTERS

While several cellulose mixed esters have been reported in the literature, only two have industrial importance, cellulose acetate butyrate and cellulose acetate propionate. The main reason for their production is their thermal properties. The mixed esters can be produced with a range of thermal properties that cellulose acetate alone would not provide.

The thermal properties change over a wide range from pure cellulose butyrate to pure cellulose acetate. The T_ms, T_gs, density and moisture adsorption decrease with increasing butyrate content. The T_m decreases from 300°C to 160°C; the density decreases from 1.32 to 1.16; and the water adsorption at 90% relative humidity varies from 12% to 1.5% by weight. Solubility varies greatly over this range as well (Eicher 1988).

The major use of mixed cellulose esters is in the production of molded plastics. This is because of transparency, high mechanical strength and toughness (Wandel,Bayer 1988). They also exhibit cold flow. This is in response to mechanical stresses applied to it. The insertion of metal parts into the molded polymer can be done without inducing stress cracking. Light stability and a glossy finish with anti-static properties insure that moldings and other visually exposed products remain unchanged for years. The products also have good damping properties which make them useful for hand tools (Wandel,Bayer 1988).

Cellulose mixed esters are usually plasticized. Plasticizers are high-boilers and are used in amounts of 3 to 25% where cellulose acetate uses 15-35%. Since the mixed esters retain much less water than cellulose acetate, they are dimensionally stable in a wider range of relative humidities.

Other uses of mixed esters are films and surface coatings. Films can be used for electrical insulation materials. The photographic industry used mixed cellulose esters until the past few years when polyesters replaced them. Lacquer coatings use

mixed esters because of their superior lightfastness, gloss, low combustibility, thermal stability and low moisture uptake (Eicher 1988).

Cellulose mixed esters are produced like cellulose acetate except that a mixture of two acid anhydrides are added together. The reactivity of the larger anhydrides decreases significantly and cost of producing them is higher than cellulose acetates.

2.1.3 HETEROGENEOUS CHEMISTRY

Cellulose acetate and triacetate are prepared by the esterification of pure cellulose with acetic anhydride. The purity of the cellulose is important because of solubility. Impure cellulose may not go into solution and fully substituted derivatives can't be produced. This can cause blockiness with sections of the polymer having no or few substituents and other sections being fully substituted. The standard purity range is 95-98% α-cellulose (Krassig 1990).

Three major processes are reported for industrial production of cellulose acetate. Solution process with acetic acid as the solvent, solution process with methylene chloride as the solvent, and completely heterogeneous reaction with a nonsolvent like benzene. The solution process with acetic acid as the solvent places cellulose, acetic anhydride and sulfuric acid into acetic acid solution. As high as 15% sulfuric acid based on cellulose weight is added to increase the solubility of the cellulose. The solution process with methylene chloride may use perchloric acid as the catalyst and methylene chloride in place of acetic acid with acetic anhydride as the

esterification agent. The heterogeneous reaction uses a nonsolvent like benzene and adds cellulose and acetic anhydride. This is done in order to keep the crystallinity of the cellulose from changing. The cellulose does not swell during the reaction, and the product looks fibrous after nearly complete substitution.

Cellulose acetate is made in four steps: preparation of cellulose, acetylation, hydrolysis and recovery of product. First, the cellulose is refined in a disk refiner. The fluffed cellulose is then typically treated with acetic acid solution for 1 hr at 25-40°C. The sulfuric acid and acetic acid mixture is then added. This activation period and temperature is adjusted depending on the DP of cellulose acetate that is desired.

This pulp slurry is mixed with acetic anhydride, acetic acid and sulfuric acid. Precooling is required to keep this exothermic reaction below 50°C. 5-15 wt % excess acetic anhydride is used for complete substitution so, over four equivalents of acetic anhydride per anhydroglucose unit is used.

The nearly fully substituted cellulose triacetate is hydrolyzed in order to produce a DS 2.4 acetate derivative. This is done by acid hydrolysis under conditions of controlled time, temperature and acidity. Typical reactions occur at 50-100°C for 1 to 24 hrs.

The precipitation is done by addition of the reaction solution into dilute acetic acid solution (10-15%) while vigorously stirring. Different size products can be produced by adjusting the stirring rate. The precipitate is filtered. The product is washed to remove acetic and sulfuric acid residues. The wet flakes are then dried to

1-5% moisture content. An extra washing step may be performed with deionized water under pressure to remove residual sulfate groups by hydrolysis. Acid recovery is also performed and this is a critical step for the economics of cellulose ester derivatives.

The other two processes use the same steps but substitute different solvents and catalysts. Continuous cellulose acetate production has been achieved, but only a few companies have invested the money for this highly automated process. In the future, the continuous process may replace batchwise operation.

2.1.4 HOMOGENEOUS CHEMISTRY

A solvent system was invented in the early 1980's that was a non-degradative organic solvent system suitable for cellulose esterification (McCormick,Callais 1987). The DMAc/ LiCl cellulose solvent system has been shown to be the best homogeneous esterification solvent system for cellulose today (Samaranayake,Glasser 1993a). Acid chloride and acid anhydride esterification agents have been used efficiently for a wide range of substituents. This solvent system allows evenly substituted derivatives with a range of DS to be made without having to produce fully substituted derivatives and subsequently hydrolyze to the desired DS. Less reagent was used to produce the same DS product while eliminating a processing step needed for heterogeneous reagent systems.

Several pro's and con's exist for homogeneous esterification in DMAc/ LiCl.

The system is similar to heterogeneous methods in that cellulose pretreatment, cellulose dissolution, esterification and precipitation are the steps involved in both systems. The cellulose pretreatment involves steps of solvent exchange with methanol and DMAc like the acetic acid and sulfuric acid activation in the heterogeneous technique. While the activation time is longer in the homogeneous phase process (about 24 to 48 hrs), the process may be performed in a similar batch system as is used today. The cellulose dissolution requires solvent addition and heat at the beginning of the process and is then cooled for the esterification step like the heterogeneous method. The esterification method seems to be longer by about 24 hrs, but it can produce fully substituted derivatives more efficiently than heterogeneous methods (Samaranayake,Glasser 1993b) (McCormick,Dawsey 1990). The precipitation process is identical except for the nonsolvent used.

The pro's for the homogeneous solvent systems are the even substitution, one pot, efficient reaction, non-degradative method and similarity to batch process used in the heterogeneous methods. The con's all extend from the toxicity and special handling needed for DMAc and LiCl. DMAc is toxic and it penetrates human skin. It is also very difficult to minimize codistillation with water, and this becomes a challenge for recycling since anhydrous conditions are needed for esterification. This adds to the cost of this system.

Despite the cost, industry has taken a serious look at the DMAc/ LiCl esterification process, and pilot plant studies are being performed today (Eastman

1992). While the products produced by this method must be high dollar specialty products to be cost effective, the outlook for this system is not as bleak as other organic solvent systems like DMSO/ SO_2/ amine. The improvement of the recycling techniques for DMAc could make this system competitive with the heterogeneous process used today.

2.2 THERMAL PROPERTIES OF CELLULOSE ESTERS

While the thermal properties of cellulose esters have been studied for many years, the T_g and T_m are still disputed in the literature. Since moisture, molecular weight and thermal history of the samples can cause significant changes in the transition temperatures, several trends are observed (Kamide,Saito 1979). Three main variables are examined in the literature: DS, substituent chain length and variable substituent types.

The higher the DS of the product the more thermally stable it is. Cellulose triacetate and acetate are thermally stable at 300°C and 260°C respectively above which they decompose (T_d)(Serad,Sanders 1988) (Manley 1990) (Bogan et al. 1990). Over a wider range of DS, the lower DS derivatives show no T_ms with weak to nonexisting T_gs. Apparently, the T_d is below the T_m.

As substituent chain length increases for fully substituted derivatives the T_m decreases until about C_8 before it levels off (Figure 1) (Malm et al. 1957) (Morooka et al. 1988). The T_g has been reported to follow the same trend, but the T_g and T_m

occur closer together as chain length increases (Morooka et al 1988). The presence of side chain crystallinity is reported for substituent lengths of C_{10}, C_{12} and higher for thiophenes and glutamates (Daly et al. 1992) (Hsu et al. 1993).

Mixed esters show several trends with fully substituted derivatives. The T_g and T_m decrease as the amount of long chain substituent increases. The density also decreases with increasing amount of bulky substituent (Wandel,Bayer 1988). These trends have been seen for several structures including cellulose acetate hexanoate. Cellulose acetate hexanoate samples also showed $\Delta(T_m - T_g)$ to decrease as the amount of hexanoate substitution increased, up to DS_H 1.0 (Glasser et al., in preparation).

Moisture acts as a plasticizer for cellulose and cellulose derivatives. The higher the moisture content the lower the T_g. The T_g of pure cellulose has been reported at 25°C from broad line NMR (Kimura et al 1972), but it is typically accepted to be at 220°C (Salmen,Back 1977). Salmen has reported an equation that can predict the T_g of cellulose as a function of the cohesive energy and the amount of water molecules present (Salmen,Back 1977). The effect of moisture in cellulose derivatives is more complex than in pure cellulose. Cellulose derivatives have free hydroxyls, substituents and impurities that interact with the moisture. The general

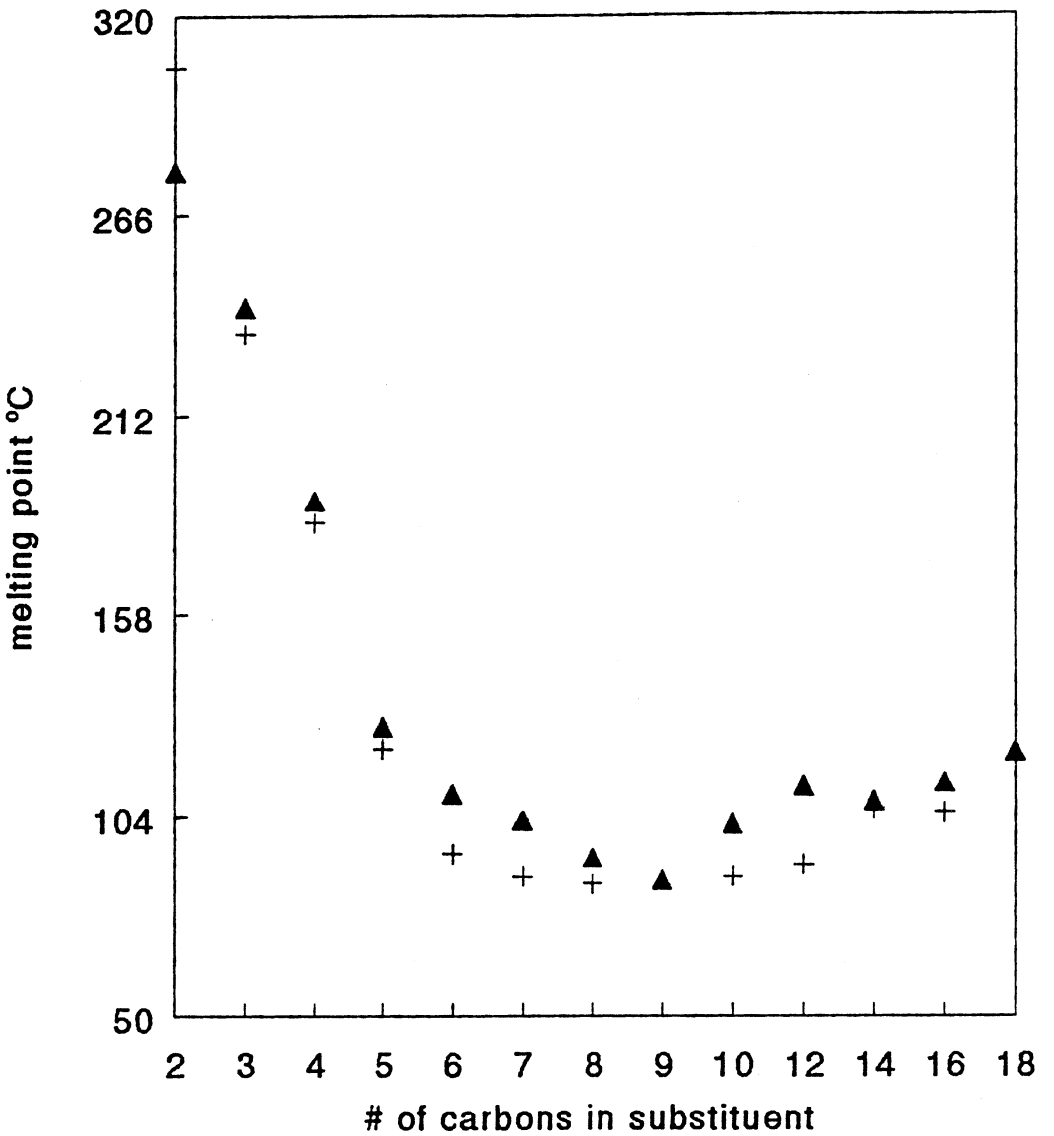

Figure 1. T_m of cellulose esters reported in the literature. Malm's (+) data was reported from visual analysis(Malm et al. 1957). Morooka's (▲) data was reported from TMA analysis (Morooka et al. 1984). Molecular weights of the cellulose derivatives were not reported.

trend for cellulose esters is that the higher the DS and the longer the substituent length, the more hydrophobic the material will become (Bogan et al. 1990) (Serad,Sanders 1988) (Ott et al 1954).

Cellulose esters reportedly have transitions caused by moisture at -73°C, 0-30°C and 100°C (Klason,Kubat 1976). The transition that causes the greatest modulus loss is at -73°C . This transition occurs after repeated scans in some cases and can mask, adjust and excite cellulose ester transitions (Balser 1988). The only way to avoid or lessen the moisture effects is to work with fully substituted derivatives.

2.3 FLUORINATED CARBOHYDRATES

Reactions between carbohydrates and fluorine have been performed for almost 200 years with mixed success. Even Moissan, the discoverer of elemental fluorine, reacted glucose with F_2 in 1900 (Kent 1990). The first real successful reaction between fluorine and carbohydrates was the synthesis of glycosyl fluoride which could be made by an exchange reaction with metallic fluorides or the reaction of liquid HF with a fully acetylated monosaccharides. It was also discovered in the 1930's that cellulose is soluble in anhydrous HF, but if a small amount of moisture was present a nonlinear glucan or 'cellan' was produced (Kent 1990).

Since the 1930's, reactions between fluoro- carbohydrates were preformed on monomeric carbohydrates. A recent study was one of the first highly successful fluorination of polymeric carbohydrates. Cellulose was directly fluorinated with the

use of dialkyaminosulphur trifluorine (DAST) and fluorine was attached to cellulose by producing a cellulose fluoro-benzyl ether (Frazier et al. 1992). Both of these reactions were performed in homogeneous phase (DMSO, SO_2, and amine), and this enabled a wide range of DS to be produced. The only drawback to this study was that both reagent chemistries were highly degradative to the starting polymer. The idea of producing cellulose fluorinated esters evolved because reactions in DMAc/LiCl, which is a cellulose solvent that is suitable for esterification, was shown to be nondegradative.

Several reasons have been given over the years for the production of fluorinated carbohydrates. They range from the interest in producing carbohydrate derivatives that are hydrophobic to the interest in studying the toxicity of fluoro-hydrocarbons. A recent study of graft copolymers of 2-(perfluorooctyl) ethyl acrylate and cellulose was reported. Homogeneous reactions were performed in DMSO-PF that produced products that ranged from 61 to 16% cellulose (Matsui,Shiraishi 1993a). The products were melt processable and had predictable moisture absorption properties. The moisture content of the products decreased with increasing amounts of fluoro copolymer. The films that were produced had a small dielectric constant and a small dielectric loss which suggest that this product would be a good insulating material. The film's surface was mainly poly-POEA with the CF_3 groups concentrating on the surface (Matsui,Shiraishi 1993b).

Another recent study examined the effects of water adsorption on

fluorochemical treated nonwoven fabrics. The fabrics were composites of wood pulp and polypropylene. The surface treatment embedded the fluorochemical into the surface fibers (mainly the polypropylene) by using heat and pressure. The fiber's surface contained about 1% of fluorochemical after pretreatment. The contact angles increased from 25° to 65° for untreated to fluorochemical treated fabrics respectively (Sarmadi et al 1993). The increase in hydrophobic nature with this slight pretreatment was surprising, and the fluorochemical treated fabric should be useful for protective garments especially for pesticide contact (Sarmadi et al 1993).

3.0 OBJECTIVES

The objectives of this study were to examine the structure property relationship for fluorinated and long linear (waxy) aliphatic cellulose esters. The reactivity of cellulose in DMAc/LiCl solution with aliphatic acids of varying size was to be determined by the degree of substitution obtained at various stoichiometric ratios and the comparison between degree of polymerization of the starting polymer and the final product. The effects of variable degree of substitution (DS) on cellulose ester properties (thermal and solubility) were to be determined for fluorinated (polar) and waxy (non-polar) cellulose esters having DS ranging from 0 to 3. The effects of alkyl substituents size on thermal properties were to be revealed using cellulose tri-alkanoates having acyl group with between 12 to 20 carbon atoms.

4.0 EXPERIMENTAL

4.1 CELLULOSE DISSOLUTION

All cellulose derivatives were made from Whatman CF-11 cellulose ($DP_n = 190$). The cellulose was dried for 18 hours at 80°C in a vacuum oven. This cellulose was solvent exchanged with methanol and then DMAc. The solvent exchange was done by stirring 100 g of cellulose with 500 mL of reagent grade solvent. The mixture was allowed to stir overnight and this was repeated three times for each solvent.

The dissolution process starts with dry DMAc which was heated under nitrogen to 80°C. A 10% LiCl/DMAc solution was made while slowly adding LiCl into briskly stirring DMAc. Once the LiCl was in solution, a 2% cellulose solution was made by adding an appropriate amount of cellulose to the solvent at 80°C. The solution was allowed to cool to room temperature and stirring was continued for 48 hrs. The solution was then stored under nitrogen (McCormick, Callais 1987).

A large 5 liter batch of cellulose solution was prepared at the beginning of this study. All derivatives were produced using this cellulose solution. This was done to ensure accurate stoichiometric ratios between reactions.

4.2 TRIFLUOROETHOXY ACETIC ACID REACTIONS

4.2.1 SYNTHESIS OF TRIFLUOROETHOXY ACETIC ACID (TFEA)

Trifluoroethoxy acetic acid was prepared from a method described by Beecham Research Laboratories (Beecham 1960). A solution of 50 g of CF_3CH_2OH in 100 mL of 20% NaOH solution was made. Separately, a solution of 58.3 g of $ClCH_2COOH$ in 125 mL of distilled water was prepared. The chloroacetic acid solution was added slowly to the trifluoroethanol solution at 0°C temperature. The mixture was allowed to reflux overnight while stirring. Then, the solution was cooled in an ice bath and the pH of the solution was adjusted to 2 with concentrated HCl. The mixture was filtered and the filtrate was extracted with diethyl ether five times. The ether extract was washed three times with water or until neutral to lithmus paper. The ether layer was dried over anhydrous sodium sulphate, filtered and concentrated under vacuum. Further purification was done by vacuum distillation (110°C, 11 mm Hg). 60% of the theoretical yield was recovered with a density of 1.4 g/mL. Product was characterized by ^1H (Figure 2) and ^{13}C NMR. The methyl ester of the acid was also made for characterization of the product.

4.2.2 SYNTHESIS OF THE METHYL ESTER OF TRIFLUOROETHOXY ACETIC ACID

The methyl ester of trifluoroethoxy acetic acid was produced by reacting diazomethane with the free acid. This method is described in Vogel's Textbook of Practical Organic Chemistry (Furniss et al. 1989). The diazomethane was produced in a smooth glass joint glass apparatus (Aldrich cat# Z10,025-0). A solution of 2.14g

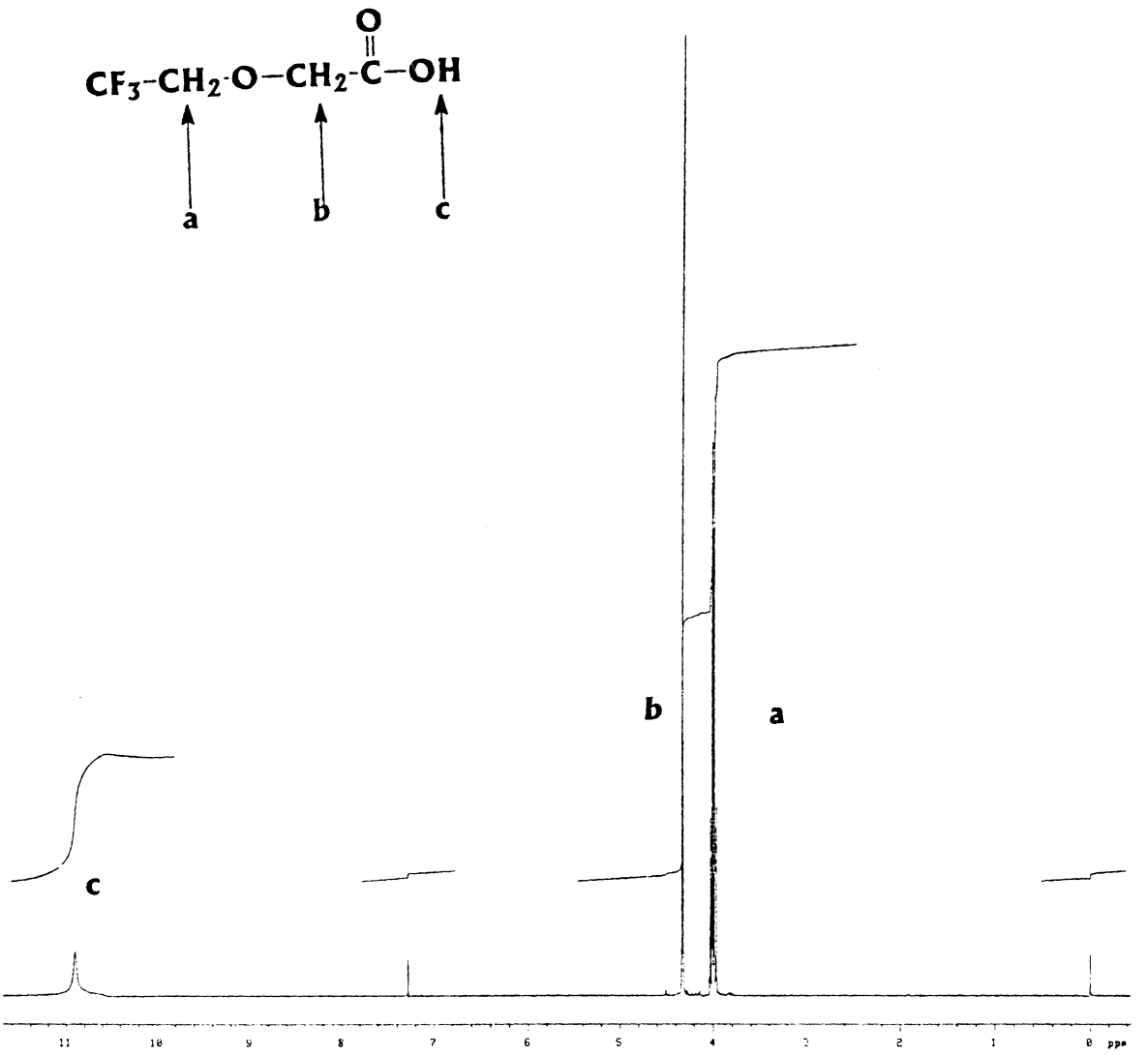

Figure 2. ^{1}H NMR of trifluoroethoxy acetic acid. This product was purified by vacuum distillation. The solvent used was deuterated chloroform.

of N-methyl-N-nitrosotoluene-p-sulphonamide in to 30 mL of ether was introduced to the apparatus and the solution was cooled in an ice bath while 0.4 g of potassium hydroxide in 10 mL of 96% ethanol solution was added slowly. More ethanol was added as necessary to prevent precipitation of reagents. The solution was allow to react for 10 min and then, ethereal diazomethane was distilled off, under gentle heat of a warm water bath, into an ice cold collecting round bottom flask.

The ethereal diazomethane solution was added drop-wise into a solution of 2 mL of free acid in 5 mL of anhydrous ether until a pale yellow color was persistent. Excess diazomethane and solvent were distilled off. The methyl ester was isolated by vacuum distillation. The product was characterized by ^{1}H NMR (Figure 3).

4.2.3 SYNTHESIS OF PYRROLIDINE DERIVATIVES

The synthesis of the pyrrolidine derivatives was done in two steps. First, the acid chloride was made by reacting the free acid with oxalyl chloride in dichloromethane. 5 mL of free acid was added to 10 mL of dichloromethane in a round bottom flask while stirring in an ice water bath. A solution of 5.6 g of oxalyl chloride in 10 mL of dichloromethane was added drop-wise through an addition funnel into the acid solution under anhydrous conditions. After addition, the ice water bath was removed and, the reaction was allowed to warm to room temperature. Total reaction time was 60 min. The acid chloride was concentrated under anhydrous conditions.

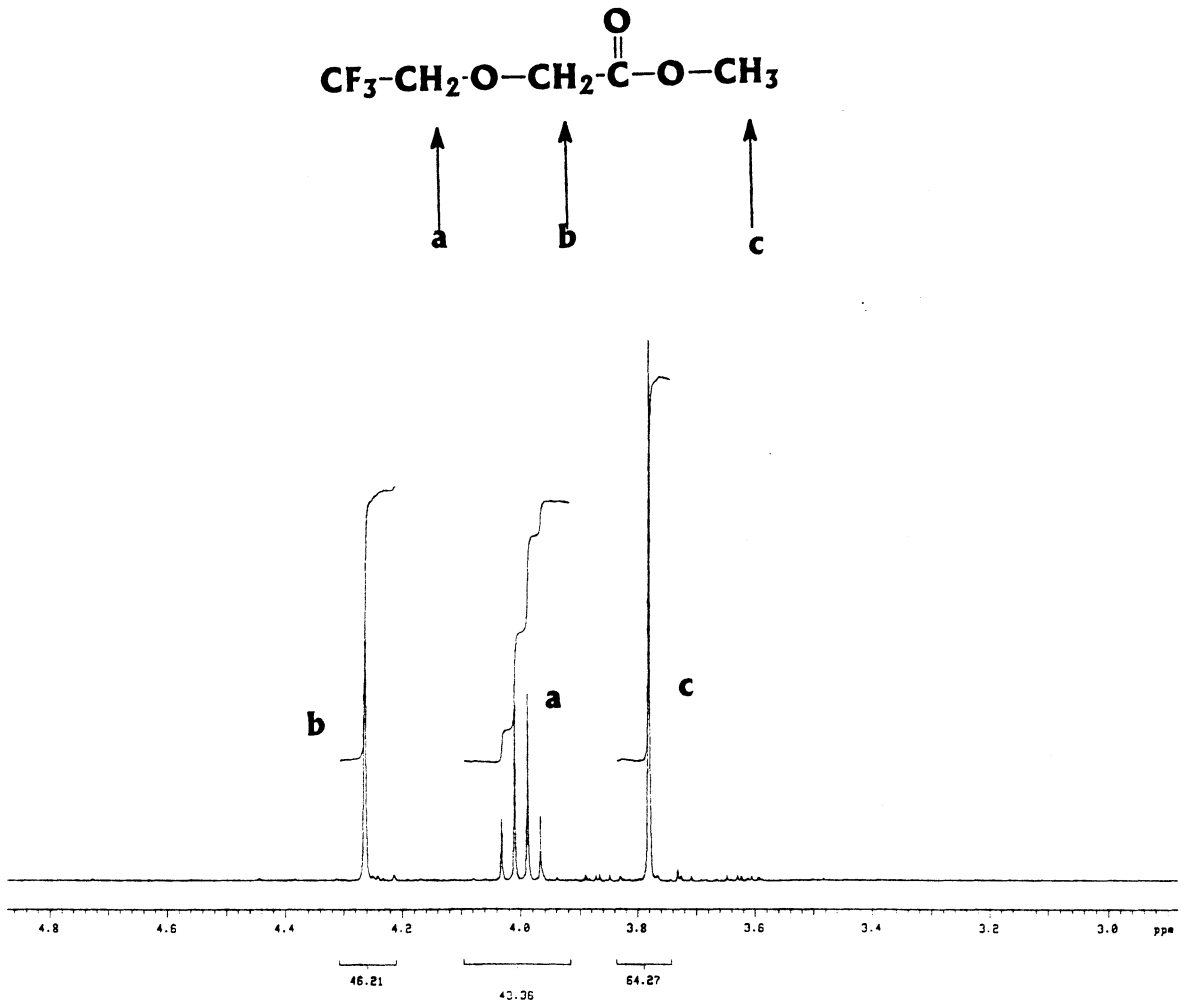

Figure 3. ^{1}H NMR of methyl ester of trifluoroethoxy acetic acid. The solvent used was deuterated chloroform. The methyl ester protons signal was seen at 3.79 ppm (δ-value).

The pyrrolidine derivative was then made by reacting the acid chloride with pyrrolidine in a stoichiometric ratio of 1 to 3, respectively. 10 mL of dichloromethane was added to 6.6 mL of pyrrolidine. While stirring in an ice water bath, the acid chloride was added drop-wise from an addition funnel. After addition, the solution was stirred for 2-3 hrs at room temperature.

Myristoyl, lauroyl and stearoyl pyrrolidine derivatives were isolated by washing the reaction product with 3N HCl. The dichloromethane layer was separated and washed with 5% sodium bicarbonate solution followed by water until neutral. Myristoyl and stearoyl pyrrolidine were isolated as a solid after evaporation, and lauroyl was isolated as a liquid and purified by vacuum distillation. Trifluoroethoxy acetyl pyrrolidine was soluble in water so no work-up could be preformed before vacuum distillation. Since the product is highly acidic, it charred significantly during distillation. The yield of clear viscous liquid was low. This product was a mixture of about 50% pyrrolidine derivative and 50% free acid by NMR. The isolation of pure trifluoroethoxy acetyl pyrrolidine was never accomplished.

4.3 ESTERIFICATION

4.3.1 DICYCLOHEXYLCARBODIIMIDE (DCC)

The acylation was done in homogeneous phase (2% cellulose solution in 10% DMAc/LiCl). The reaction conditions were three equivalents of trifluoroethoxy acetic

acid and DCC per hydroxyl group and, 0.01 equivalent of pyrrolidine pyridine (PP) per hydroxyl group.

A typical reaction involves a cellulose solution placed in a three neck round bottom flask under nitrogen. The flask was placed in a heating mantle on top of a stir plate. The PP is added to the flask and allowed to stir. The DCC and free acid were mixed together in a round bottom flask with 50 mL of DMAc. This was added to the cellulose solution. The solutions were allowed to stir for 48 hrs at room temperature or 50°C. The solutions were then precipitated into hot 50/50 methanol/water solution. The product was filtered under vacuum and extracted in a soxhlet with methanol for 48 hrs. The product was dried in a vacuum oven at 50°C. Characterization was performed by NMR and FTIR.

4.3.2 PARA-TOLUENE SULPHONYL CHLORIDE (TsCl)

The acylation of cellulose in homogeneous phase with a free acid and TsCl was done under the following conditions. TsCl and the free acid were used in a 1 to 1 ratio. Pyridine was added in a 3 to 1 ratio with TsCl and, The reaction was heated to 40°C or 50°C for 24 hrs.

The cellulose solution is placed in a three neck round bottom flask under nitrogen. The flask is placed in a heating mantle on top of a stir plate. The solution is stirred by a magnetic stir bar while diluting the solution with additional DMAc. The amount of dilution needed depended on the type of free acid and the

stoichiometric ratio. This ranged from additional 0 to 60 mL of DMAc for a 1 g cellulose reaction. Pyridine was added and allowed to stir for 15 min. The free acid was added slowly and allowed to stir for 5 min. A DMAc solution of TsCl was then added to the solution. If the free acid was a solid, it was also placed into DMAc solution before addition.

The solution was precipitated into water if it was a fluoro-ester and into hot 50/50 methanol water solution if it was a bulky ester. The product was filtered under vacuum and then extracted in a soxhlet for 48 hrs (solvent depends on the derivative). The product is dried in a vacuum oven at 50°C. The product was characterized by NMR, FTIR, GC and GPC. Thermal analysis was performed by DSC, DMTA, TMA and melting point apparatus.

4.3.3 PERACETYLATION

A solution with 200 mg of sample in 10 mL of pyridine was added to 3 mL of acetic anhydride and the solution is heated at 60°C for 12-18 hrs or until all the starting material was dissolved. The product was precipitated into water, solvent extracted and vacuum dried at 50°C .

4.4 CHEMICAL ANALYSIS

4.4.1 NUCLEAR MAGNETIC RESONANCE (NMR)

All NMR spectra were done on a Varian 400 MHz spectrometer. Wilmad 507

or 550 PP tubes were used for all samples.

^{1}H NMR samples were prepared from 25-35 mg of dry sample, 1 mL of deuterated solvent and three drops of trifluoroacetic acid (TFAA). The solution was made by stirring the sample and the solvent in a 5 mL round bottom flask with a magnetic stir bar. Before addition of the solution into the NMR tubes, the three drops of TFAA were added. The spectrum was run within 2 hrs of sample preparation.

^{19}F NMR samples were prepared from 20 mg of sample, 5-10 mg of 3-trifluoromethyl-benzophenone (internal standard) and 1 mL of dry deuterated solvent. Solutions were prepared as above but no TFAA was added and the sample weight was recorded accurately.

^{13}C NMR was performed only on trifluoroethoxy acetic acid. The sample was prepared by adding four drops of acid into 3/4 mL of deuterated solvent already in the NMR tube.

The type of deuterated solvent used depended on the ester derivative. DMSO was avoided whenever possible, and most experiments were preformed in acetone or chloroform.

4.4.2 FOURIER TRANSFORM INFRARED SPECTROSCOPY (FTIR)

FTIR spectroscopy was performed on a Nicolet 5 SXC spectrophotometer. A thin solvent cast film was used for soluble samples and, KBr pellets were made from

the rest of the samples. The solvent cast films were dried in a vacuum oven before testing.

4.4.3 DEGREE OF SUBSTITUTION DETERMINED BY GAS CHROMATOGRAPHY (Samaranayake,Glasser 1993a)(Mansson,Samuelsson 1981)

SAMPLE PREPARATION

The procedure of Mansson as refined by Samaranayake and Glasser (1993a) was used. This procedure used a dry cellulose alkanoate sample of 10 to 50 mg. It was suspended in 1 to 2 mL of appropriate internal standard solution. The internal standard (synthesis described in section 4.2.3) used was determined by which internal standard would provide peak separation resolved by GC analysis (several seconds between peaks allowing the detector to return to the baseline between peaks). For example, A cellulose laurate would use a myristoyl pyrrolidine internal standard. The internal standard solution was 3-10 mg/ mL pyrrolidine derivative in a 1 to 1 mixture of pyridine and pyrrolidine. The reaction was done in a glass vial with a triangular magnetic stir bar and a Reactivial (supelco) fitting. The reaction lasted 12 hrs at 80°C. After cooling, the sample mixture was filtered and a portion was injected into the GC.

EQUIPMENT

A Varian model 3700 with a HP integrator model 3394 equipped with a packed-column was used in GC analysis. A 3% OV-17 on 80/100 Supelcoport column

was used with helium as the carrier gas.

DS CALCULATION

The degree of substitution was calculated using the following formula:

$$DS = A * D * V * 162 / (W (M + 70.12) - V * D * A (M - 1))$$

WHERE A= sample concentration in mg/ml
D= dilution factor (D=1 for no dilution)
V= solvent volume used in aminolysis
W= mass of the unknown sample
M= molecular weight of the acyl moiety, and 70.12 is the molecular weight of the pyrrolidine group.

4.4.4 ELEMENTAL ANALYSIS

Elemental analysis was preformed at Galbraith Laboratories PO. Box 51610, Knoxville, TN 37950. The samples were analyzed for carbon, hydrogen, chlorine, fluorine and sulfur.

4.4.5 GPC

The GPC molecular weight analysis used the following equipment:

Columns- Waters Ultrastyragel, length 30 cm, 7.8 mm ID, styrenedivinylbenzene copolymer packed with $10^{3,4,6}$ angstrom pore size.

Pumps- Waters model 510 HPLC pump

Detectors- (RI) Waters model 410 differential refractometer

(Differential viscosity) Viscotek model 1000

Software- Viscotek Unical

Standard- Polymer Laboratories polystyrene; 3rd order polynomial was used to fit the data with hydrodynamic volume = η * MW.

The solvent used was HPLC tetrahydrofuran from Fisher. Sample preparation was done by adding 10 mg of dry cellulose derivative into 10 mL of solvent. All samples were in solution by 24 hrs without stirring. Column temperature was 40°C.

CARBANILATION

Carbanilation was performed on samples that were not THF soluble. This reaction was performed in the following manner: 250 mg of dry cellulose derivative was added to a 50 mL Erlenmeyer flask with a stirbar, 25 mL of dry pyridine and 5 ml of phenyl isocyanate was added. The temperature was raised to 80°C, and the reaction was allowed to continue for 24 hrs or until the solution was clear. The reaction mixture was precipitated in 250 mL of 50/50 MeOH/ H_2O. The product was filtered and dried in vacuum oven at 60°C overnight.

4.4.6 SOLUBILITY TEST

The solubility test used a solvent to solid ratio of 9 to 1 by weight. The mixtures were stirred at room temperature for 24 hrs. The sample was then examined visually to determine solubility. Partially soluble samples were labeled insoluble in that solvent.

4.5 THERMAL ANALYSIS

4.5.1 DIFFERENTIAL SCANNING CALORIMETRY (DSC)

All samples were tested using a Perkin-Elmer DSC 4 with a TADS software package. Samples were typically heated at 10°C/min and cooled at 5°C/min for three consecutive scans between -50°C and 5°C below the decomposition temperature. This temperature was determined by visual discoloration in a melting point apparatus. Glass transition temperature (T_g) was defined as the midpoint of an endothermic step function. This temperature was calculated by the TADS software package. The recorded T_g was taken from the second heating. The melting temperature (T_m) was defined as the temperature at the maximum peak height of an endothermic transition. The range of the T_m was the point the endotherm leaves the baseline to the point at which it returns to the baseline. These temperatures weree also calculated by the software package. The samples were prepared by cold pressing powders into films under pressure (10 tons). They were cut into squares and placed in the aluminum DSC pans (10 mg was the average weight).

4.5.2 DYNAMIC MECHANICAL THERMAL ANALYSIS (DMTA)

The DMTA used was a Polymer Laboratories system with a Plus Five software package. Most samples were tested from -120°C to the melting point of the polymer. The samples were prepared by hot pressing powders to form films. The samples were allowed to cool slowly in the press to room temperature. The films

were then cut into rectangular samples for testing. Flat edge clamps were used in single cantilever bending at a frequency of 1 Hz . One pound of torque was used for clamping.

α and β-transitions were defined as the midpoint of the tan δ or the loss modulus transition. The α-transition was the first transition going from high to low temperature and, β-transition was the second.

4.5.3 THERMAL MECHANICAL ANALYSIS (TMA)

A Perkin Elmer TM-2 TMA was used with Polymer Laboratories Plus Five software package. Expansion probe test used one gram weight which was 1 g/10.7 mm^2 of force. Samples were cut from cold pressed films and heated above their T_g's to let the polymer relax while in contact with the probe. The samples were allowed to cool to room temperature, then liquid nitrogen was added to cool to -150°C. The samples were scanned from -150°C at 2.5°C/min until flow was recorded. Transitions were defined as the onset of expansion. The penatration probe test was preformed with a 5°C/min ramp and 10g of force.

4.5.4 HOT STAGE MICROSCOPY

Optical microscopy was conducted on a Zeiss Axioplan microscope fitted with a TMS 90 hot stage and a Zeiss ML 100 camera. The presence of birefringence and the temperature at which it disappears was studied for the fluoro-esters, and the re-

occurring birefringence above T_m was examined for the bulky esters. Solution concentrations of 0.01 g/ mL were in THF and chloroform. Samples were made by placing a drop of solution on a glass plate and air drying.

5.0 CELLULOSE TRIFLUOROETHOXY ACETATE (CT)

5.1 INTRODUCTION

Since miscible blends between fluorine containing polymers and polyesters have been reported, one objective in chemically bonding fluorine to cellulose is to produce miscible blends with polyesters. Polymer-polymer miscibility occurs whenever the free energy of mixing is negative. Since the entropy of mixing is negligible for polymeric constituents, enthalpy of mixing is the main variable that influences miscibility. One way of changing the enthalpy of mixing is to induce strong interactions between polymers. Hydrogen bonding, charge-transfer, dipolar, Van der Waals and electrostatic interactions are forces between polymers that can induce miscibility (Olabisi 1988). Cellulose fluoro-ester should induce strong dipolar-dipolar interactions with polyesters, and this could induce miscible blends between the two polymers .

Recent work done by Paul and Barlow show that poly(vinylidene fluoride) is miscible with oxygen containing polymers (Paul, et al. 1978). They use melting point depression between two semi-crystalline polymers to determine miscibility. T_m depressions of 20°C were seen with several polyesters and PVF. These blends also show only one T_g and one T_m transition. It has been suggested that only 1°C of the T_m depression could be related to entropic consideration; and the driving force for T_m depression and miscibility is due to enthalpic changes.

Cellulose fluorination has been performed by Frazier in a recent study (Frazier et al 1992). Direct cellulose fluorination and cellulose derivatives of aromatic fluoro-ethers were synthesized and blended with polycaprolactone. Interactions between the two polymers were increased with fluorine content, but miscible blends were not created. It was believed that a cellulose derivative with aliphatic fluorine may be able to induce a miscible blend with a polyester.

Trifluoroethoxy acetic acid was chosen for several reasons. The ease of synthesis was one. The aqueous reaction between chloroacetic acid and trifluoroethanol enabled large scale reactions to be done that produced high yields of free acid with only a few isolation steps. The esterification of this free acid with cellulose produced a derivative that not only has fluorine, but also incorporates a carbonyl group that would enhance dipole-dipole interactions with polyesters (Figure 4). The free acid was synthesized according to the method described in a British patent (patent # 873,244). This acid was produced to make various penicillin derivatives that were hydrophobic (Beacham 1960). This acid is apparently quite novel because this patent is the only publication that describes its synthesis.

Cellulose esters were chosen because the synthesis of esters with a wide range of DS could be accomplished with little to no degradation to the starting polymer (Samaranayake, Glasser 1993a) (McCormick,Callais 1987). The DCC esterification technique can react free acids with cellulose in homogeneous phase (DMAc/ LiCl), and this reaction could be done in a single reaction vessel (ie, in "one pot").

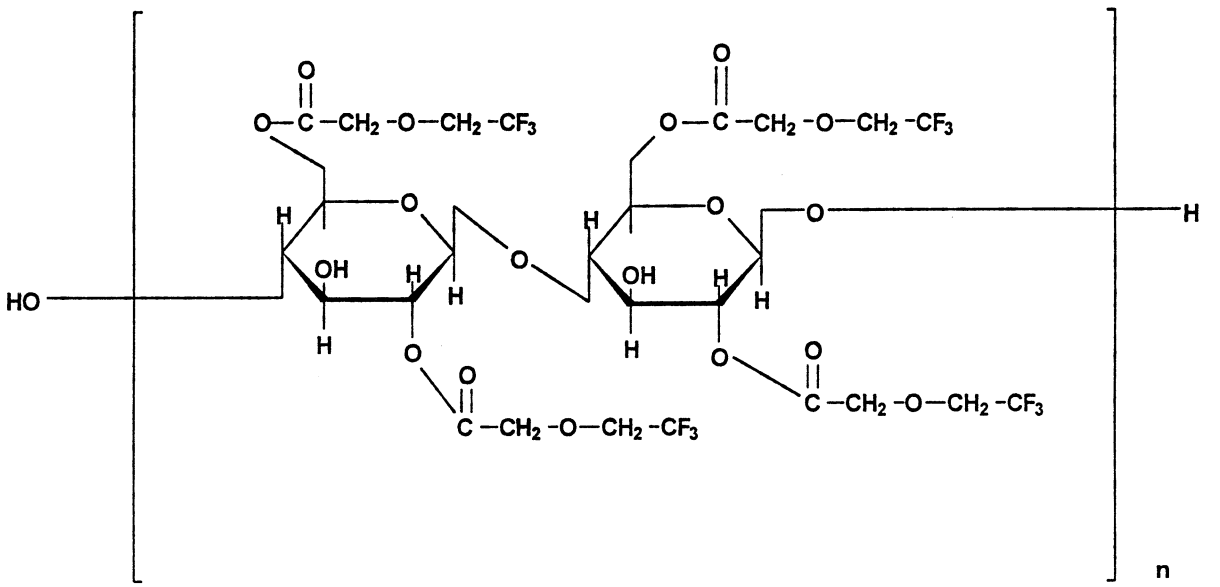

Figure 4. CT chemical structure. This structure represents a DS of 2.0. All CT structures have free hydroxyls present except DS 3.0 derivatives.

Cellulose esters have also been reported as thermally stable which will be needed for melt processing blends (Serad,Sanders 1988).

The objective of this study was to create a cellulose ester with a wide range of uniformly substituted aliphatic fluorine derivatives, and to characterize them by chemical and thermal analysis. The reactivity and the extent of degradation during the reaction was determined.

5.2 RESULTS AND DISCUSSION

5.2.1 REACTIONS AND REACTIVITY

The DCC esterification reagent system was performed with trifluoroethoxy acetic acid (Figure 5). While this reagent system worked well for alkanoates from C_2 to C_6 in length, only very low DS derivatives were produced with trifluoroethoxy acetic acid while using elevated temperatures and high stoichiometric ratios (3 EQ. acid/OH). The products were insoluble and showed small to non-existing ester absorption by FTIR analysis. Apparently, the acid anhydride was insoluble in the DMAc/ LiCl solution (Hassner, Alexanin 1978). This problem was noticed for long linear aliphatic acids with the DCC method, but it was surprising to see this problem with this small polar acid.

The TsCl esterification reagent system was then investigated with trifluoroethoxy acetic acid (Figure 6). This system, which was used for

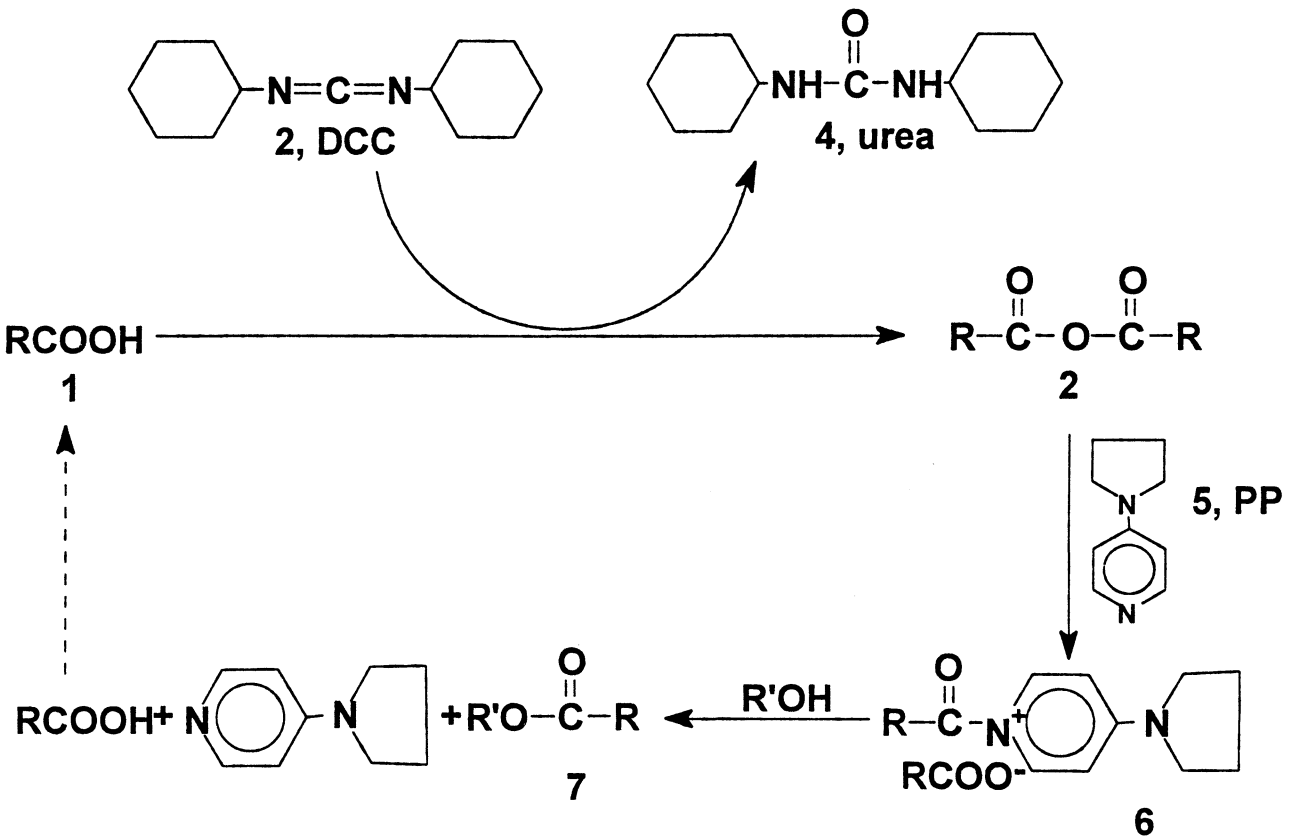

Figure 5. DCC esterification reagent system. This system was recently reported for aliphatic cellulose esters (Samaranayake,Glasser 1993a).

TsCl / PYRIDINE

REAGENT SYSTEM

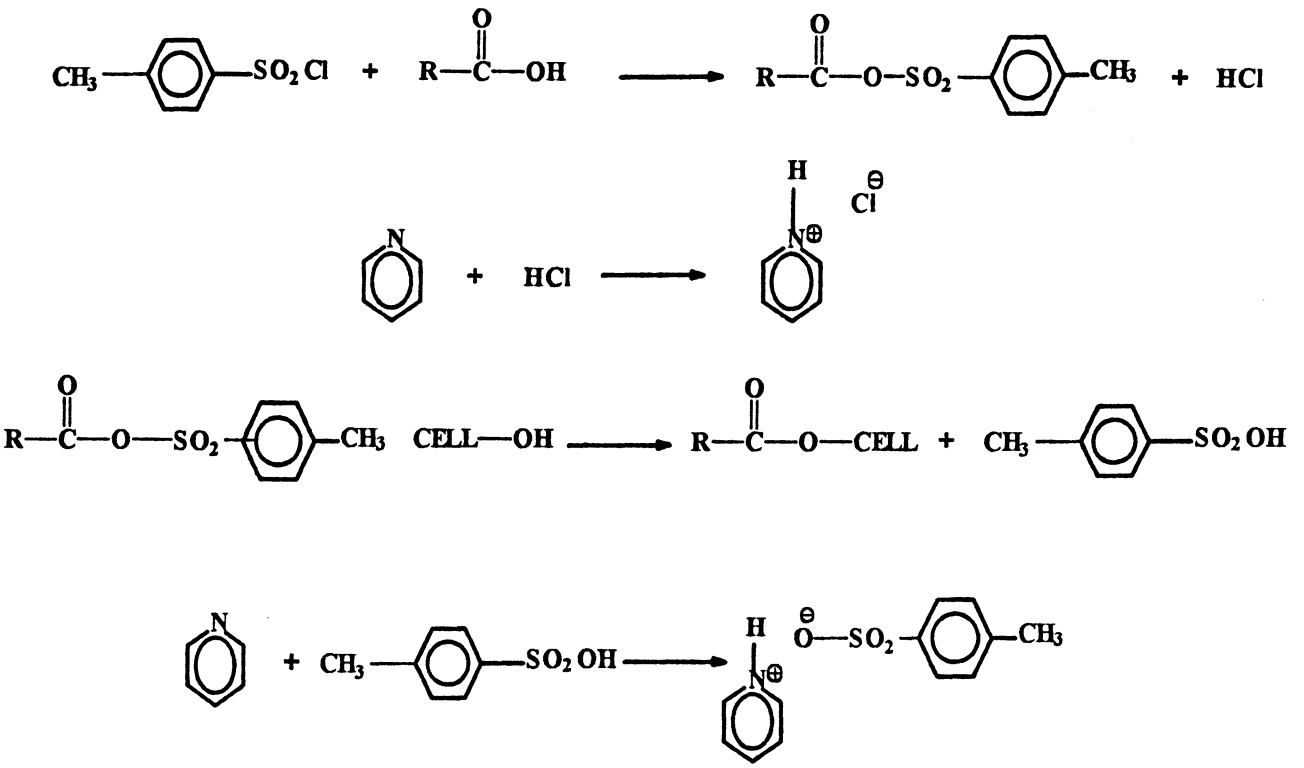

Figure 6. TsCl esterification reagent system. This system incorporated the pyridine acid anhydride esterification method with TsCl esterification method reported by Shimizu (Shimizu,Hayashi 1989).

heterogeneous cellulose esterification by Shimizu, showed surprising reactivity (Shimizu, Hayashi 1989). Nearly fully substituted aromatic and long linear aliphatic cellulose esters were produced with low stoichiometric ratios of acid per OH. However, this was the first time this reagent system was used in homogeneous phase reaction of cellulose (comparison in section 7.2.1). A time study was performed for 2 EQ. of acid/OH at 40°C (Figure 7). After three hours, over 80% of the substitution had occurred. No benefit was gained from reaction times over 24 hrs. The degree of polymerization remains the same over a 30 hrs reaction time with no depolymerization detected for the 40°C reaction (Figure 8). Another time study was performed at 50°C with 1 eq. of acid/OH (Figure 7). This reaction condition proved to be more efficient while using 50% less free acid compared with the 40°C reaction. No degradation was detected for this reaction either. However, reactions at 50°C with higher stoichiometric ratios (greater than 1.0 acid/OH unit) do show significant degradation (Figure 8). This will be examined in section 5.2.2.

The reaction conditions of 50°C for 24 hrs with a range of stoichiometric ratio between 0.5 to 2 acid/OH unit were used for the rest of this study. The stoichiometric control of the TsCl esterification method was linear (Figure 9) and predictable. DS between 0.04 to 3.0 were created with a high efficiency compared to published techniques (McCormick,Dawsey 1990).

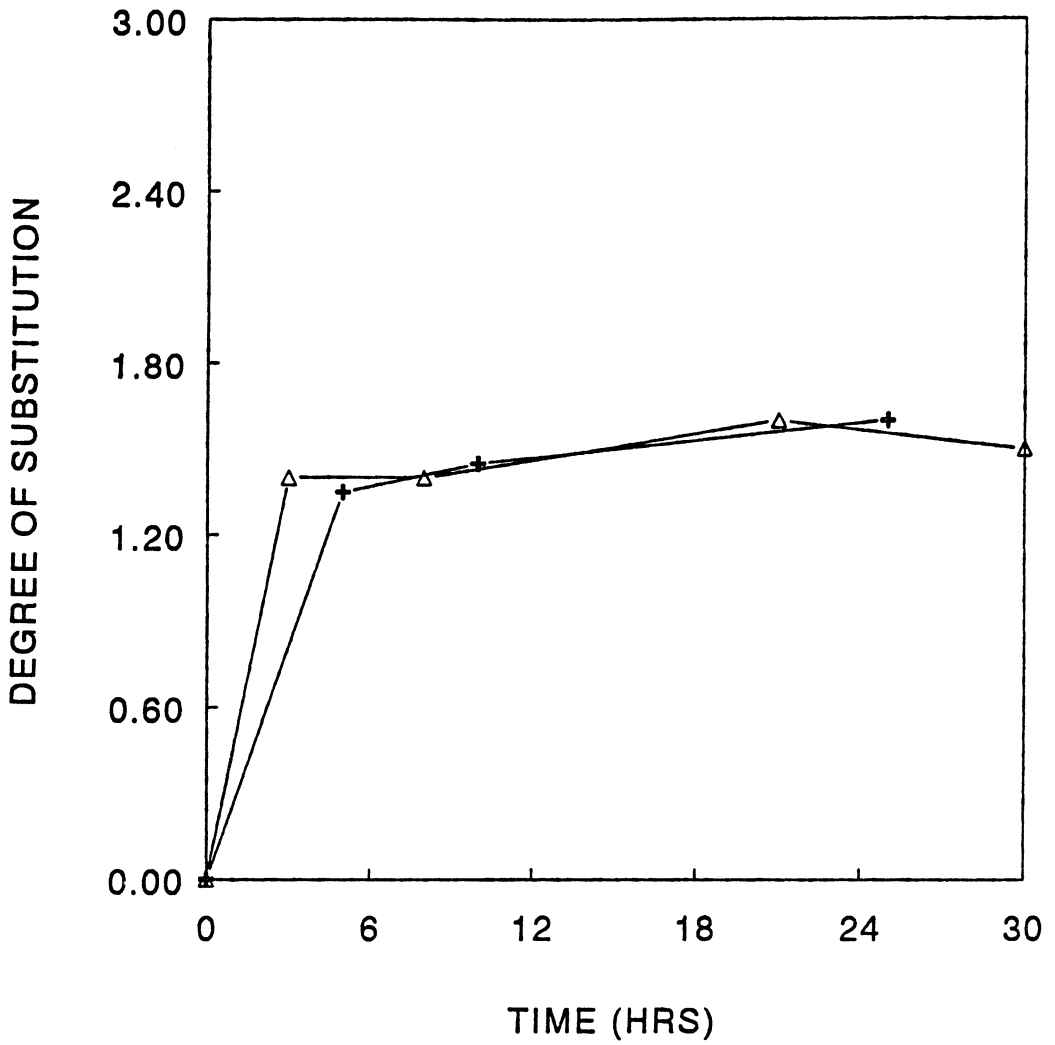

Figure 7. Time study vs DS at reaction temperatures of 40°C (Δ) and 50°C (+). The 40°C reaction was performed with 2 EQ. of free acid per OH. The 50°C reaction was performed with 1 EQ. of free acid per OH.

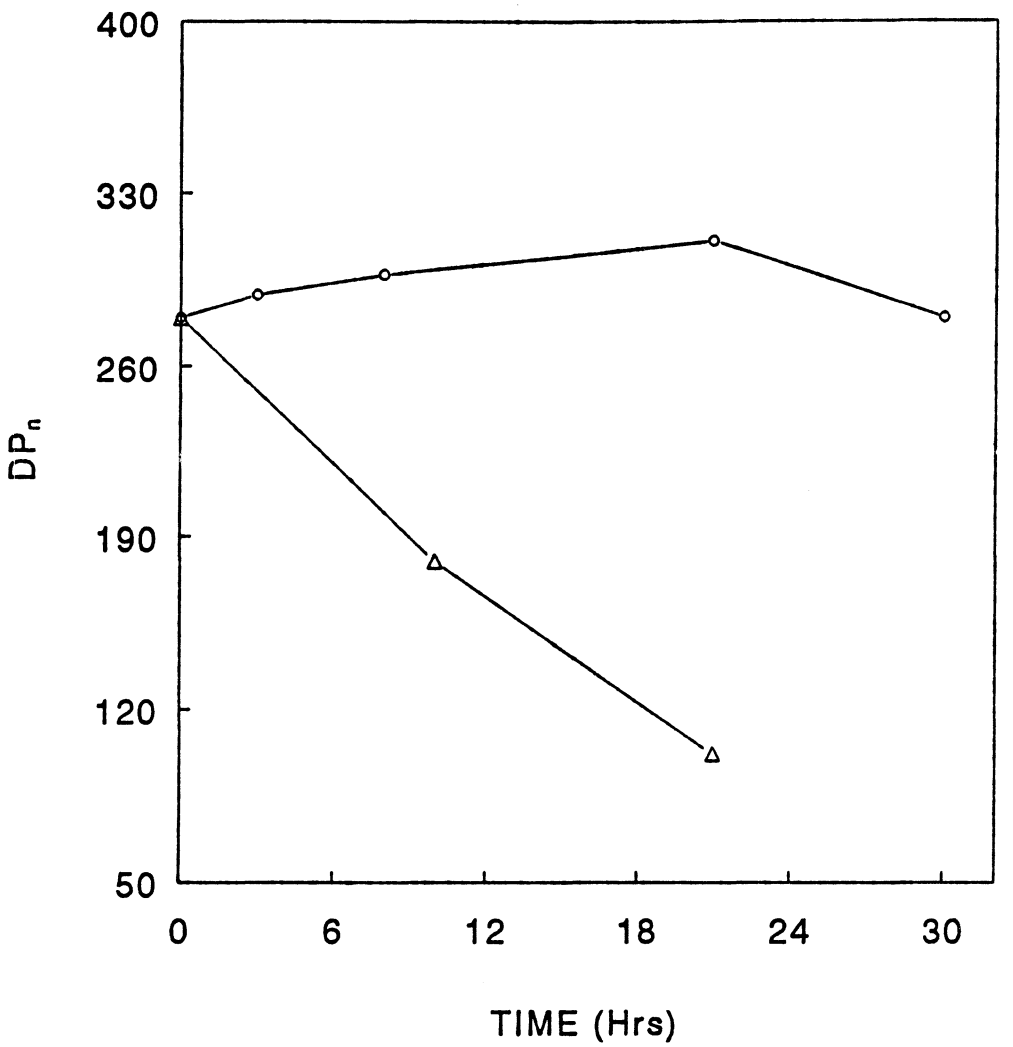

Figure 8. Time study vs DP_n at reaction temperatures 40°C (O) and 50°C (Δ). The 40°C reaction was performed with 2 EQ. of free acid per OH. The 50°C reaction was performed with 2 EQ. of acid per OH.

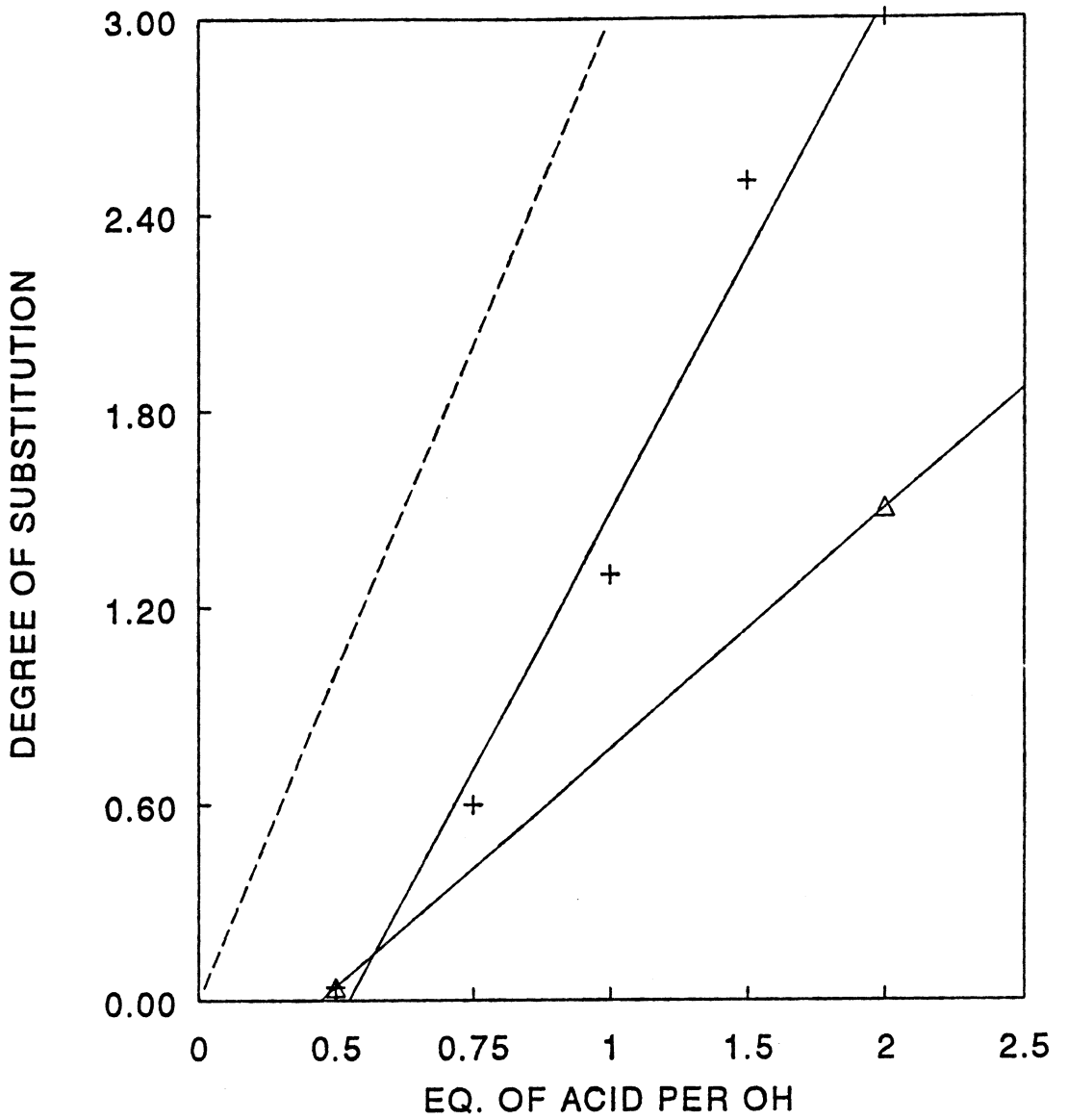

Figure 9. Stoichiometric reactivity of the TsCl esterification system with the TFEA. (---) 100% theoretical reactivity, (+) DS produced at a reaction temperature of 50°C, (Δ) DS produced at a reaction temperature of 40°C.

5.2.2 CHEMICAL ANALYSIS

^{1}H and ^{19}F NMR techniques are used to characterize and calculate DS for CT. A typical ^{1}H NMR spectrum shows broad peaks for the seven backbone protons between 3.7 to 5.5 ppm δ (Figure 10)(Buchanan,Edger et al. 1991). The four proton signals from the trifluoroethoxy group overlap the backbone protons at 4.2 and 4.35 ppm δ. The multiple peaks from 7.8 to 8.3 ppm δ represent the protons from the internal standard 3-trifluoromethyl-benzophenone. The 2.1 ppm δ peak is for deuterated acetone. The overlapping of the substituent protons with the backbone protons made it impossible to calculate DS by ^{1}H NMR.

The ^{19}F NMR spectrum shows only two regions of interest (Figure 11). The peak at -64.2 ppm δ is the internal standard of 3-trifluoromethyl-benzophenone. The second region is for the CT derivative. The three triplets seen in the fully substituted derivative are from the fluorines in each of the substituted sites in anhydroglucose unit. While no definite assignments can be made with the present data, the middle triplet appears to have a higher intensity. DS is calculated by comparing the integration of the two regions to the accurate weight of the sample and internal standard. Each sample is duplicated, and the averages are taken. This technique has been compared to other DS determination technique, and it has at least an accuracy of $>$DS$\pm$ 0.3 (Frazier et al 1992). Lower substituted derivatives do not reveal the sharp triplets of a fully substituted product. The signal becomes increasingly broad as DS decreases.

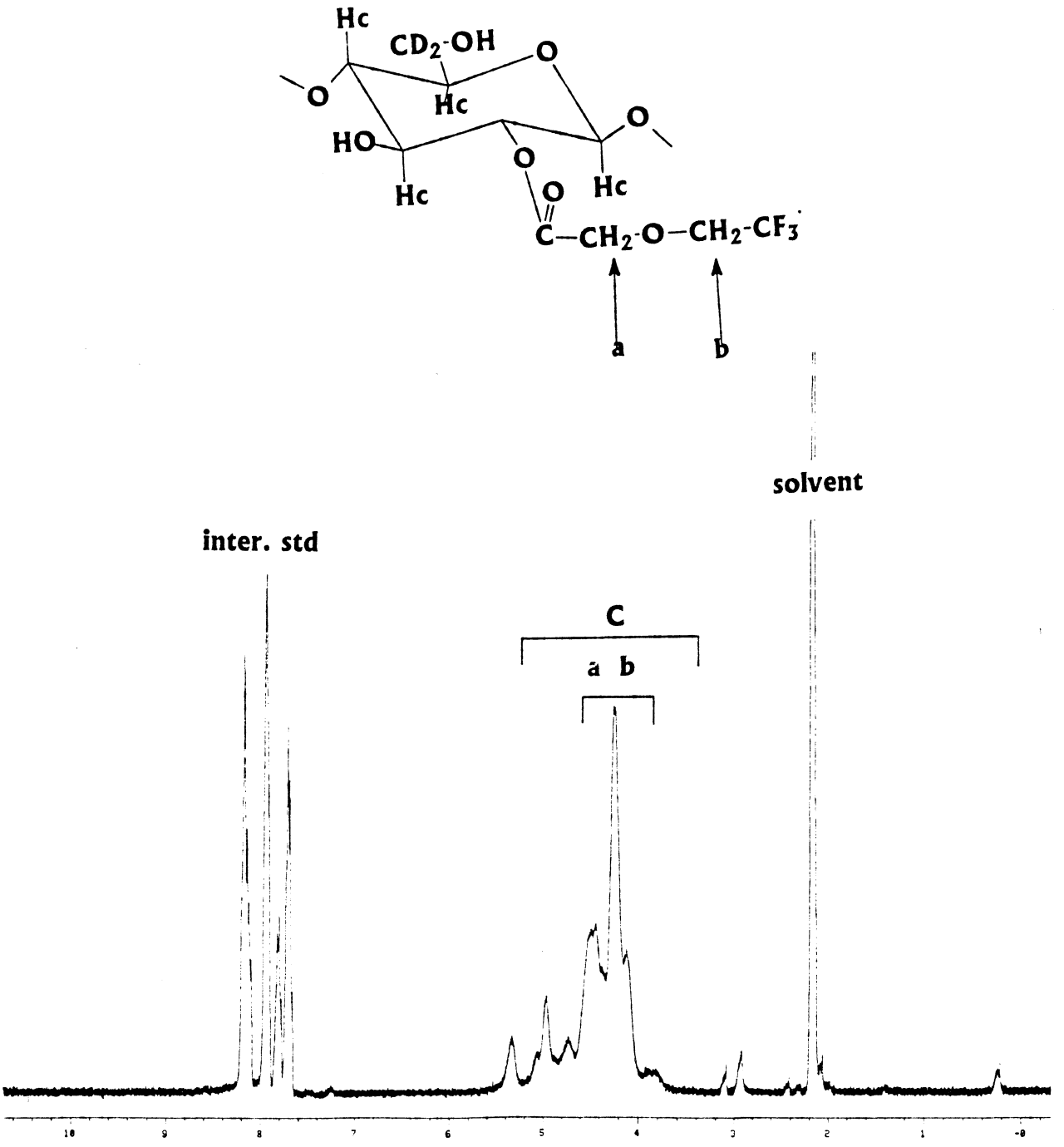

Figure 10. ^{1}H NMR of CT derivative with a DS 2.9. The substituent's proton signals overlap cellulose's backbone proton signals. The solvent used was deuterated acetone.

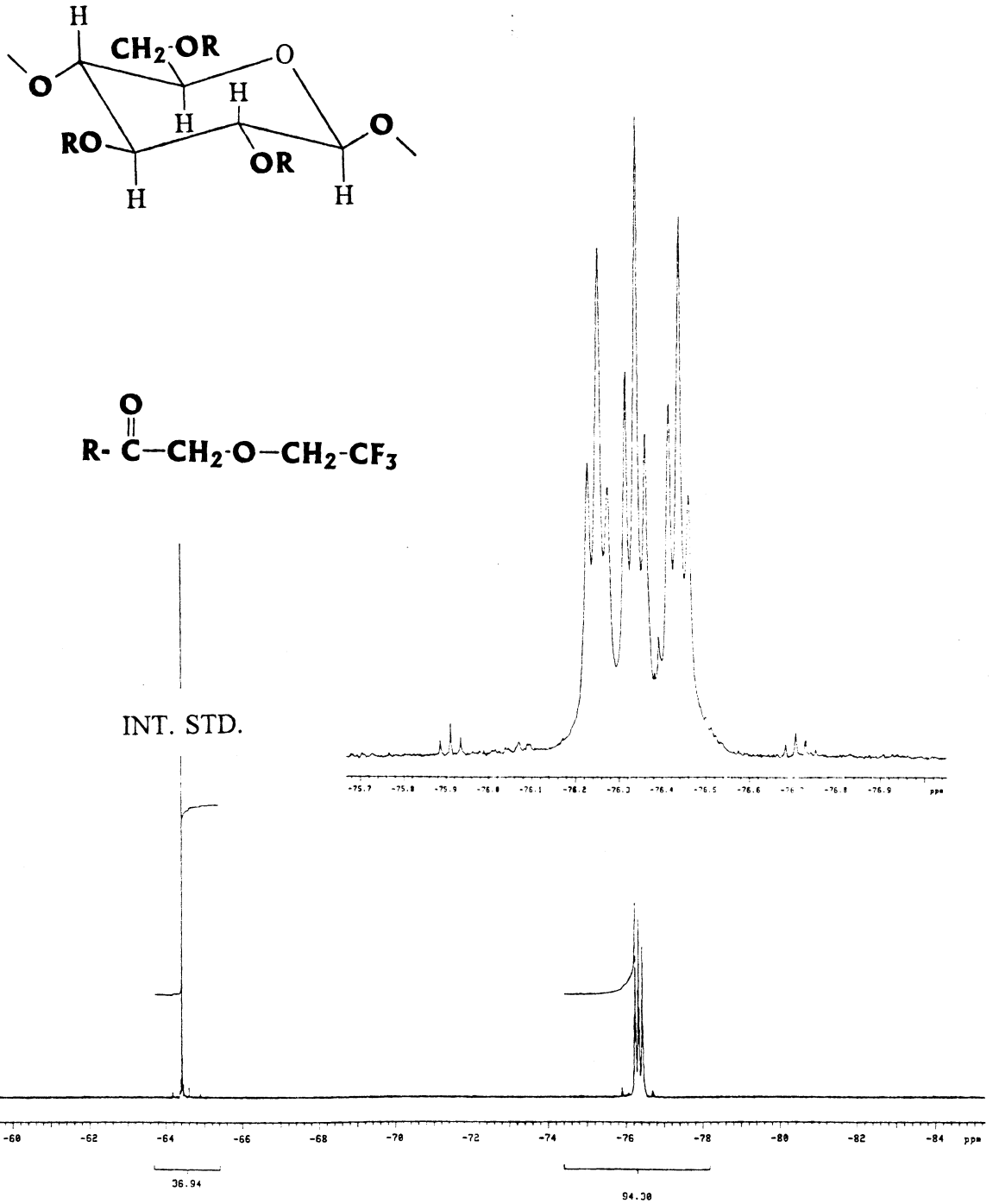

Figure 11. ^{19}F NMR of CT derivatives with a DS 3.0. 3-trifluoromethyl-benzophenone was used as the internal standard.

The FTIR spectrum for a dry solvent cast film of a fully substituted CT has a flat hydroxyl region absorption compared to cellulose (Figure 12). All derivatives showed a strong ester absorption at 1735 cm^{-1} (Blackwell, Marchessault 1970). The absence of a absorption in the 1350 and 1195 cm^{-1} regions suggests absence of tosylation (McCormick, Dawsey 1990).

Elemental analysis (for a DS 2.0 sample: carbon 36.65%, hydrogen 3.48%, fluorine 19.61%, chlorine 0.53%, sulfur 0.13%) reinforced the FTIR data by detecting only a trace amount of sulfur in highly substituted derivatives. The percent chlorine in the samples was also in trace amounts. Since Shimizu discussed the possibility of tosylation, it was surprising to reveal the absence of this side reaction. It was believed to be mainly due to the reaction conditions. The TsCl was not added until the free acid was well mixed in the solution. This caused the TsCl to react with the free acid and not the cellulose.

The solubility of the CT derivatives was tested with a range of solvents (Table 1). No report of a cellulose ester that was methanol soluble has been presented until now (Malm et al. 1957). The solubility of DS 0.6 in acetone was also surprising. This solubility of a wide range of DS allowed NMR analysis to be preformed with free hydroxyls. Typically a mixed ester has to be made inorder to make the product soluble. This minimized the complexity of the spectrum. This wide range of solubilities could also prove important for fiber spinning. Water and hexane were the

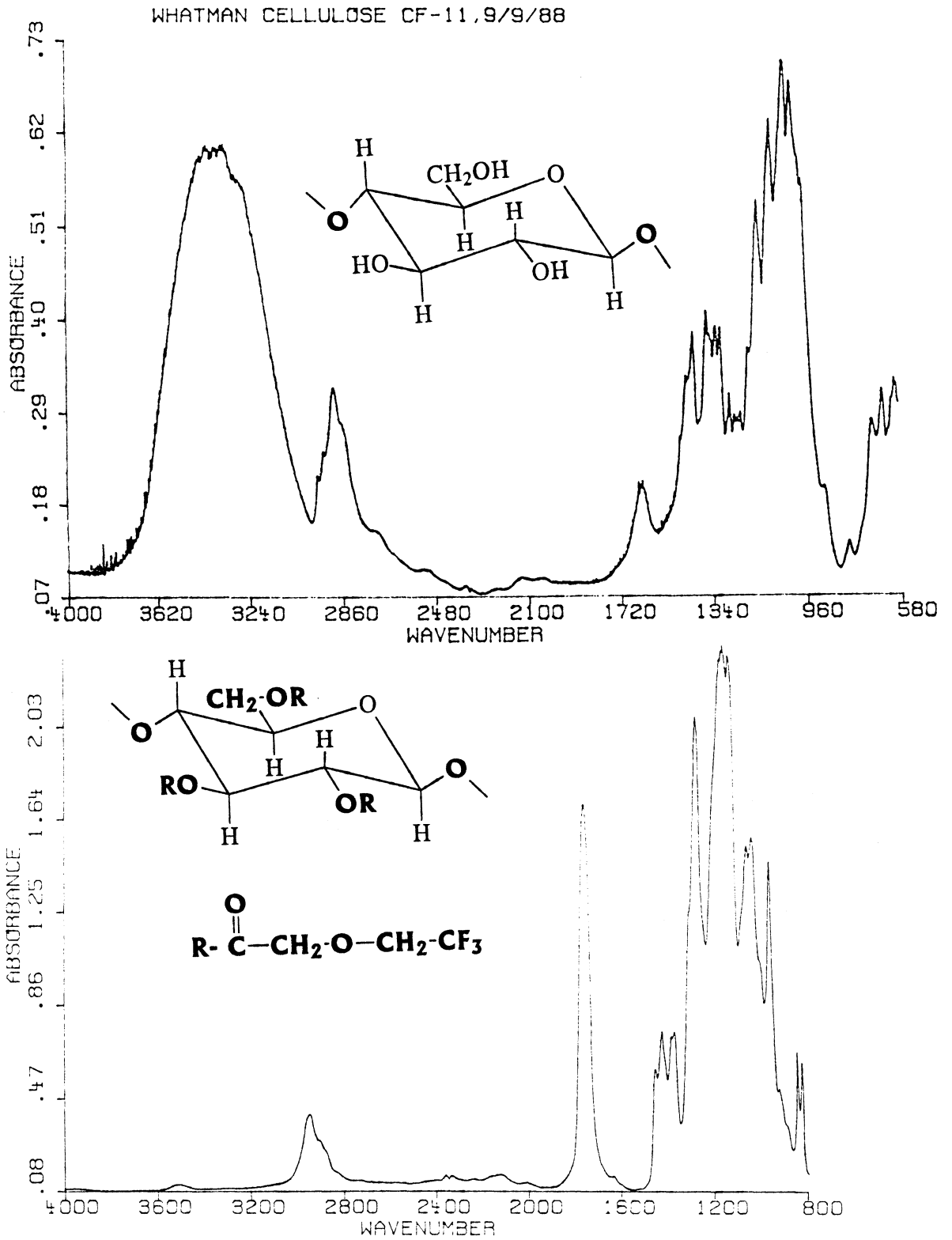

Figure 12. FTIR of pure cellulose (top) and DS 3.0 CT derivative (bottom). The OH response was almost zero.

Table 1 CT solubility. ■ soluble — insoluble DS of zero is pure cellulose.

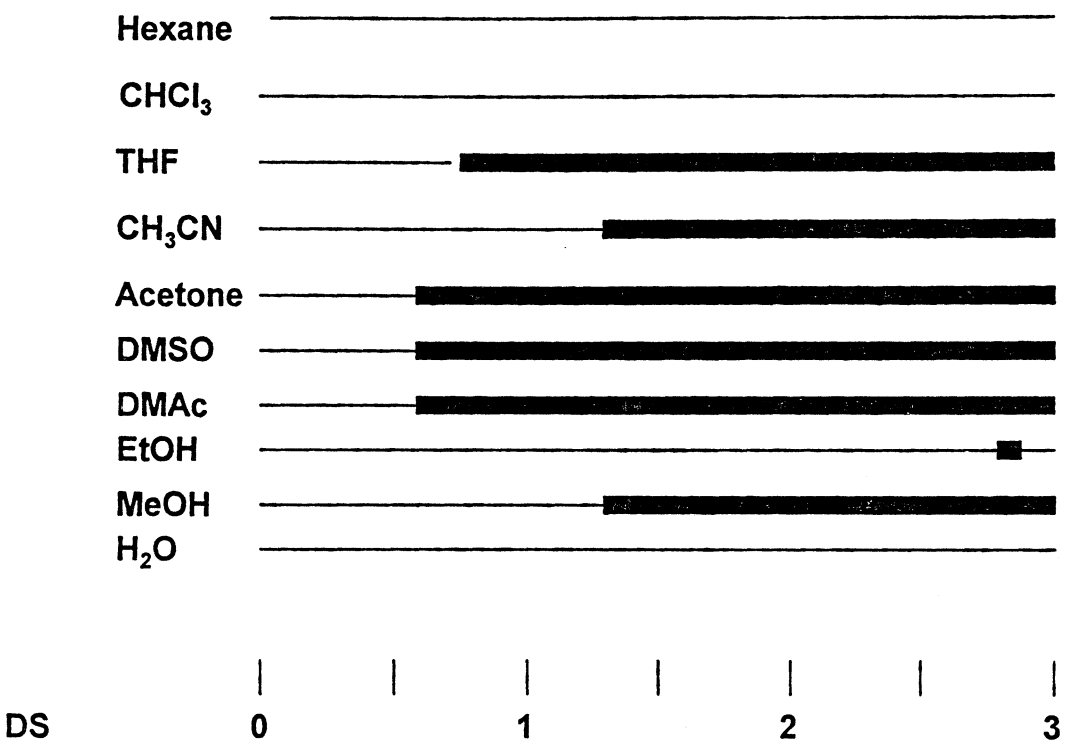

best nonsolvents and they were used in the work-up of CT. DS above 1.3 was even soluble in hot diethyl ether.

Molecular weight analysis revealed significant degradation for three products (Table 2). Elevated reaction temperature seems to be responsible for the degradation during reaction with high stoichiometric ratios. It was also observed that trans-glycosidation resulting in branching may be present because of high DP_w / DP_n ratios. The reaction at 40°C showed no degradation or evidence of side reaction at high stoichiometric ratios, but the products produced with reaction condition of high stoichiometric ratios and at 50°C were significantly degraded.

5.2.3 THERMAL ANALYSIS

Thermal analysis was done by DSC, DMTA and TMA. For this study, the TMA analysis was done in expansion mode only, and all transitions were the onset of expansion which was evidence of a T_g transition (Figure 13). Flow occurred within 15°C after expansion. The T_g and β-transitions were reported using different analysis techniques (Table 3). None of the CT derivatives revealed a clear T_m except fully substituted ones and, they all flowed within 15°C above T_g except for DS 0.6 and below. All the derivatives in powder form discolored at 240 to 250°C, but weight loss occurred above 300°C.

DSC analysis was performed by repeated scans between -50°C and at least

Table 2 CT MOLECULAR WEIGHT ANALYSIS

DS	MW of repeat unit	YIELD	DP_n	DP_w	DP_W/DP_N
0.04[1]	564	90%	128	184	1.4
0.6[1]	568	75%	165	317	1.9
0.7	260	100%	149	450	3.0
1.3	344	100%	9	169	18
1.5	372	70%	102	219	2.2
2.0[2]	442	95%	278	405	1.5
2.5	512	60%	3	213	71
2.8	554	72%	49	213	4
3.0	582	10%	199	469	2.4
3.0	582	62%	6	72	12
3.0	582	66%	101	332	3.3

1) These samples were carbanilated to make them THF soluble. This is why the MW of the repeat unit was so high.
2) This sample was reacted at 40°C. The rest of the samples were reacted at 50°C.

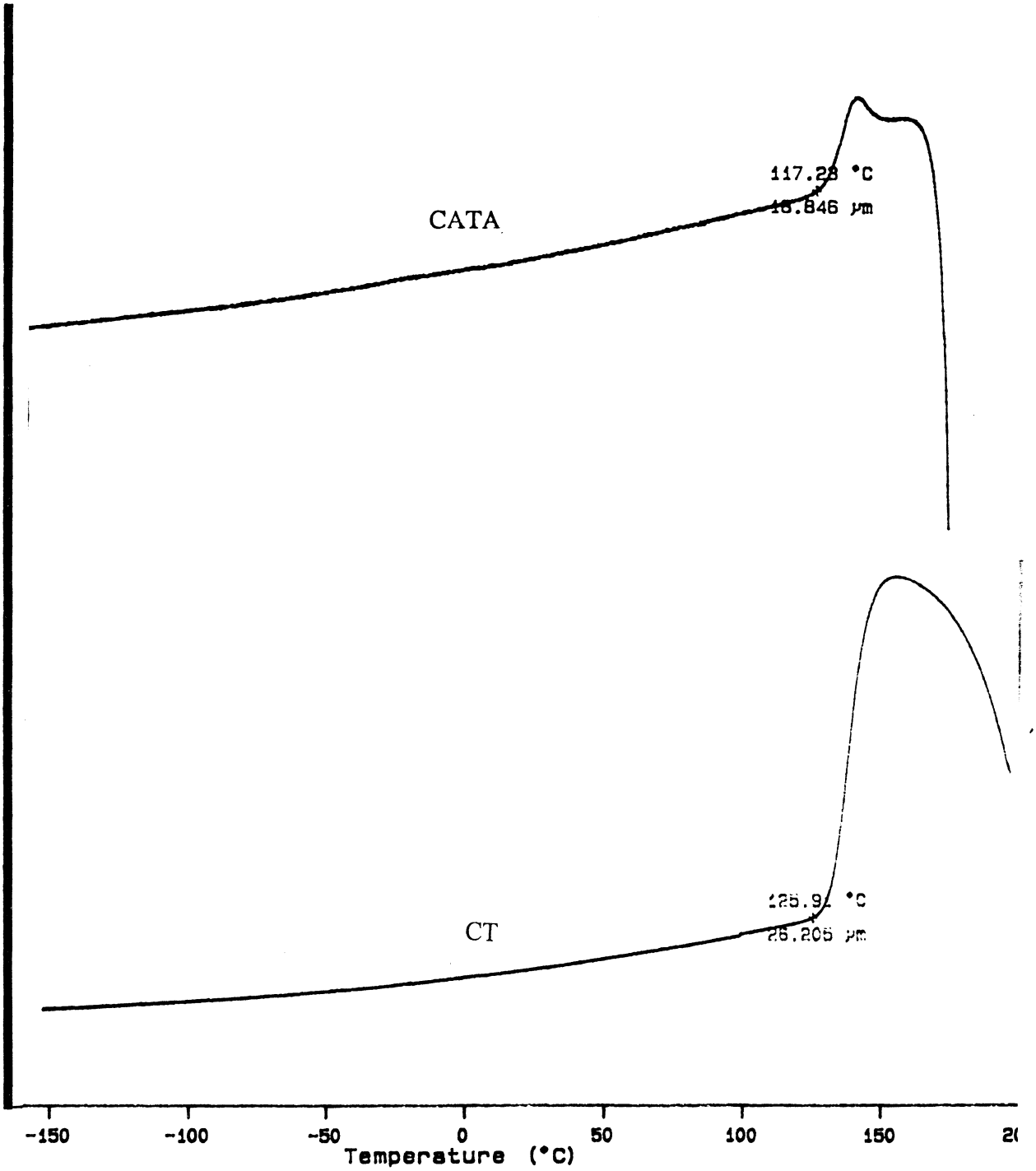

Figure 13. TMA expansion mode data of DS 1.3 CT derivative (bottom) and DS_f 1.7 CATA derivative (top). The onset of a change in expansion was the T_g was recorded. This test was performed with an expansion probe with 1 g/ 10.7 mm^2 of force placed on the sample.

Table 3 CT Thermal transitions

DS	T_g		
	TMA	DMTA	DSC
0.04	218		NS
0.6	162		NS
0.7	144		142
1.3	109	113	125
1.7	126		96
2.0[1]	112	97	65
2.5	87	73	74
2.8[2]	37	49	62
3.0	55		46
3.0[3]	57	34	35

1) Has β-transition at -6°C (DMTA) and 15°C (TMA).

2) Has β-transition at -20°C (TMA) and 5°C (DMTA).

3) This low molecular weight sample revealed a T_m at 95°C on the first heat and a T_m at 90°C after annealing for 4.5 hrs at 70°C; and it occurred over a wide range of 28°C (82-110°C).

5°C below decomposition temperature (Figure 14). This was done for several reasons. The first scan erased all thermal history and releases water from the polymer. To completely remove moisture from cellulose esters has been nearly impossible especially with low substituted derivatives (Glasser et al. pending) (Nakamura et al. 1971) (Cowie, Ranson 1971) (Seymour, Johnson 1978). The moisture creates a broad endotherm between 40-100°C and greatly complicates transitions. The CT derivatives, which apparently have hydrophobic character, showed no broad endotherm after the first scan. The T_g was clearly seen. The second and third scan was done in order to prove reproducibility. The T_g was recorded from the second scan, but the ΔT_g was $< 5°C$ between the second and third scan. The T_gs had a linear relationship with DS (Figure 15). The T_g range from 142°C to 46°C for CT derivatives with DS 0.7 to 3.0 respectively.

A CT sample with a DS 2 was solvent-cast in THF. The solvent was evaporated over a period of seven days. This sample's thermal response was completely different than the cold pressed film scanned by the DSC. The T_g could not be located by DSC (no thermal transition was detected by DSC analysis). Visual analysis showed that the solvent casted film degraded without melt flow or softening (the material chard), but the cold pressed film flowed 30°C before discoloration. A significant amount of crystallinity may have been induced by solvent casting.

Since the TMA analysis was done in expansion mode, the T_g can be easily detected. Since the volume of the polymer increases after the T_g, T_gs were reported

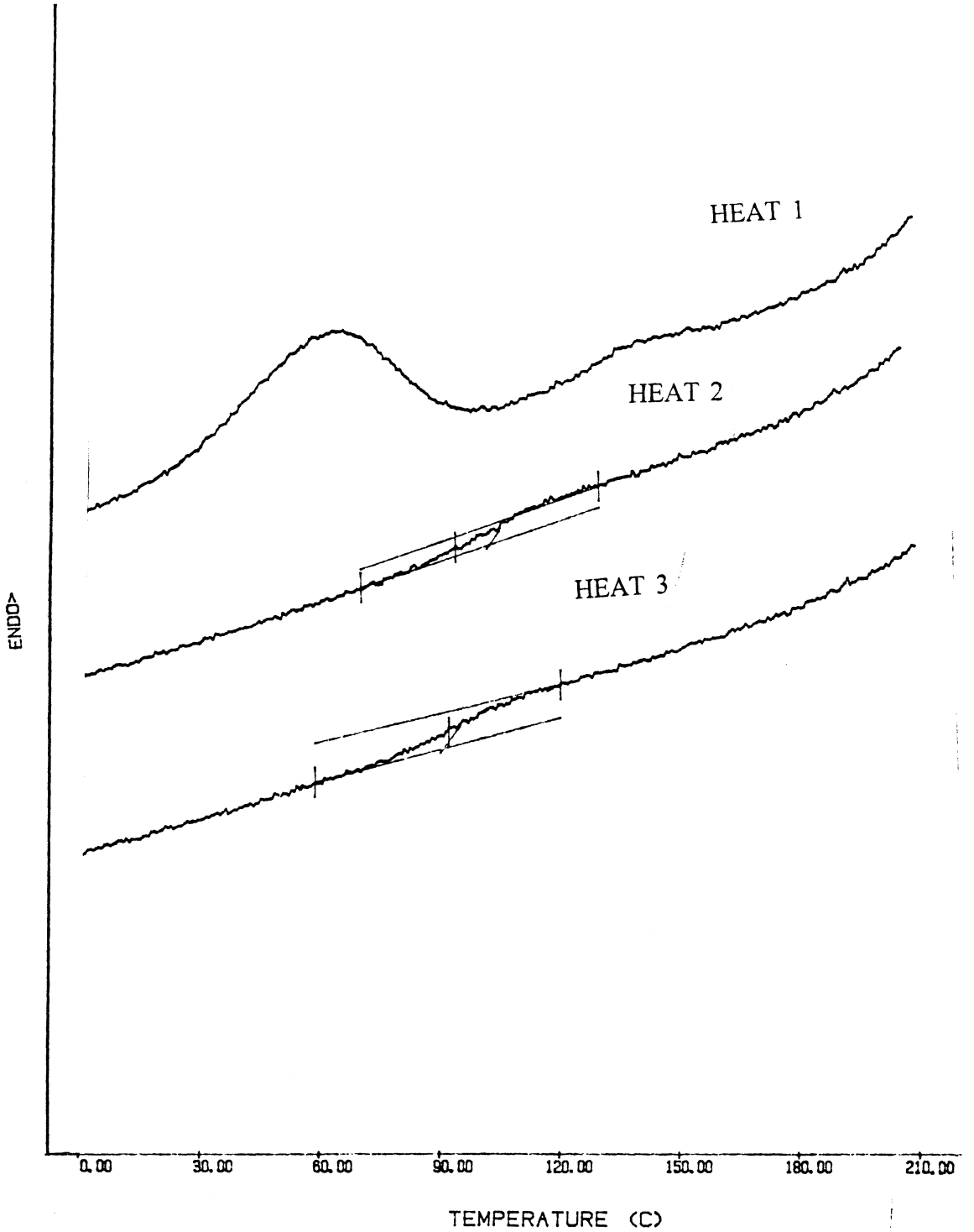

Figure 14. DSC scans of DS 1.5 CT derivative. Each heating scan was performed at 10°C per minute, and each cooling scan was performed at 5°C per minute. The T_g was easily isolated after the first heat.

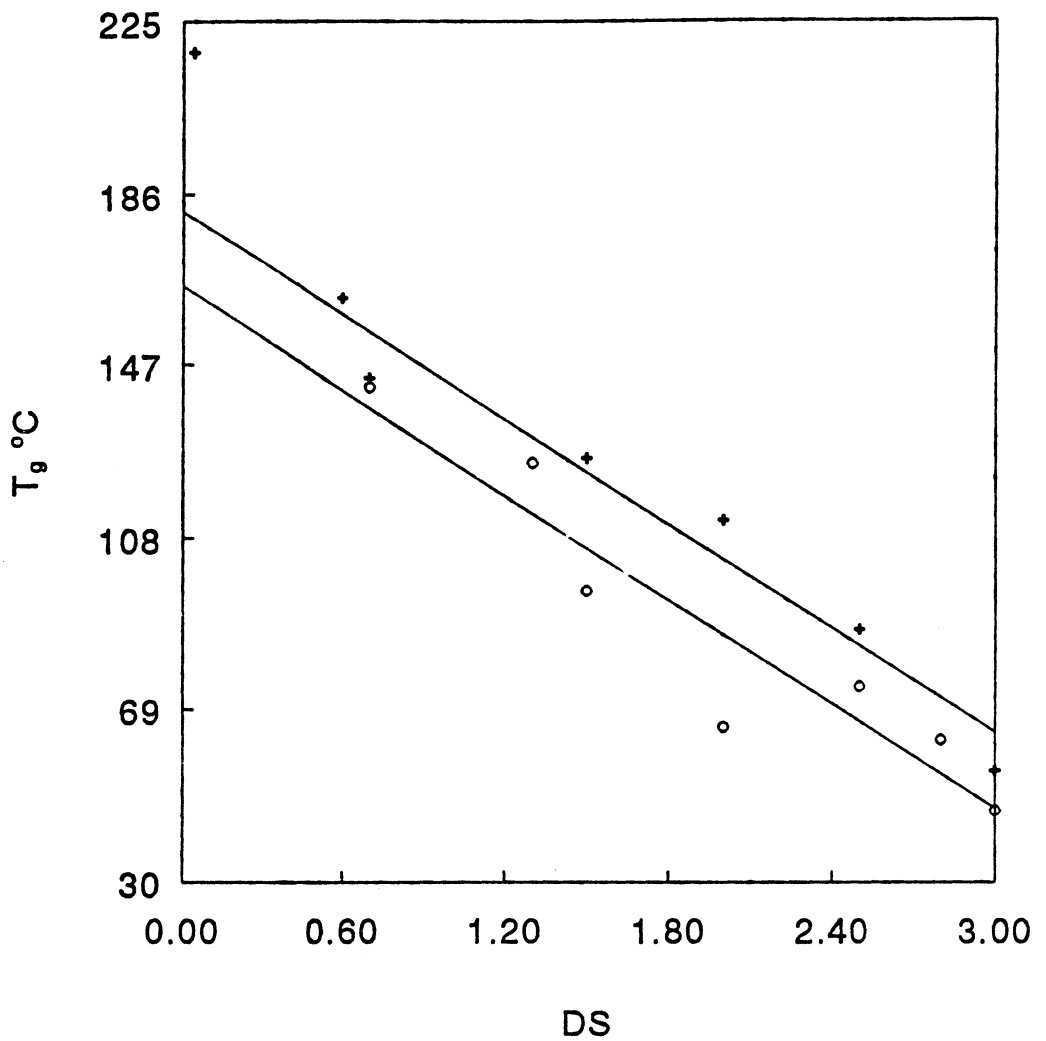

Figure 15. T_g vs DS of CT derivatives from TMA analysis (--+--) and DSC analysis (-O-). A strong linear relationship between DS and T_g was observed for both techniques.

as the onset of expansion (Figure 13). This volume increase after T_g was due to the relaxation and expansion of the amorphous regions of the polymer. Two transitions were seen, β and α. The β- transitions which were seen at low temperature could represent the T_g of the side chain and may be similar to β-transitions seen from the DMTA . The α- transition (T_g of the mainchain) of polymers measured by TMA agreed well with the DSC, but the transitions differed 10-20°C between the two techniques (Figure 15). The main reason the TMA was used was because it can analyze very low substituted samples. This linear relationship between T_g and DS continued for low substituted derivatives also.

The DMTA analysis also showed a strong linear relationship between T_g and DS (Figure 16). The T_g was predictable over a wide range of DS. The β- transition showed a declining trend as DS increased even though it is subtle. Since complete thermal characterization was not possible for aliphatic cellulose esters over this range of DS, comparisons were difficult to make.

5.2.4 CONCLUSION

The synthesis of cellulose trifluoroethoxy acetate could not be achieved by the DCC acid anhydride esterification technique. Apparently, trifluoroethoxy acetic anhydride was not soluble in the DMAc/ LiCl solvent system. The TsCl mixed anhydride esterification technique proved to be highly effective. Reaction conditions of 40°C and 2.0 or above EQ/ OH of free acid produced a highly substituted product

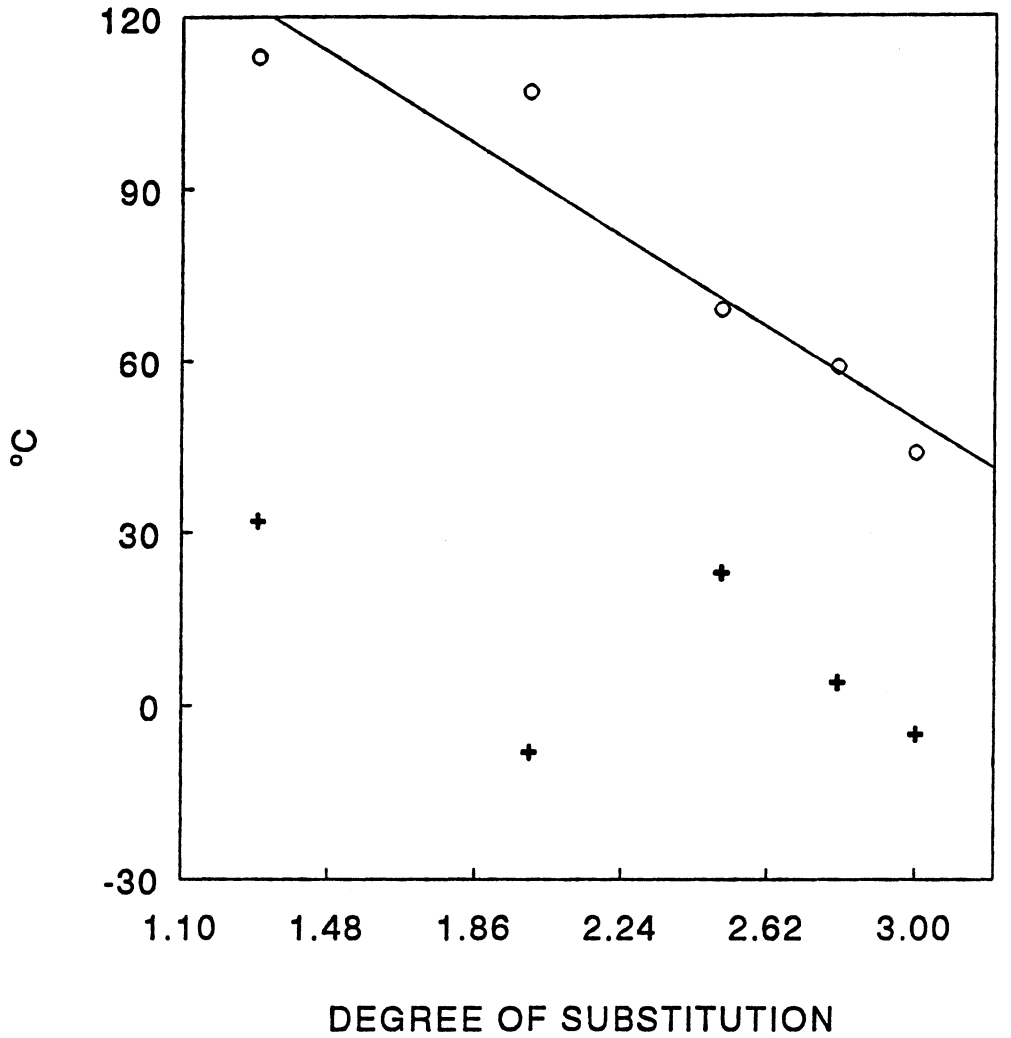

Figure 16. DMTA transitions vs DS of CT derivative(O) α- transition (+) β- transition. The α- transition temperature declined linearly with increasing DS while the β- transitions temperatures stayed about the same.

with little to no degradation to the starting polymer, and elemental analysis revealed little to no presence of side reactions. Since the TsCl esterification showed a strong linear relationship between stoichiometric ratio and DS, the reaction was easy to control and predict.

Chemical characterization was clearly shown with the combination of FTIR, ^{1}H NMR,and ^{19}F NMR. The increase in the ester adsorption and the decrease in the hydroxyl adsorption was seen with increasing DS derivative. ^{1}H NMR spectra revealed sharp peaks representing the hydroxyls on the trifluoroethoxy substituent, but these peaks overlapped the cellulose backbone protons, and this made it impossible to determine DS by ^{1}H NMR. ^{19}F NMR was effective in calculating DS, and fully substituted derivatives revealed three sharp triplets that represent substitution in each of the three hydroxyl groups of the repeat unit.

Thermal analysis reveal a strong linear relationship between DS and T_g. T_g transitions were seen for DS 0.7 to 3.0 from 142°C to 46°C respectively; with a slope of 42°C/ DS unit by DSC analysis. This was the first time T_gs could be seen for this wide of a DS range because aliphatic cellulose esters have moisture transitions that mask the T_gs below DS 2.0. Apparently, the fluoro-ester's hydrophobic nature allows the moisture to leave when the polymer was heated above it's T_g.

Since CT derivatives with DS 0.7 and above all flowed without discoloration, and the DSC analysis showed no T_m transition throughout the entire temperature range (-60 to 250°C); the CT derivative must be mainly amorphous. However, crystallinity

seemed to be induced by solvent casting.

6.0 CELLULOSE ACETATE AND TRIFLUOROETHOXY ACETATE (CATA)

6.1 INTRODUCTION

Mixed esters were made in order to do complete thermal analysis on the CT derivatives (Figure 17). In the literature, mixed esters had to be made in order to isolate the T_g and T_m for cellulose aliphatic esters because derivatives with DS 2.0 and below do not reveal reproducible thermal transitions. This was believed to be due to moisture effects (Glasser et al. pending). Since CT derivatives with free hydroxyls reveal reproducible thermal transitions, the effects of free hydroxyls on T_g can be studied. A comparison can be made between the thermal analysis of the CT and CATA derivatives which may produce a relationship that can be applied to aliphatic cellulose esters with a similar substituent size.

It has also been observed in the literature that acetylated hydroxyl samples reveal T_ms but derivatives with free hydroxyl do not. This has been studied extensively for cellulose hexanoate derivatives (Glasser et al. pending). One conclusion of this study was that the T_m was lowered below the T_d when the free hydroxyls were acetylated. This conclusions seemed reasonable for cellulose hexanoate derivatives with DS 0.7 and below, but hexanoate derivatives with DS 0.8 to above 2.0 flowed without discoloration or any sign of degradation while still revealing no T_m during thermal analysis. This implies that the material was mainly

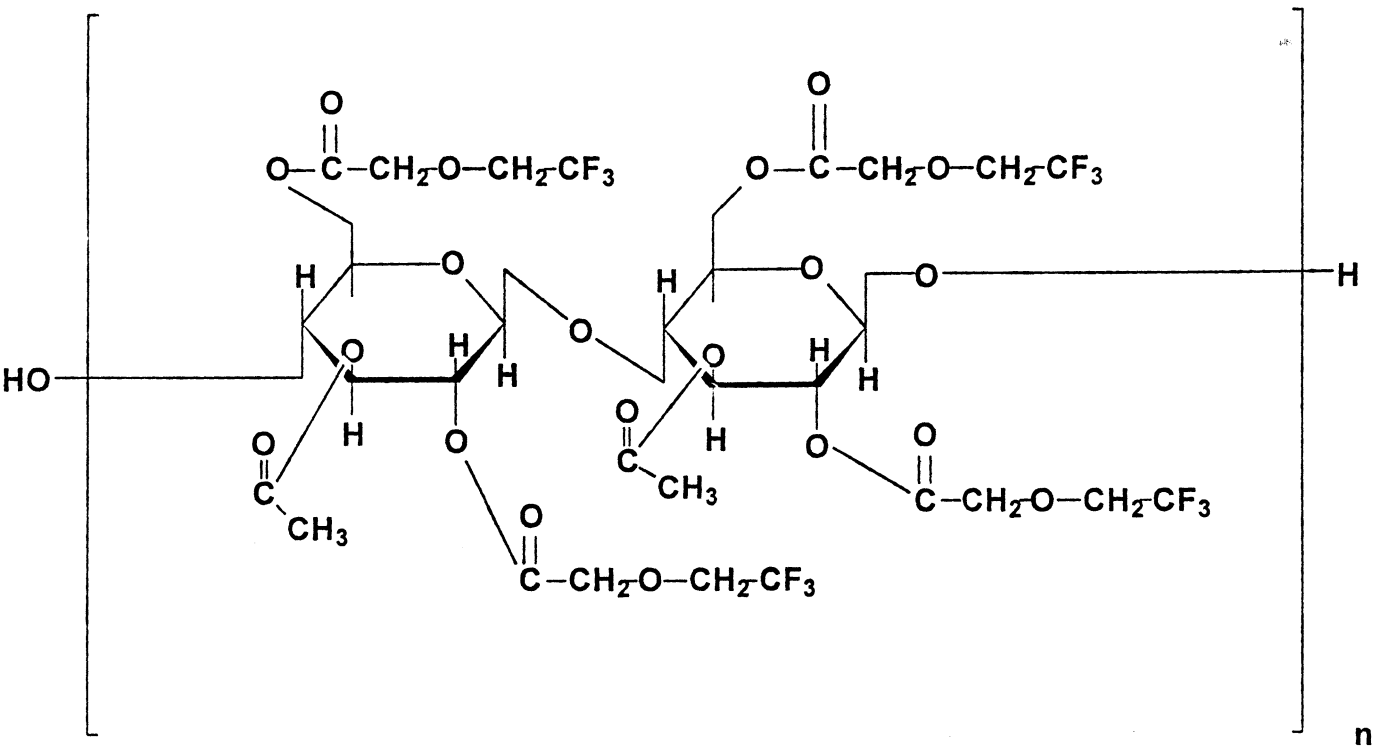

Figure 17. CATA molecular structure. This structure represents a DS_f 2.0 and a DS_a 1.0. All CATA structures were fully substituted.

amorphous. This observation for the hexanoate derivatives was surprising because substitution of free hydroxyl with acetates would seem to reduce crystallinity by eliminating the sites that make pure cellulose highly crystalline. The comparison between CT and CATA derivatives will also be used to examine this trend.

The objectives of this study are to analyze the structure property relationship of CATA derivatives.

6.2 RESULTS AND DISCUSSION

6.2.1 REACTIONS AND REACTIVITY

Most of the mixed esters were created by peracetylation described in section 4.3.3, but mixed esters were also created by a "one pot" reaction using the TsCl esterification method. "Consecutive" and "simultaneous" mixed ester reaction were tested. The consecutive method was performed by first reacting one free acid (trifluoroethoxy acetic acid) for 24 hrs at 35°C then, reacting the second free acid (acetic acid) for another 24 hrs in the same pot. This method wasn't degradative but, fully substituted derivatives were not produced even with a combined stoichiometric ratio of 3 eq. of acid/OH. Simultaneous reaction was performed with both free acids at the same time. The reaction was performed for 24 hrs at 50°C with 1.5 EQ. of acid/OH for each acid. The product was fully substituted, but moderate degradation occurred. This reaction produced a DS_f 2.8/DS_{ac}0.2 derivative which was

surprisingly high, but this reaction was not truly simultaneous. The fluoro-acid was added first with its TsCl and then within two minutes, the time needed to measure out the acetic acid and its TsCl, the acetic acid was added with the comparable amount of TsCl. Apparently, a substantial amount of the reaction occurred within the first few minutes of the reaction because the reaction should favor the acetate substitution.

6.2.2 CHEMICAL ANALYSIS

A typical ^{1}H NMR spectrum shows a multiple peak between 1.9 to 2.1 ppm δ which represents the acetyl methyl protons and a broad multiple peaks between 3.5 to 5.2 ppm δ which represents the seven backbone protons on cellulose (Figure 18). The sharp peaks at 4.0 and 4.3 ppm δ are represent the four protons on the trifluoroethoxy substituent. The acetyl methyl protons are integrated against the rest, and the DS of the trifluoroethoxy acetate is determined separately by ^{19}F NMR after peracetylation.

All FTIR spectra indicated almost no absorption in the hydroxyl region which would indicate a fully substituted cellulose derivative. The ester response had two overlapping carbonyl absorption bands. One from each ester substituent (Figure 19).

The molecular weight of the derivatives increased after peracetylation (Table 4). This is due to the isolation technique since only 70% yield is recovered on average. The low molecular weight material was removed during work-up. Apparently, peracetylation had no significant effect on molecular weight.

Solubility of the CATA's changed significantly from CT for methanol and

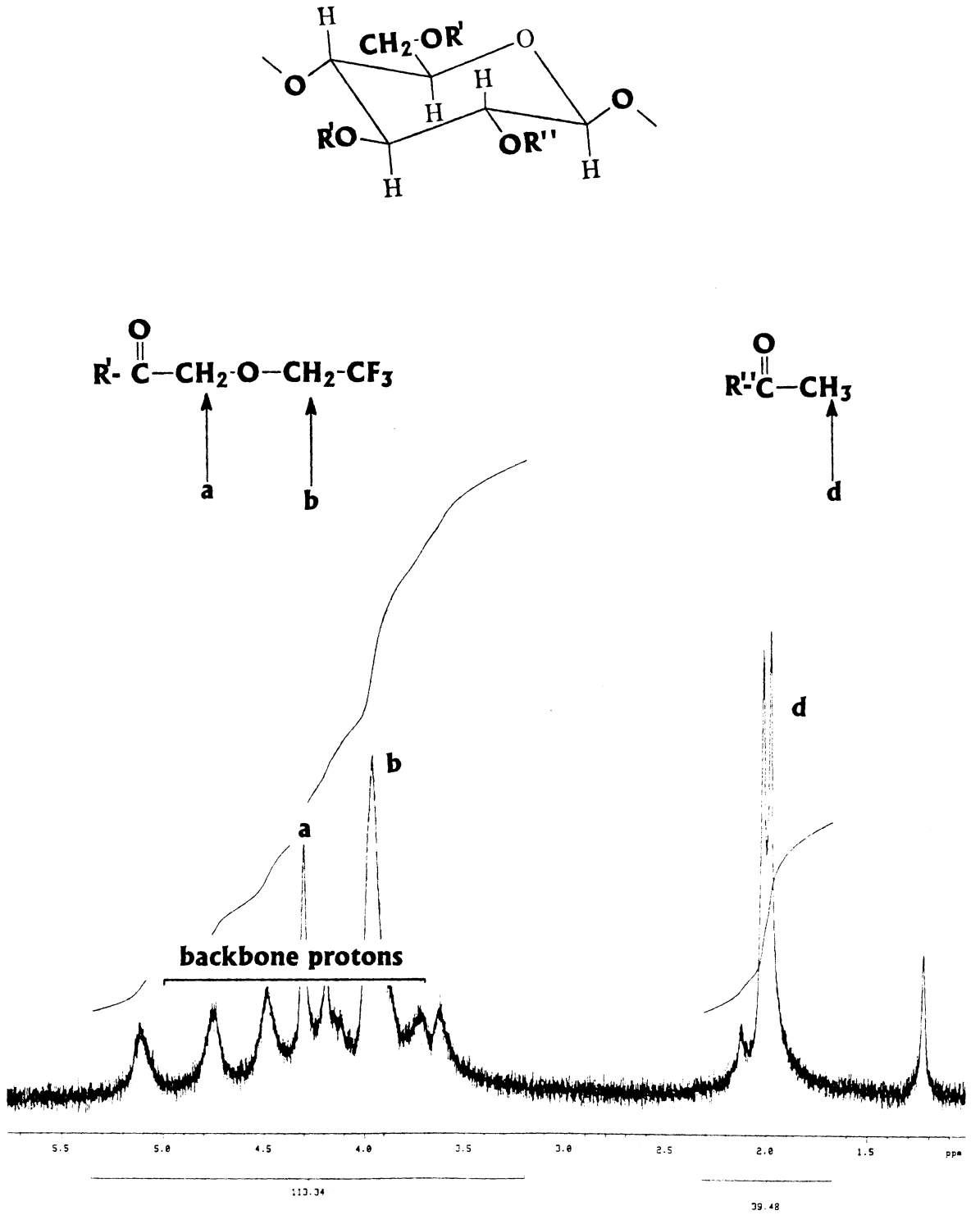

Figure 18. ^{1}H NMR of CATA derivative with DS_f 1.7 and DS_a 1.3. The fluoro substituent's protons overlap with cellulose's backbone protons but they can still be identified. The acetate protons were seen at 2.0 ppm δ.

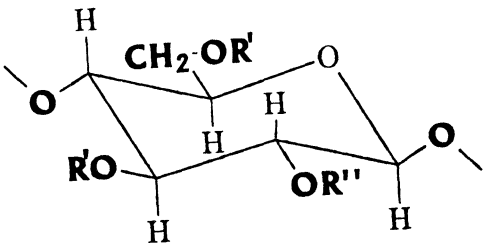

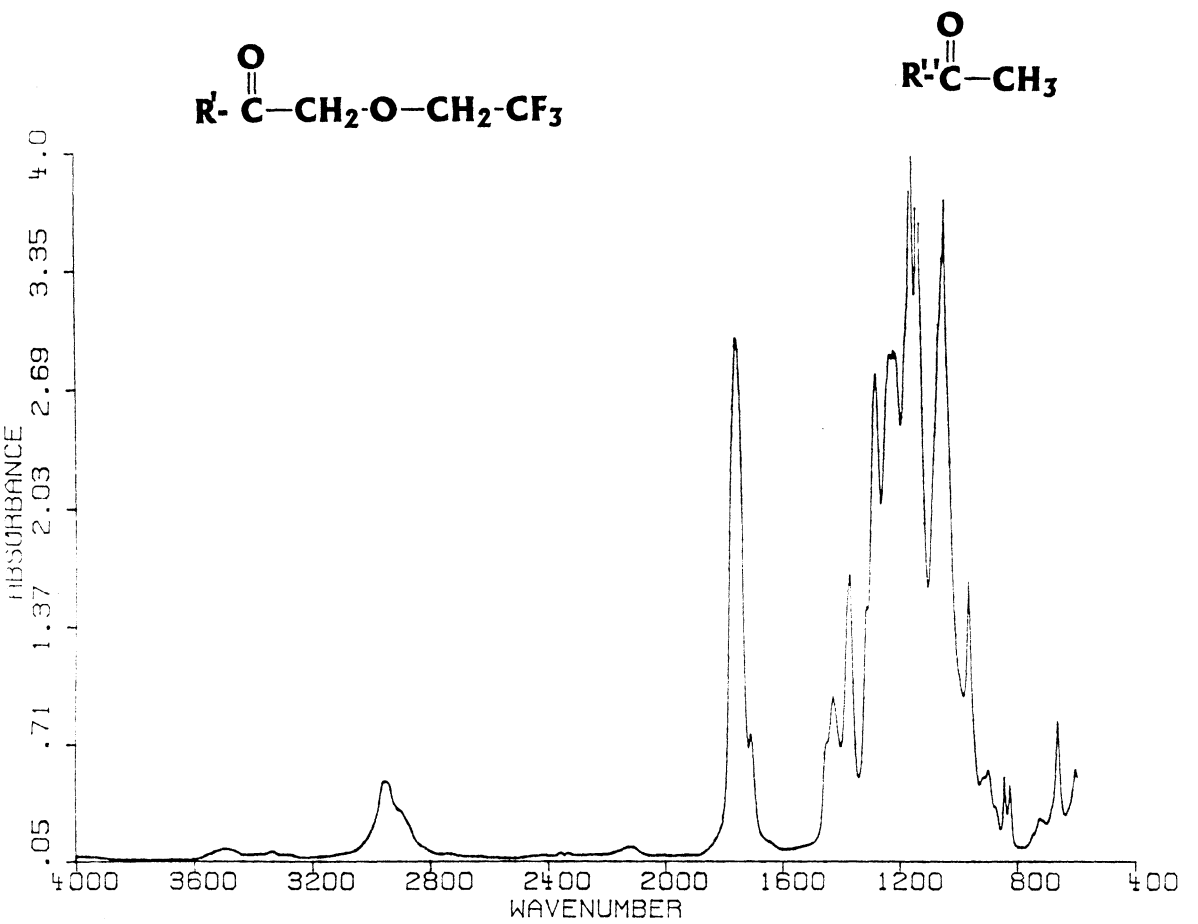

Figure 19. FTIR of CATA derivative DS_f 2.1 and DS_a 0.9. A strong ester response was seen at 1735 wavenumber while also no OH response was detected.

Table 4 Molecular weights before and after peracetylation.

DSF	BEFORE		AFTER	
	DP_n	DP_w	DP_n	DP_w
1.1	9	169	82	227
1.7	102	219	186	292
2.1	278	405	109	264
2.5	3	213	196	315
2.8[1]	-------	--------	59	310

1) Was produced in a simultaneuos esterification reaction by the TsCl method.

chloroform (Table 5). Chloroform solubility is induced for derivatives with DS_f of 1.7 and less; and CATA with DS_f of 1.7 and below are not methanol soluble. The presence of acetylated hydroxyl has a significant effect on solubility.

6.3 THERMAL ANALYSIS

The DSC and TMA analysis were used for thermal characterization of CATA derivatives (Table 6). The DSC samples were analyzed by four consecutive heats on the DSC. The first heat revealed a broad endotherm which represents a T_g, crystallization and T_m (Figure 20). The cooling curves showed an exotherm but, this exotherm had a distinct step function in it. The second heating curve revealed a T_g with no real T_m. The next cooling curve was the same as the first and, the third heating curve was the same as the second. The sample was then annealed at about 10°C above the T_g for at least four hours. The fourth heating curve typically showed two T_m transitions. The T_g s were reported from the second heat and, the T_m were reported from the first and fourth heating curve.

The T_gs, which were separated by only a few degrees from the T_m, can now be isolated by melting all the crystals and not allowing them enough time to reform. This thermal processing produces a mainly amorphous material which only had a T_g. Since the CATA derivative's T_g and T_m are difficult to separate from one another, this allowed a comparison between T_gs with and without free hydroxyls (Figure 21). Surprisingly, the presence of free hydroxyls had no effect on T_g. The T_g had a linear

Table 5 CATA solubility. ■ soluble — insoluble DS_F of zero is cellulose triacetate.

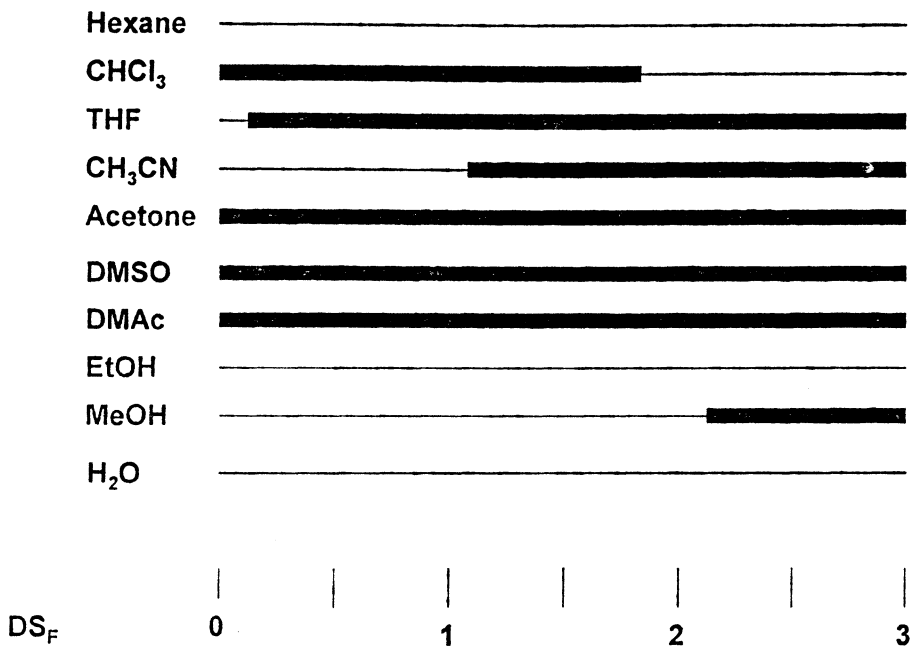

Table 6 CATA Thermal transitions

DS_F	DS_A	T_g°C		T_m°C	
		TMA	DSC	initial	after annealing
1.1	2.0	140	125	150	160 anneal (140)
1.7	1.6	117	99	159	129 anneal (110)
2.1	0.9	98	82	134	131 anneal (90)
2.5	0.2	79	66	131	105 anneal (85)
2.8	0.2	74	66	102	95 anneal (76)

DS_F= DEGREE OF SUBSTITUTION OF FLUOROESTER
DS_A= DEGREE OF SUBSTITUTION OF ACETATE
EQ_F= EQUIVALENCE OF FLUORO-ACID TO CELLULOSE HYDROXYLS
Tm1=Tm seen during first scan.
Tm2=Tm seen in fourth scan after annealing for at least four hours.
The addition on DSF and DSA exceeds three in some cases. This is due to error in NMR intergration. The accuratcy is 0.2 of DS which can cause a 0.4 DS error with the two test.
(number) = The annealing temperture.

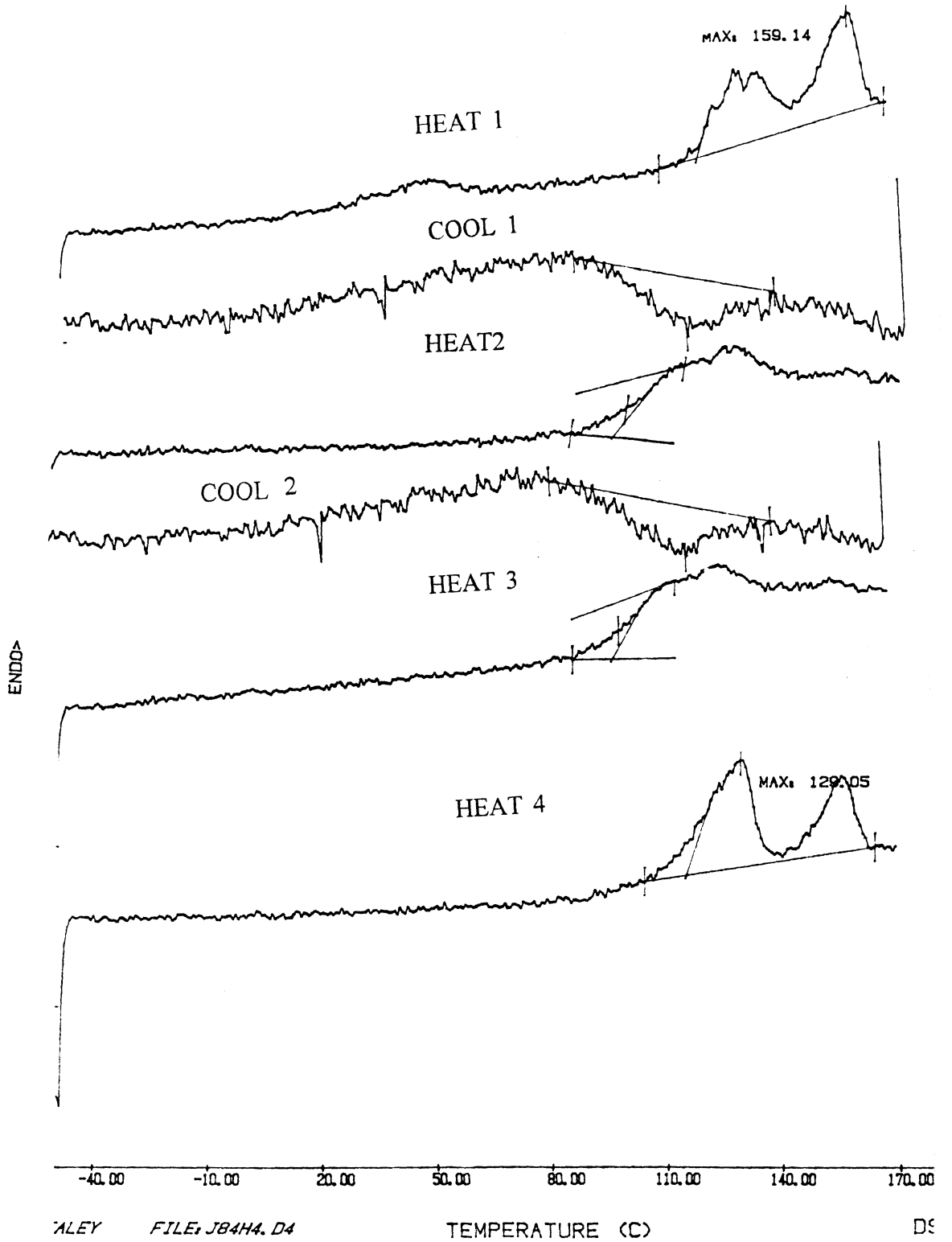

Figure 20. DSC scans of 1.7 DS_F CATA derivative. Each heating scan was performed at 10°C per minute while each cooling scan was performed at 5°C per minute. The fourth heating scan was produced after annealing at 10°C above the T_g for over four hours.

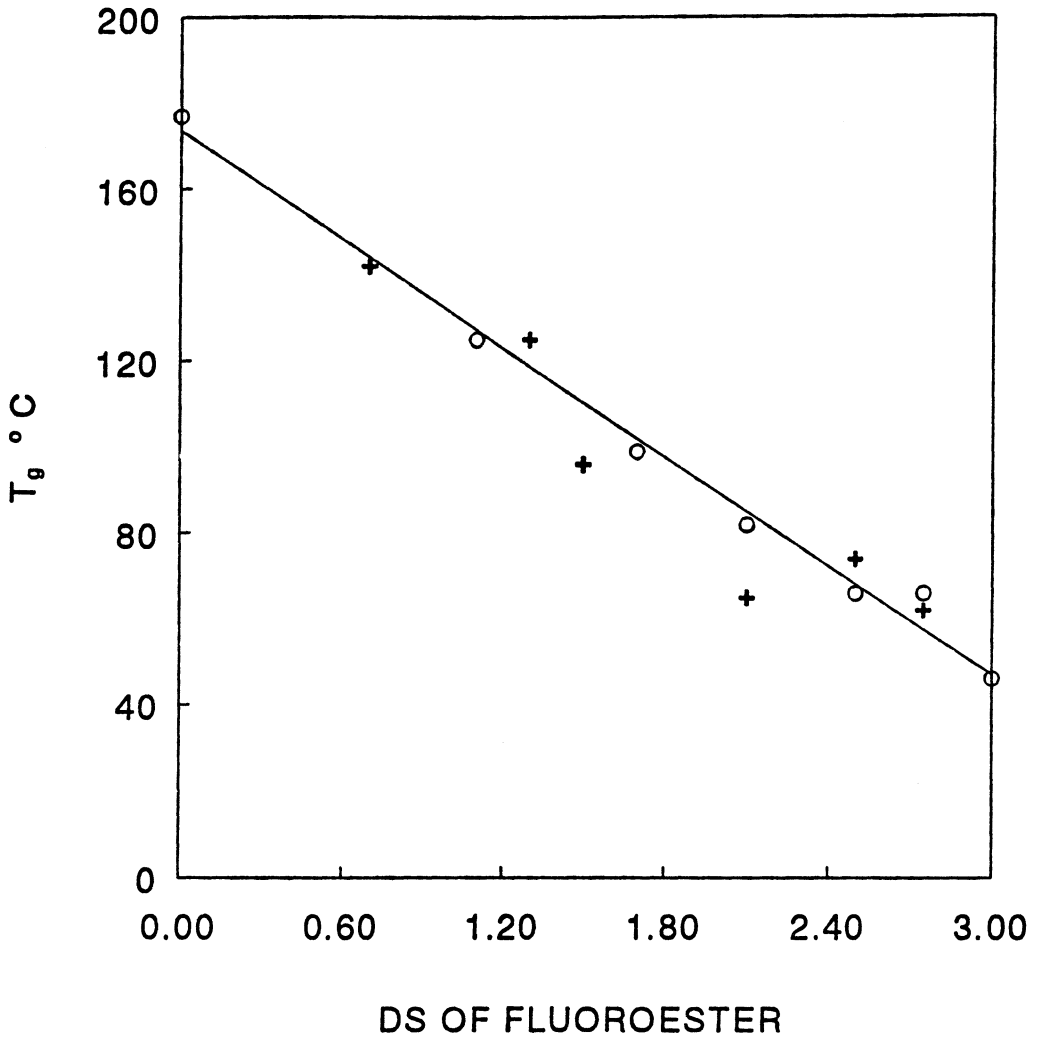

Figure 21. T_g vs DS_F of CATA and CT derivative. CATA (O); CT (+). Almost no difference was detected between the T_gs of the CT and CATA. The strong linear relationship between DS and transition temperature remained.

relationship with DS_f from triacetate to completely substituted CT.

The CATA derivatives have crystalline character while the CT derivatives do not. Acetylating the free hydroxyls apparently induces crystallinity. The T_ms of CATA show a linear relationship with DS_f between 1.0 and 3.0 (Figure 22). This linear relationship was also observed for the hexanoate (C_6) mixed esters. The T_m for CATA can be expressed by the following:

$$T_m = 160 - (36.7) * DS_f \qquad \text{(between } DS_f \text{ of 1 to 3)}$$

The T_g for CATA and CT can be expressed by the following:

$$T_g = 177 - (42.2) * DS_f$$

The $\Delta(T_m-T_g)$ for CATA derivatives ranged from 29 to 49°C revealing a roughly constant difference between T_g and T_m.

6.3 CONCLUSION

A fully substituted mixed ester can be created in a one pot simultaneous reaction using the TsCl esterification method. Since the "simultaneous" reaction wasn't truly simultaneous, the trifluoroethoxy substitution was favored with the same stoichiometric ratios of both acids. Apparently, the esterification reaction with trifluoroethoxy acetic acid was rapid; it occurs within the first few minutes of the TsCl esterification reaction.

The solubility of CT and CATA derivatives changes widely. Fully acetylated derivatives with DS_f 1.7 and below were soluble in chloroform while derivatives with the same amount of fluoro substitution but having free hydroxyls were not. Methanol

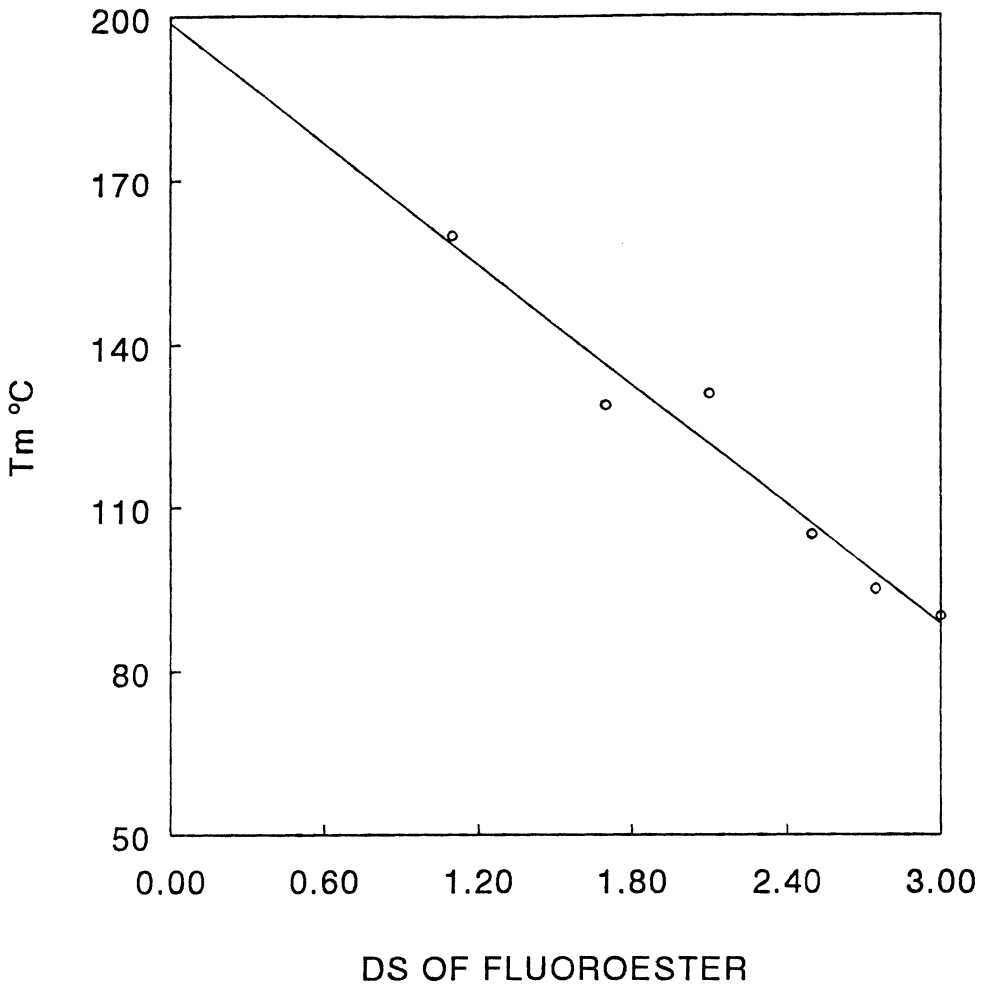

Figure 22. T_m vs DS_F of CATA derivative. A linear relationship between T_m and DS was observed for derivatives with DS_f of 1.1 and greater.

solubility was also lost after acetylating the free hydroxyls.

Thermal analysis revealed T_m transitions for CATA derivatives that were within a few degrees of the T_g. Dual T_m transitions were observed after annealing which could represent dual or multiple crystal morphologies. Surprisingly, the T_g transitions did not change between the CT and CATA derivatives. The acetylation of the free hydroxyls of the CT derivatives seems to induce crystallinity, but the relaxation temperature of the amorphous region does not change.

7.0 CELLULOSE ESTERS WITH LONG CHAIN LINEAR ALIPHATIC ACIDS

7.1 INTRODUCTION

Aliphatic cellulose esters represent a class of commercial biopolymers with excellent fiber and film forming characteristics, and with melt processability. Cellulose esters are conventionally produced by heterogeneous phase reaction chemistries involving acid, anhydride, and acyl chlorides. Although cellulose esters with large fatty and waxy ester substituents have been reported, only those cellulose esters having acyl groups as large as C_4 (butyryl) are commercially available. Cellulose esters with larger substituents are apparently difficult to manufacture using heterogeneous phase reaction chemistry (Ott et al. 1954).

Bulky esters with acids having between C_2 to C_{18} number of carbons in the acyl substituent have been made through heterogeneous reaction techniques. Melting point and T_g have been reported from visual, TMA and thermal dielectric analysis. Malm et al reported from visual analysis melting points decreasing from cellulose triacetate to tricaprylate (C_8). He also reported melting points slightly increasing from C_8 to C_{16} (Malm et al. 1957).

Cellulose valerate (C_5) to palmitate (C_{16}) were characterized by dielectric thermal analysis by Morooka et al. Three types of transitions were detected

(Morooka, et al. 1984). The α- transition, which was the highest temperature second order transition, occurs within a few degrees of the melt. This was attributed to the T_g of the main chain. The β- transition, which was the next transition observed at lower temperature, was considered to represent the motion of the long linear aliphatic side chain. The γ- transition, which is the lowest temperature transition, was due to the molecular relaxation of 2 or 3 carbon groups in the side chain. The α-transition dropped significantly from C_5 to C_6 and then leveled off like the melting points. The β-transition temperature increased from -15°C to 34°C for C_{12} to C_{18}, and the γ-transition temperature stayed about the same at -150°C.

Polyglutamates with side chain lengths of C_{10} to C_{18} have been made by alcoholysis (Daly,Poche 1989) (Sakamoto,Osawa 1987). These structures showed side chain crystallinity with broad T_ms during heating, and broad T_cs in the cooling curve (Schrauwen et al. 1992) (Poche et al. 1990). The T_ms were found to be subjected to shifting over a 100°C range by annealing and several crystal types were observed. Two distinct T_ms were detected for C_{10} to C_{18}, a low temperature- T_m below 20°C, and a high temperature- T_m which was more energetic. Annealing above the lower T_m would induce only the high temperature T_m in the next heat. DMTA analysis for C_{10} to C_{18} detected three transitions that correlated with Morooka's data. The β-transition temperature increased with increasing length of the side chain. The α-transition temperature increased slightly and was always between 0 to 50°C while the γ-transition stayed about the same at -150°C. It is also reported that these

structures have lyotropic and thermotropic liquid crystal phases which were observed by hot stage microscopy (Watanabe,Ono 1987) (Watanabe, Goto 1987). Poly(3-alkyl thiophene) has also shown side chain crystallinity with sidechains of C_{12} and higher (Hsu et al. pending).

The objectives of this study were to test the reactivity of the tosic acid/ carboxylic acid mixed anhydride with cellulose dissolved in DMAc/LiCl(i.e., in homogeneous phase). The main variables to be tested were the acyl substitution size (C_{12} to C_{20}) while keeping the stoichiometric ratio of free acid to hydroxyl group constant. The thermal characterization of the resulting cellulose esters was to be examined in relation to acyl substituent size and distribution.

7.2 REACTIONS AND REACTIVITY

The TsCl esterification system, briefly described in section 5.2.1, was adapted for homogeneous phase chemistry from heterogeneous phase reaction reported by Shimizu. Several changes to this system were made beyond the solvent system. The amount of reagents and the sequence of addition were altered to create a nondegradative reagent system (Figure 23). For example, a DS 2.9 cellulose laurate was produced with a 1 to 1 free acid to TsCl ratio. The heterogeneous system used at least a 2 to 3 TsCl to free acid ratio. Both systems used 2 moles of TsCl per OH of cellulose. The homogeneous system added pyridine to complex with the tosic and HCl acid produced during the reaction. The heterogeneous system did not use any

TO PRODUCE DS 2.9 CELLULOSE LAURATE
HETEROGENEOUS vs HOMOGENEOUS
TsCl esterification method

HETEROGENEOUS	HOMOGENEOUS
STEP 1 cellulose solvent exchanged with water then DMF.	**STEP 1** cellulose solvent exchange with MeOH then DMAc.
STEP 2 add cellulose to DMF.	**STEP 2** add LiCl to DMAc then add cellulose.
STEP 3 add TsCl (2 moles TsCl and 3 moles of free acid per cellulose OH.)	**STEP 3** add pyridine (3 moles per mole of TsCl).
STEP 4 add free acid.	**STEP 4** add free acid (2 moles of free acid and 2 moles of TsCl per cellulose OH.)
STEP 5 react for 20 hrs at 50°C or higher.	**STEP 5** add TsCl and react for 24 hrs at 50°C.
PRODUCT yellow color ? low DP ? chlorination or tosylation	**PRODUCT** white color no loss in DP of the starting polymer no evidence of chlorination or tosylation.

Figure 23. Comparison of Homo and Heterogeneous reaction systems (TsCl).

buffer. The homogeneous system also added the free acid before TsCl while the heterogeneous system added them in reverse order.

The order of addition was critical for the success of the reagent system because the cellulose will be significantly degraded if TsCl was added before the free acid. When this addition was tried the reaction mixture turned black, and no precipitate was formed with water. Reacting TsCl and the free acid in DMAc before addition into the cellulose solution produced the same result. While Shimizu did not report MW data, the reported a "yellow" product and a "red" colored reaction mixture. This implies to the presence of degradation. Both of these conditions were observed for reactions performed at 70°C in homogeneous phase which produced severely degraded products.

The steps of the synthesis caused several phase changes. Once the free acid was added, the solution became cloudy and hard to stir. Within 5 min after the TsCl was added, the solution became completely homogeneous and easy to stir. The solubility of the aliphatic free acid seems to be responsible. The relatively nonpolar waxy free acid was not soluble in the polar DMAc/ LiCl solution, but once the mixed anhydride was formed the waxy acid was soluble. This facilitates the esterification reaction.

A DS of 2.8 to 2.9 was obtained from a reaction with two moles of acid and TsCl per cellulose OH for C_{12},C_{14},C_{18} and C_{20} esters (Figure 24). This result was not expected since decreasing reaction rates with increasing acid length were reported for

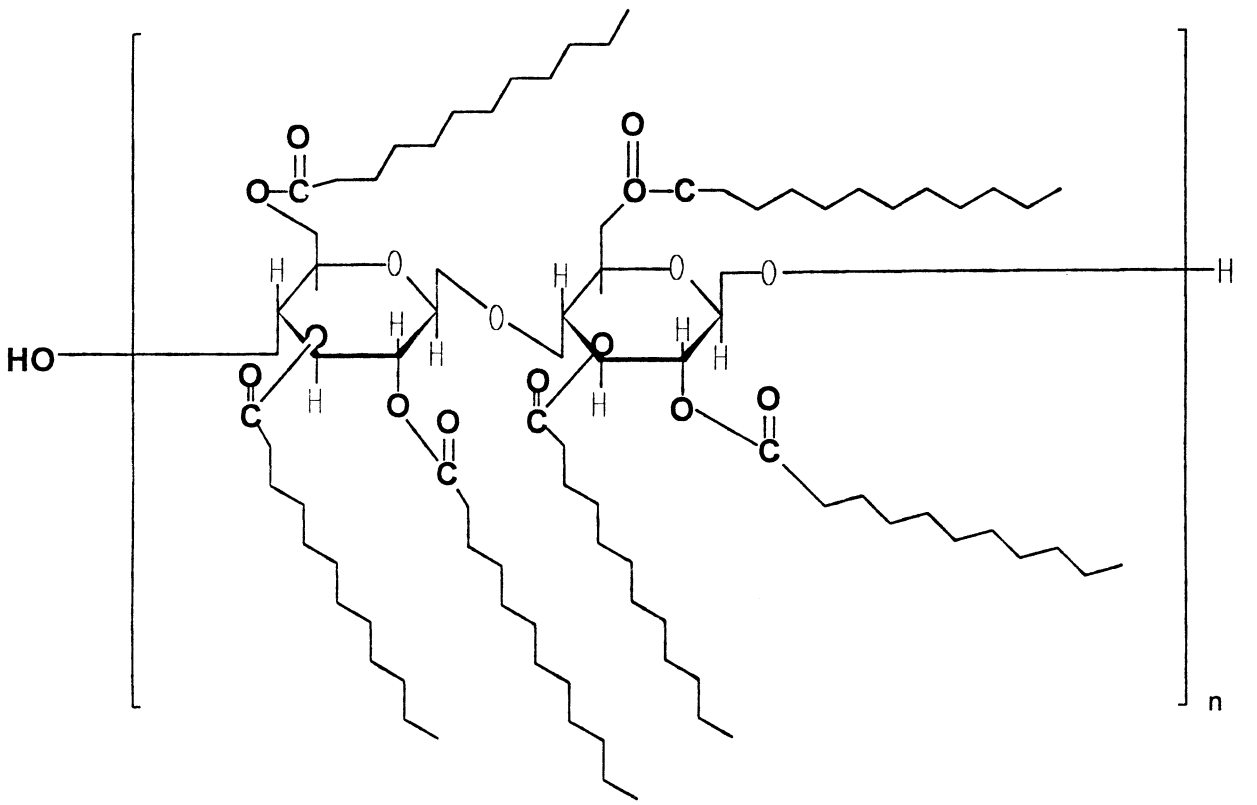

Figure 24. Long linear aliphatic cellulose ester molecular structure. This structure represents a fully substituted cellulose laurate. The structures studied range between the substituent length of C_{12} (laurate) to C_{20} (eicosanate).

other reagent systems. The TsCl reaction method again proves to be a very efficient esterification method.

Since the elemental analysis detected no significant sulfur or chlorine in a highly substituted derivative, the presence of chlorination or tosylation is negligible. Shimizu discussed the possibility of tosylation and suggested that, since tosyl cellulose did not react with free acids in DMF at 50°C for 20 hrs, tosylation did not occur. No elemental analysis was presented. While Shimizu reported reaction conditions of 50 to 80°C and various molar ratios of TsCl and free acid, the homogeneous reagent system had a limited range of successful (nondegradative) reaction conditions.

7.3 RESULTS AND DISCUSSION

7.3.1 CHEMICAL ANALYSIS

The ^{1}H NMR spectra are similar for all the bulky esters (Figure 25). Since trifluoroacetic acid is added to the samples, the water protons are shifted to around 9.0 ppm (δ) and a clear spectra is produced (Buchanan et al. 1987). The multiple broad peaks between 5.3 and 3.3 ppm (δ) represent the seven backbone protons. If the cellulose derivative is fully substituted, these peaks become sharp. This is due to the elimination of all the free hydroxyl protons that can couple with the backbone protons and cause broad, unassignable peaks. Even though these derivatives are

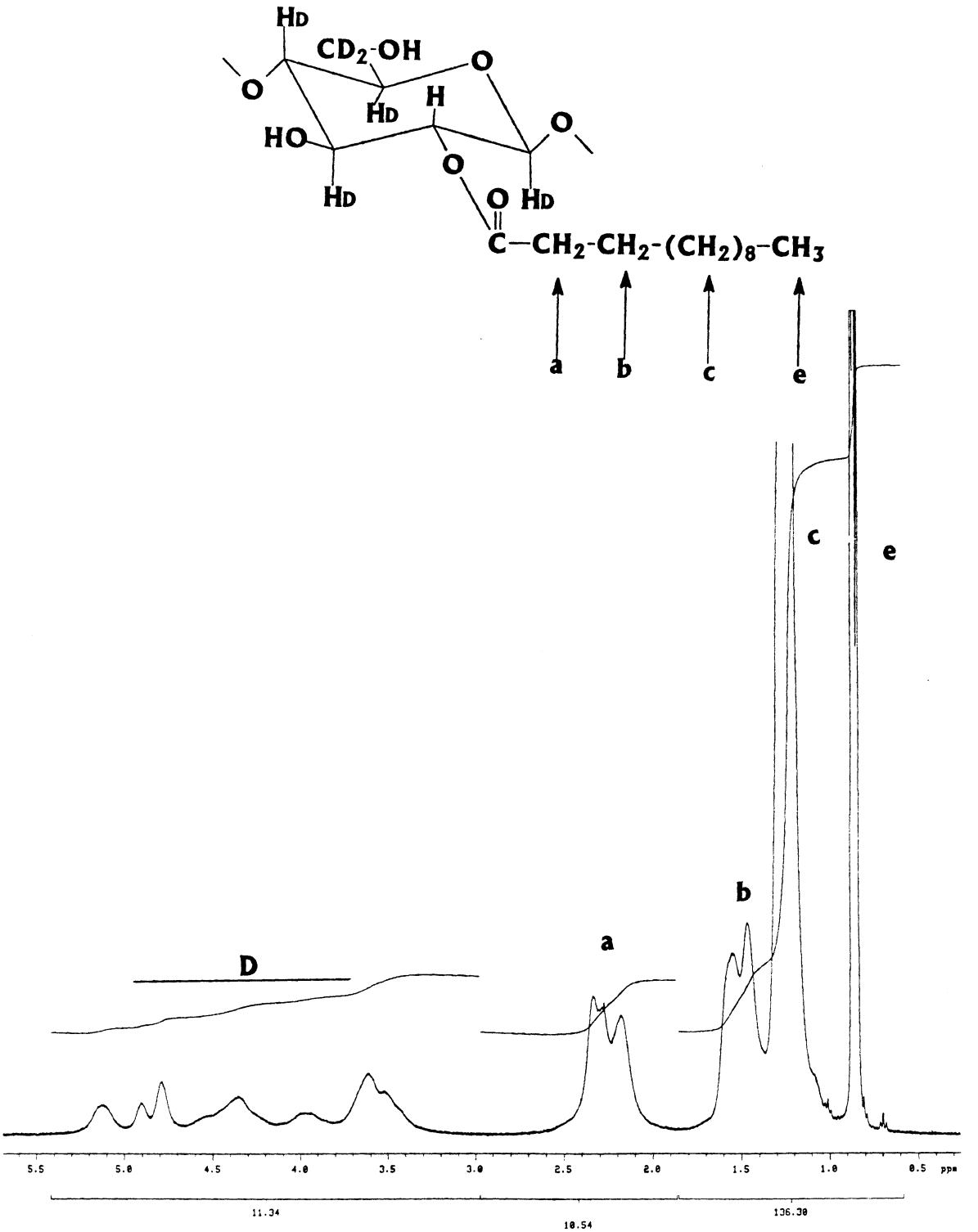

Figure 25. ^{1}H NMR of cellulose laurate DS 2.9. The long linear substituent's protons produced four separate regions of response.

highly substituted, the presence of only a few hydroxyls complicates the spectra and makes the backbone protons unassignable.

The bulky substituent has four regions in the ^1H NMR spectra. The region between 2.5 to 2.0 ppm (δ) represents the resonance of the two protons next to the ester group, and the region between 1.6 to 1.35 ppm (δ) represents the resonance of the protons on the next carbon. These two regions are a triplet that is caused by the substituents having three substitution positions on the anhydroglucose repeat unit. The rest of the protons are represented by the resonance between 1.3 to 1.1 ppm (δ) except for the three methyl protons. These form a triplet at 0.85 ppm (δ).

The DS is calculated by comparing the integration of the backbone protons to the substituent protons. It is also calculated by GC analysis. The GC DS analysis corresponded closely with the NMR data for C_{12} to C_{20} highly substituted derivatives. However the C_{18} ester is apparently 50% C_{18} and 50% C_{17} ester.

FTIR spectra showed minimal absorption from the hydroxyl region for the highly substituted C_{12} to C_{20} esters (Figure 26). They also showed a strong, sharp ester absorption at 1735 cm^{-1}.

The molecular weight analysis indicates no degradation for the bulky esters. The only sample that shows slight degradation is the C_{20} ester (Table 7). This is due to the reaction temperature being raised to 60°C for 15 min. This is done in order to soften the free acid so stirring could continue. The bulky esters seem to be more resistant to degradation than the CT esters. This could be due to the bulky esters

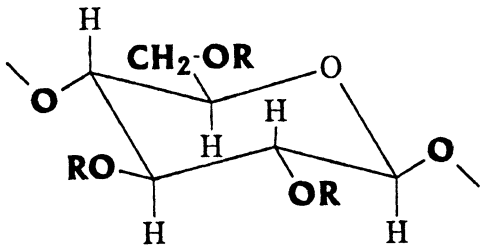

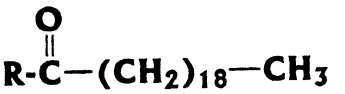

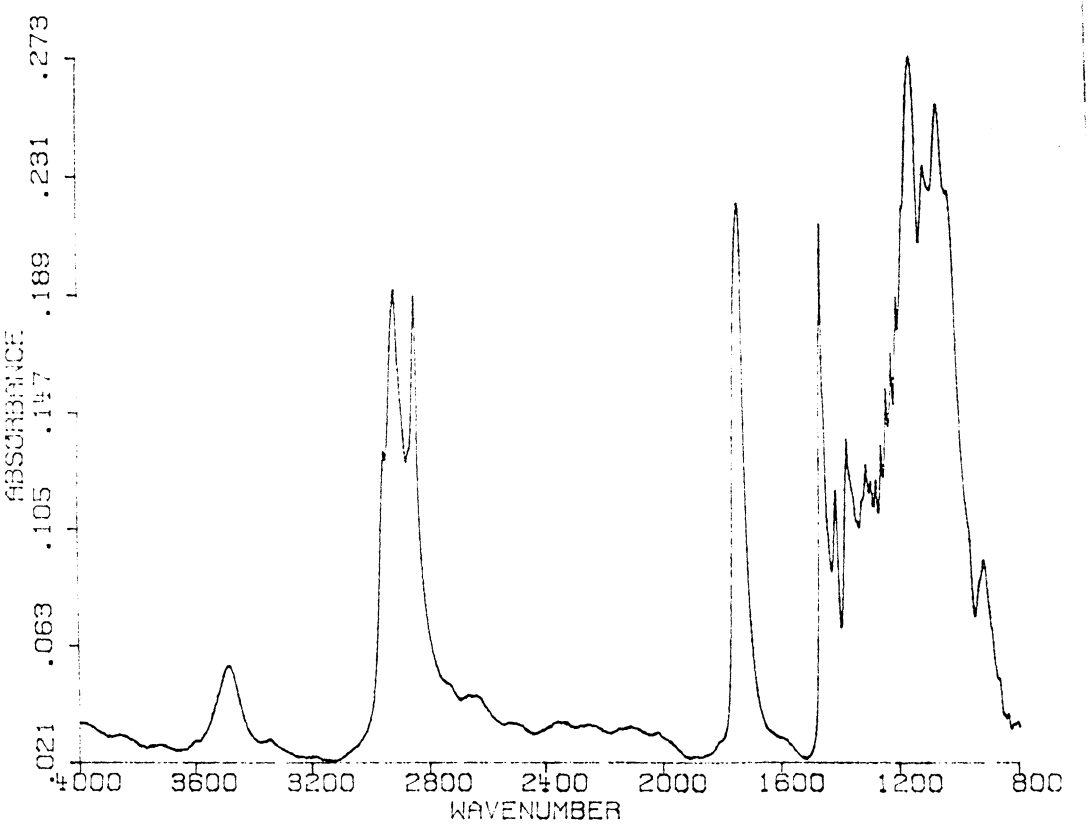

Figure 26. FTIR of DS 2.9 C_{20} ester. The strong ester response was seen with a small OH response.

Table 7 Molecular weight analysis for the bulky esters.

CHAIN LENGTH	DS (by ^{1}H NMR)	DP_n	DP_w
C_{12}	2.9	240	364
C_{12}	2.5	185	274
C_{12}	2.1	212	288
C_{12}	1.4	164	308
C_{12}	1.3	300	708
C_{12}	0.6	245	446
C_{14}	2.8	216	360
C_{18}	2.8	169	369
C_{20}	2.9	132	274

All reactions were preformed at 50°C.

forming a configuration that makes the glycosidic bond resistant to acid attack. The acidity of the reactant acid could also be a factor since the free acid is stirred with the cellulose for 5 min before the TsCl is added.

7.3.2 THERMAL ANALYSIS

The DMTA, DSC and TMA analysis results are used to characterize the thermal properties of the bulky esters (Table 8). The DMTA of C_{12} to C_{20} esters have T_g's of the main chain that are slightly declining, but the β- transitions, or the T_g's of the side chain, increase (Figure 27). Morooka reported the same trend with dielectric analysis. The C_{20} ester, which is not reported in the literature, shows no β-transition. It appears that the T_g of the side chain and main chain come together at this chain length or the crystallinity becomes so high that the T_g's disappear.

The DSC analysis is done by repetitive heating and cooling scans described in section 6.3. Two main trends are observed. C_{12} and C_{14} esters have main and side chain T_m's with a T_g transition temperature of the main chain between the two endothermic first order transition (Figure 28). No sidechain T_g is detected, and this could be due to the limited temperature range of the instrument used because the sidechain T_m began within a few degrees of the -50°C starting scan temperature of the DSC. C_{18} and C_{20} have only one broad endothermic transition, and no T_g is observed. The second trend is the drop in T_m between C_{14} and C_{18} esters. While the T_m of C_{14} seems excessively high, this could be partly due to slightly lower DS than the other

Table 8 Thermal transitions of the bulky esters

CHAIN LENGTH	DS	β-Transition (°C)		T_g (°C)			T_m (°C)
		TMA	DMTA	TMA	DMTA	DSC	DSC
C_{12}	2.9	-55	-54	103	50	87	107 Δ 98 - 135
C_{12}	2.5	-48	-52	124	56	145	NS
C_{12}	2.1	-45	-45	150	76	175	200 Δ177-241
C_{12}	1.4	-53	----	188	-------	NS	NS
C_{12}	1.3	-49	-48	158	74	180	222 Δ 194-239
C_{12}	0.6	-58	-----	200	-------	NS	NS
C_{14}	2.8	-54	-59	45	35	113	225 Δ200-230
C_{18}	2.8	-75	-28	36	20	NS	34 Δ43 -111
C_{20}	2.9	NS	NS	-5	25	NS	53 Δ2-98

Δ = The range of the T_m. The temperature where the endotherm broke away from the baseline to the temperature the endotherm returned to the baseline.

NS- not seen.

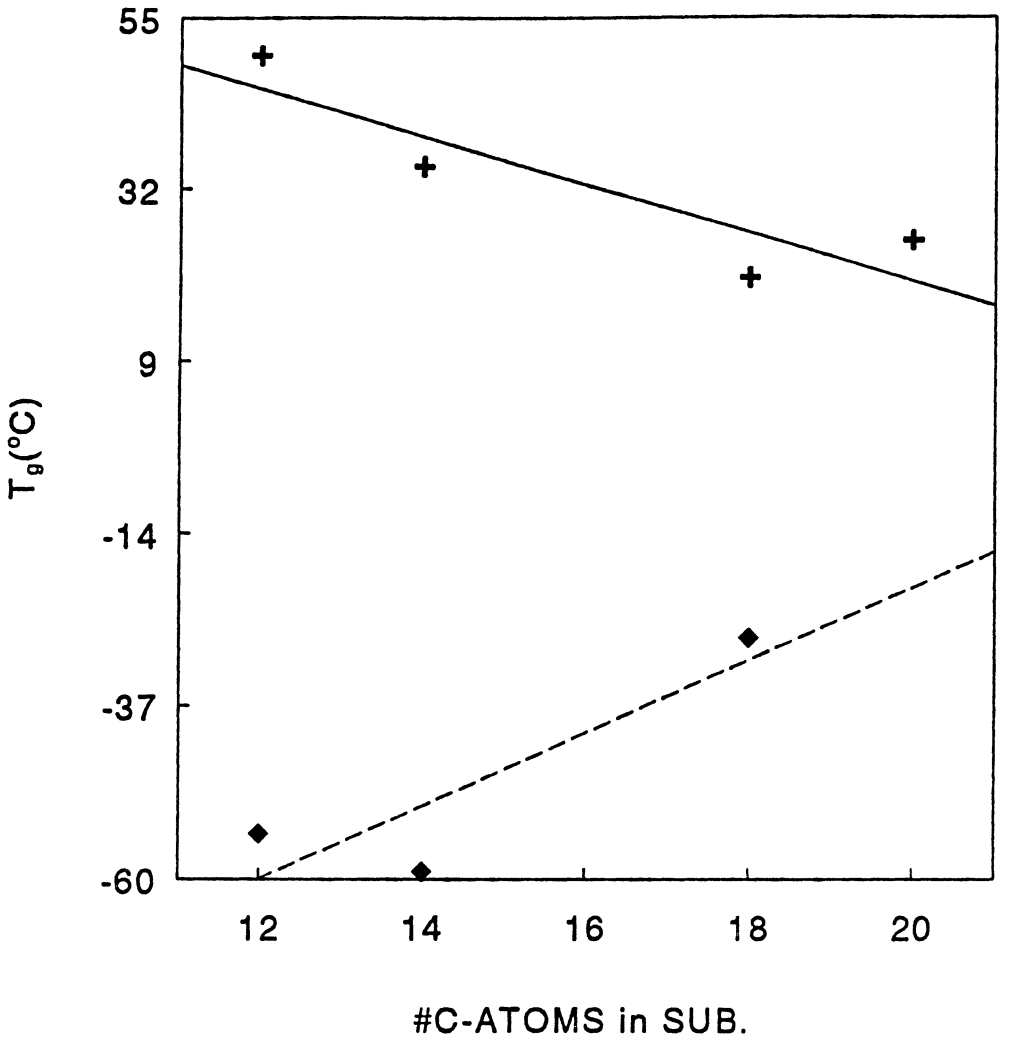

Figure 27. DMTA thermal transition temperatures of Bulky esters α- transitions (+); β-transitions (◆). The long linear aliphatic cellulose ester T_gs decline with increasing substituent length, but the β- transitions increases and seems to merge at C_{20}.

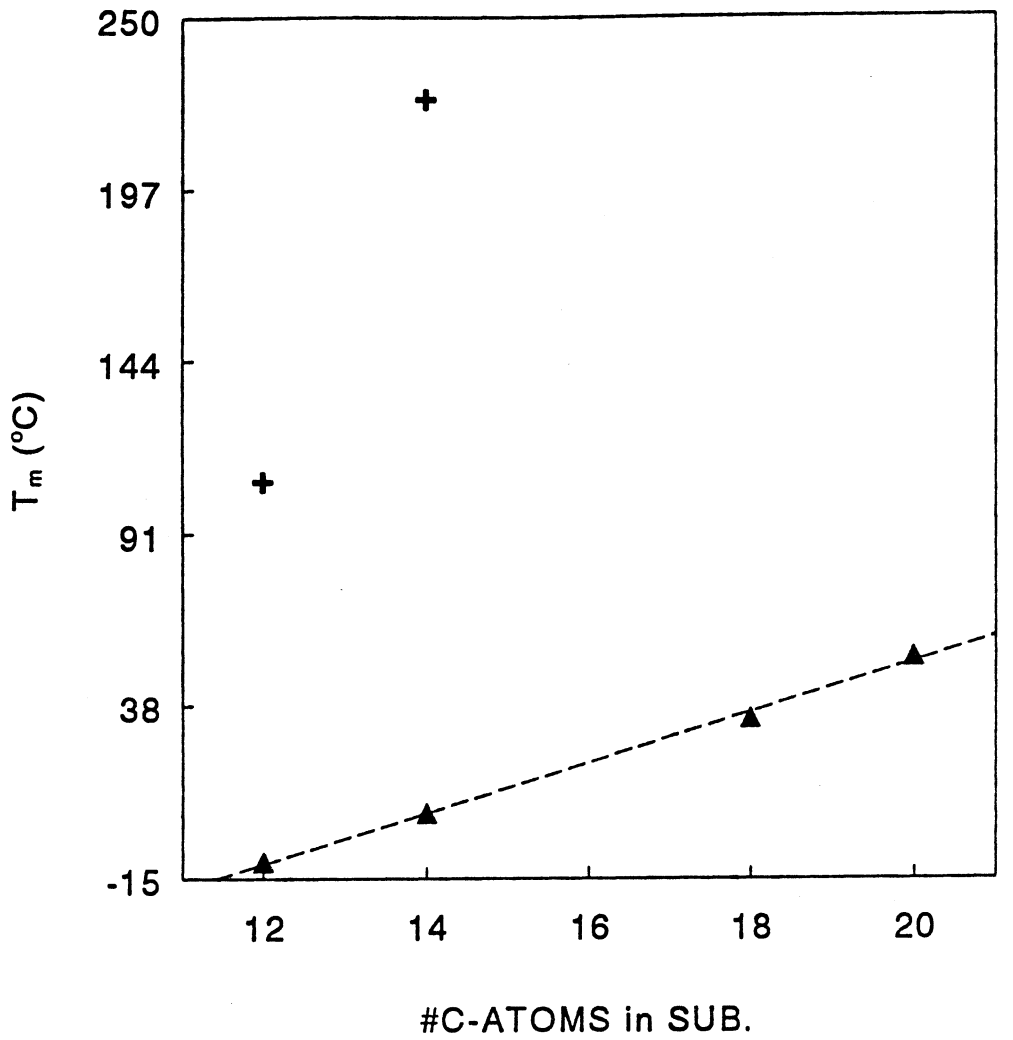

Figure 28. T_m vs substituent #C length of bulky esters. Main chain T_m (+); side chain T_m (♦). Assuming that the T_ms of C_{18} and C_{20} were from side chain melting only, the side chain T_m increases linearly with side chain length.

derivatives, the decrease in T_m is significant. The T_m of the C_{20} ester enforces this trend. If the assumption that the T_ms for C_{18} and C_{20} are due to side chain melting only, a linear relationship is observed between T_m of the side chain and number of carbons in the substituent. This assumption seems reasonable since only side chain crystallinity is observed for the polyglutamates with a side chain length of C_{18} (Daly et al. 1989)(Watanabe,Ono 1987). The T_m's become broader as the side chain length increases, and after annealing two slightly separated endotherms are observed. The breadth of the endotherm could be due to a wide range of crystal sizes and the presence of more than one crystal type. The presence of more than one crystal type and the increasing breadth and complexity of the endothermic transitions is also reported for the bulky glutamates (Daly,Poche 1989).

To eliminate the suspicion that the low temperature T_m for C_{12} and C_{14} might be due to moisture, several experiments were performed. First, the material is scanned numerous times above the T_m of the product (200 to 250°C) without the disappearance of this transition. Then, both esters were peracetylated to eliminate the free hydroxyls. After thorough drying in the vacuum oven, the acetylated samples were tested (Figure 29). While the main chain T_m decreased (from 225°C to 83°C) for the acetylated C_{14}, the side chain T_m is relatively unaffected (Table 8). C_{12} DS 2.9 ester's transitions stayed the same (compare Tables 8 and 9) . The samples were annealed at the peak crystallization temperatures calculated from the cooling

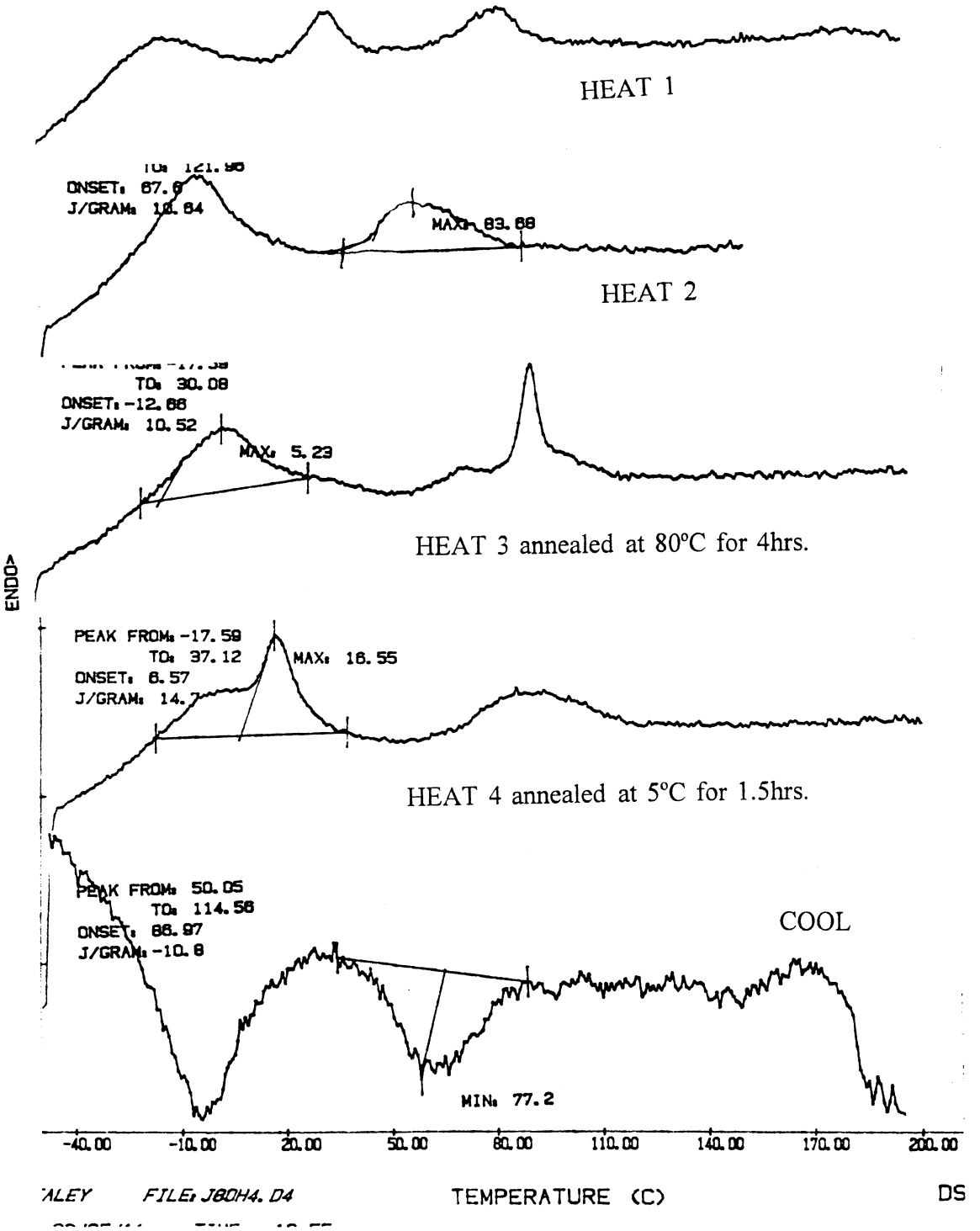

Figure 29. DSC scans of C_{14} mixed ester DS_M 2.8. The side chain and main chain crystals could be annealed separately.

Table 9 Thermal transitions for cellulose acetate laurate (C_{12}).

DS LAURATE	DS ACETATE	FLOW°C	T_m°C[1]
		TMA	DSC 2nd HEAT
0.6	2.5	112	165 range(27)
1.3	1.5	141	161 range(18)
1.4	1.0	140	153 range(18)
2.1	0.8	113	142 range(24)
2.5	0.4	128	125 range(34)
2.9	0.2	122	97 range(64)

1) T_m's were recorded from second heat after quench-cooling at 200°C/min by the DSC.

curve. The T_ms responded by becoming sharper. The annealing for one crystal type seemed to decrease the intensity of the other. These experiments strongly suggest that the low temperature T_m transition was not due to moisture effects.

The drop in C_{14}'s T_m from 225°C to 84°C for unacetylated and acetylated samples were surprising. Since the DSC of the unacetylated sample was rerun producing the same T_m and the DS calculations from NMR and GC were 2.8 and 2.7 respectively, The slightly lower DS could be the cause for elevating the T_m a few degrees, but this seems to be an unlikely cause for the observed trend. While examing the tremal transitions of a range of C_{14} substituted derivatives was beyond the scope of this study, the presence of free hydroxyls seems to have a significant effect on the T_m but a smaller effect on the T_g.

The TMA analysis in penetration mode showed a linear relationship between onset of flow and side chain length (Figure 30). The TMA in expansion mode for C_{12} to C_{18} expanded at low temperatures (-55 to -75°C) which would represent the T_g of the side chain, but C_{20} did not (Figure 31). This supports the DMTA data which was also devoid of a T_g of the sidechain transition for C_{20}. One explanation for this trend was that there were differences in the degree of crystallinity. C_{20} ester derivative was so highly crystalline that the T_g's disappeared. X-Ray analysis is needed to verify this.

Since the DSC data suggest a step function or sudden drop in the relationship between T_m and side chain length, viscosity could be the cause of the observed linear

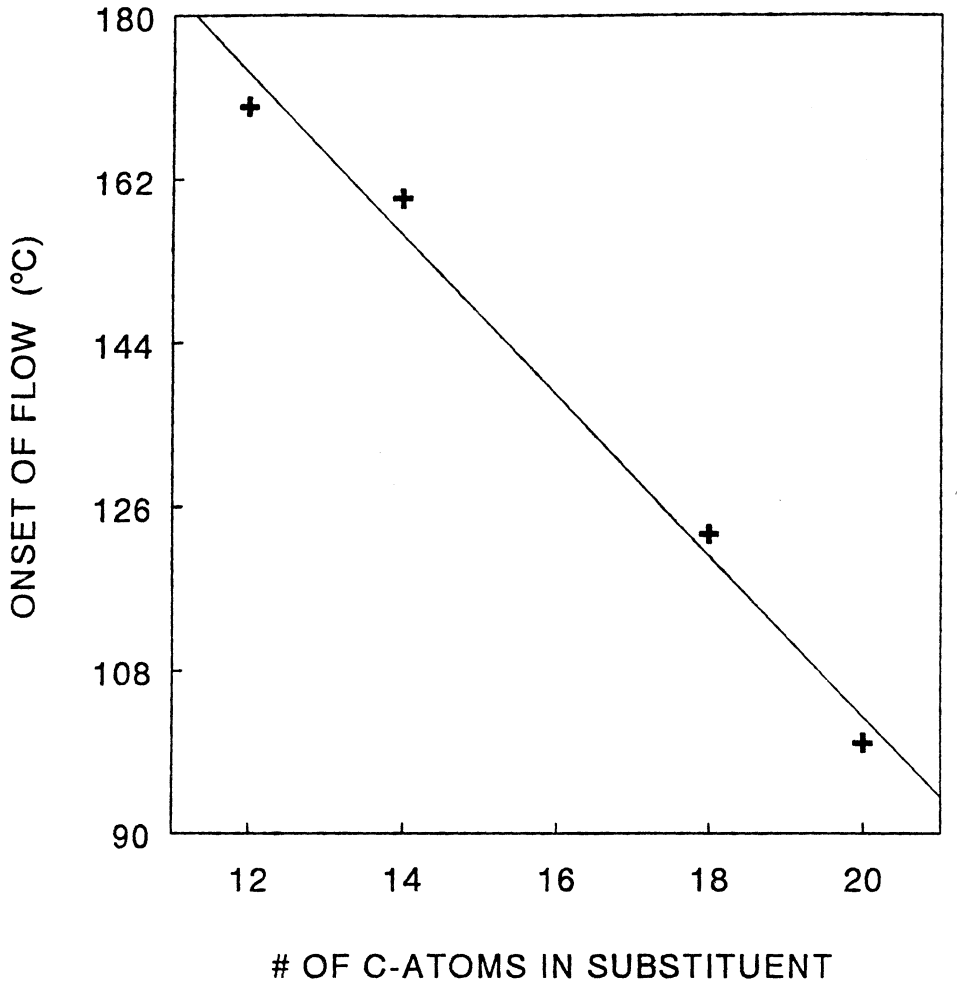

Figure 30. TMA penetration mode flow temperatures for bulky esters. The onset of flow decreased in temperature with increasing substituent length.

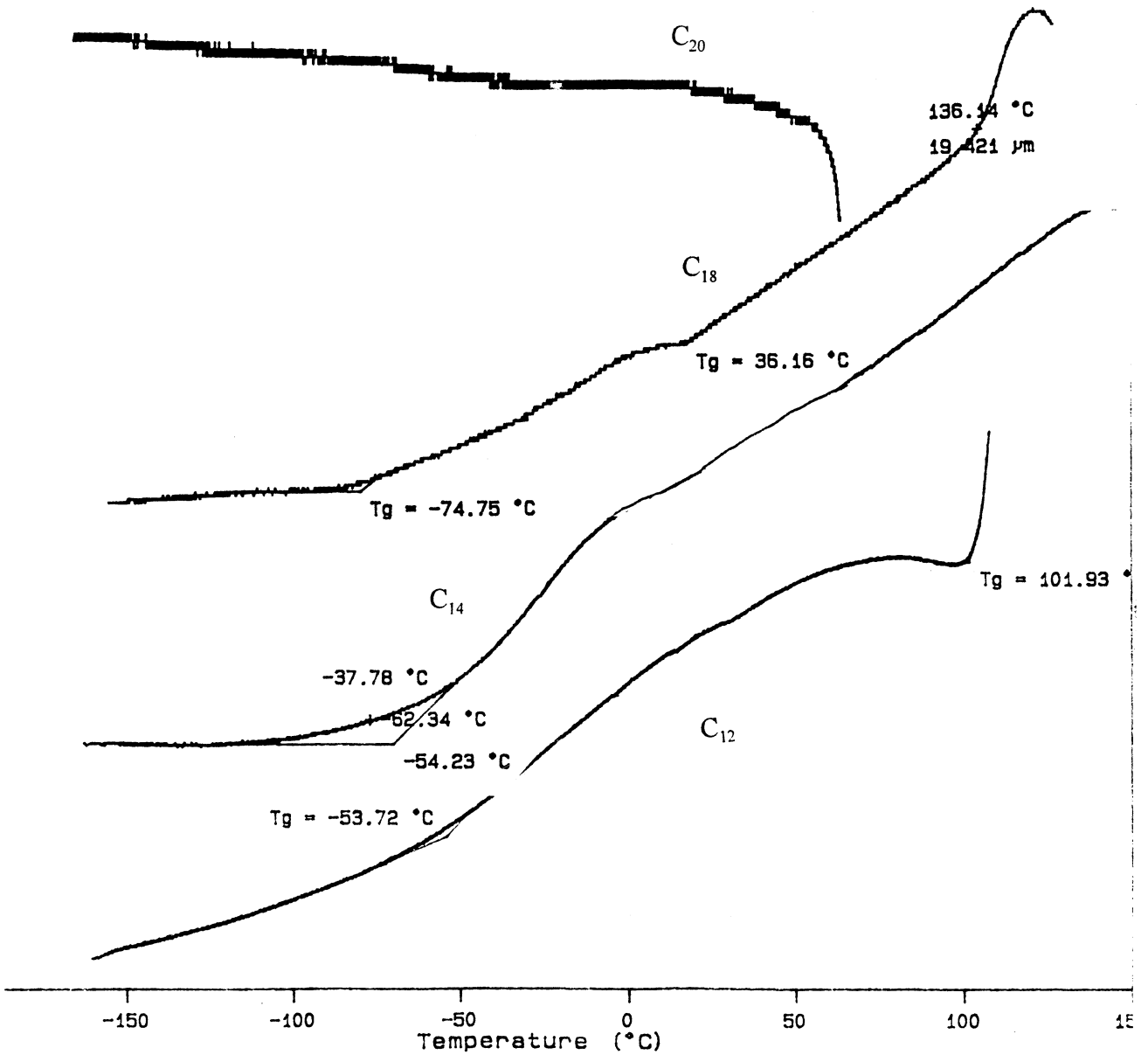

Figure 31. TMA expansion mode T_g for bulky esters. An increase in expansion rate was detected for C_{12} to C_{18} derivative, but C_{20} did not.

relationship between flow temperature and side chain length. The longer side chain of C_{18} increased viscosity which in turn increased flow temperature. The thermotropic liquid crystal behavior (described later) of C_{20} lowered the viscosity and lowered its flow temperature creating the linear relationship between C_{12} to C_{20} ester derivative.

Thermotropic liquid crystal behavior was examined by hot stage microscopy for C_{12} to C_{20} highly substituted derivatives. This was done to determine if the weak sharp endotherms seen 30 to 50°C above the T_m of the product by DSC analysis for C_{18} and C_{20} esters were due to liquid crystal melting transitions. The samples were scanned at 10°C intervals and examined for birefringence. C_{20} ester was the only sample that revealed substantial birefringence reappearing above the T_m reported by DSC. This occurred at 110°C which had a T_m at 50°C. This would suggest that C_{20} cellulose ester had thermotropic liquid crystal behavior, but further research is needed to confirm this.

7.4 CONCLUSION

The esterification of cellulose in homogeneous phase using a mixed anhydride consisting of toslic acid and carboxylic acid was highly effective when the mixed anhydride was produced in the presence of pyridine and cellulose. Waxy ester derivatives with high DS and unchanged DP can be isolated. The reaction temperature at 50°C, which were degradative for the fluoro-esters, proved to be nondegradative and highly efficient. Apparently, the esterification of long linear

aliphatic esters was more resistant to degradation than the trifluoroethoxy esters.

The thermal transitions exhibited by the waxy ester derivatives revealed signs of a distinct olefinic morphology as well as main chain motion. Transitions due to side group motion give rise to a T_g (β-transition), T_c and T_m. The main chain T_g (α) transition converges with T_m as the substituent size increases. The C_{12} and C_{14} esters showed T_g and T_m of the sidechain; T_g and T_m of the main chain; and T_c of the sidechain and mainchain. They clearly showed two distinct crystal types. The C_{18} ester revealed only T_g of the sidechain and mainchain and only one T_m. The T_m was broad (70°C breadth) but could be significantly sharpened by annealing. The C_{20} ester derivative revealed only one T_g and T_m. The T_m was also broad, but after annealing, which occurred at room temperature, became very sharp with a breadth of about 5°C.

8.0 CELLULOSE ACETATE LAURATE MIXED ESTERS

8.1 INTRODUCTION

Since most polysaccharide ester derivatives show considerable affinity for water due to the presence of oxygen and unsubstituted hydroxyl groups, moisture may cause several mechanical and thermal transitions. It may alter or mask transitions and make them unreproducable. Mandelkern and Flory have reported transitions that are believed to be caused by moisture for cellulose triacetate at 30°C and 105°C in dilatometric studies and 60°C and 120°C for cellulose acetate (DS 2.4) (Mandelkern,Flory 1951). Several publications disagree with these transition temperatures (Nakamara et al. 1971) (Cowie,Ranson 1971) (Seymour,Johnson 1978), but Klason reported that the main mechanical loss factor is at -73°C (Klason,Kubat 1976). This is believed to be due to the increased motion at the C-6 carbon bond. The increase in damping at about 140°C seems to indicate proximity to the T_g. It is also reported from dielectric and broad line NMR measurements that the -73°C transition is seen for different types of unsubstituted celluloses (I and II) as well as for different cellulose derivatives including esters (Kimura,Saito 1979).

The effects of moisture in cellulose and cellulose derivatives are complex and, highly disputed in the literature. It was the aim of this study to avoid this problem by examining mixed esters. The goal of this study is to produce cellulose laurate (CL)

with a wide range of DS, with (CAL) and without (CL) acetylated hydroxyls, and examine the structure property relationship. A comparison to hexanoate derivatives from a earlier study should reveal the effects of a longer substituents (Glasser et al. in preparation).

8.2 REACTIONS AND REACTIVITY

The TsCl reagent system described earlier again proved to be highly effective. The stoichiometric control of the reaction produced CL with a linear relationship between DS and eq of free acid per cellulose hydroxyl group (Figure 32) (Figure 33). Derivatives with DS between 0.6 and 2.9 were created with a 0.75 to 2.0 equilavants of free acid per cellulose hydroxyl group. The reaction substituted about 1 out of every 3 moles of free acid. TsCl and free acid were added with a 1 to 1 ratio at 50°C producing derivatives with little to no degradation of the starting cellulose polymer (Table 7 in section 7.3.1). The CAL derivatives were created by peracetylating the CL products. The DP_n before and after peracetylation is almost identical. The only change to the MW was due to the increase in weight of the repeat unit after acetylation.

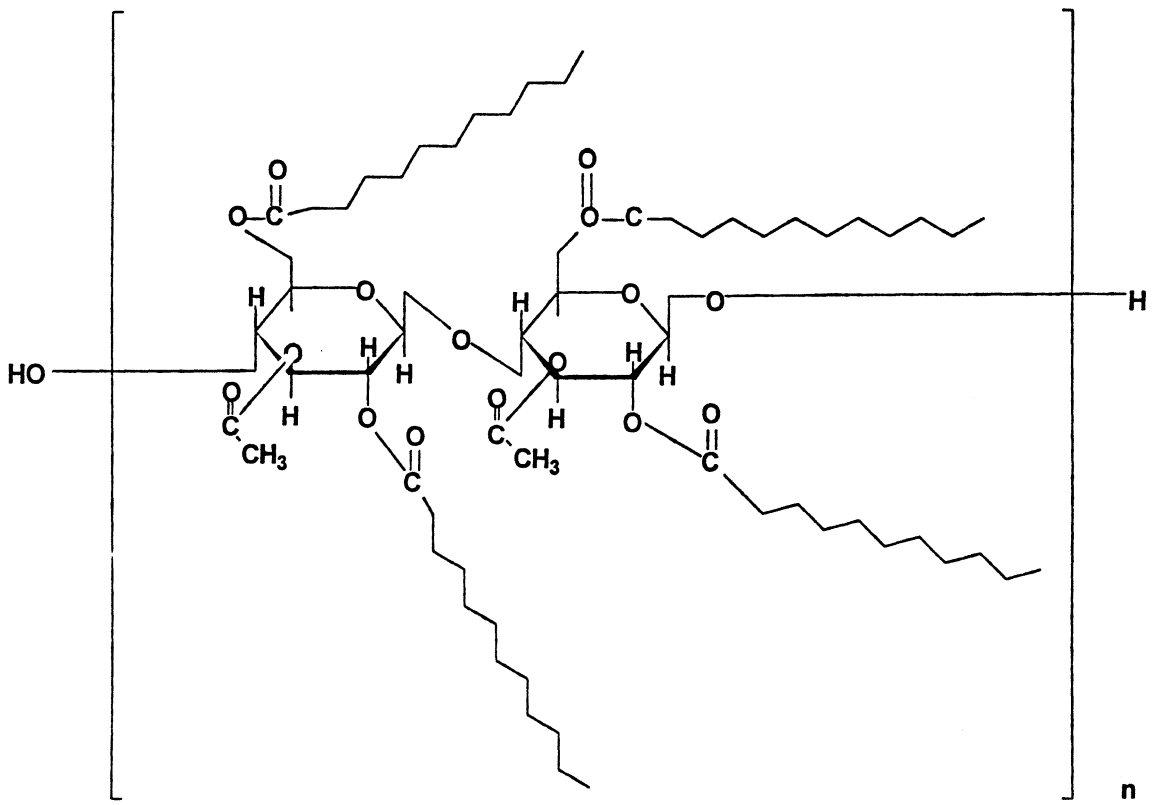

Figure 32. CAL molecular structure. This structure represents a DS_l 2.0 and DS_a 1.0 derivative. All CAL derivatives are fully substituted.

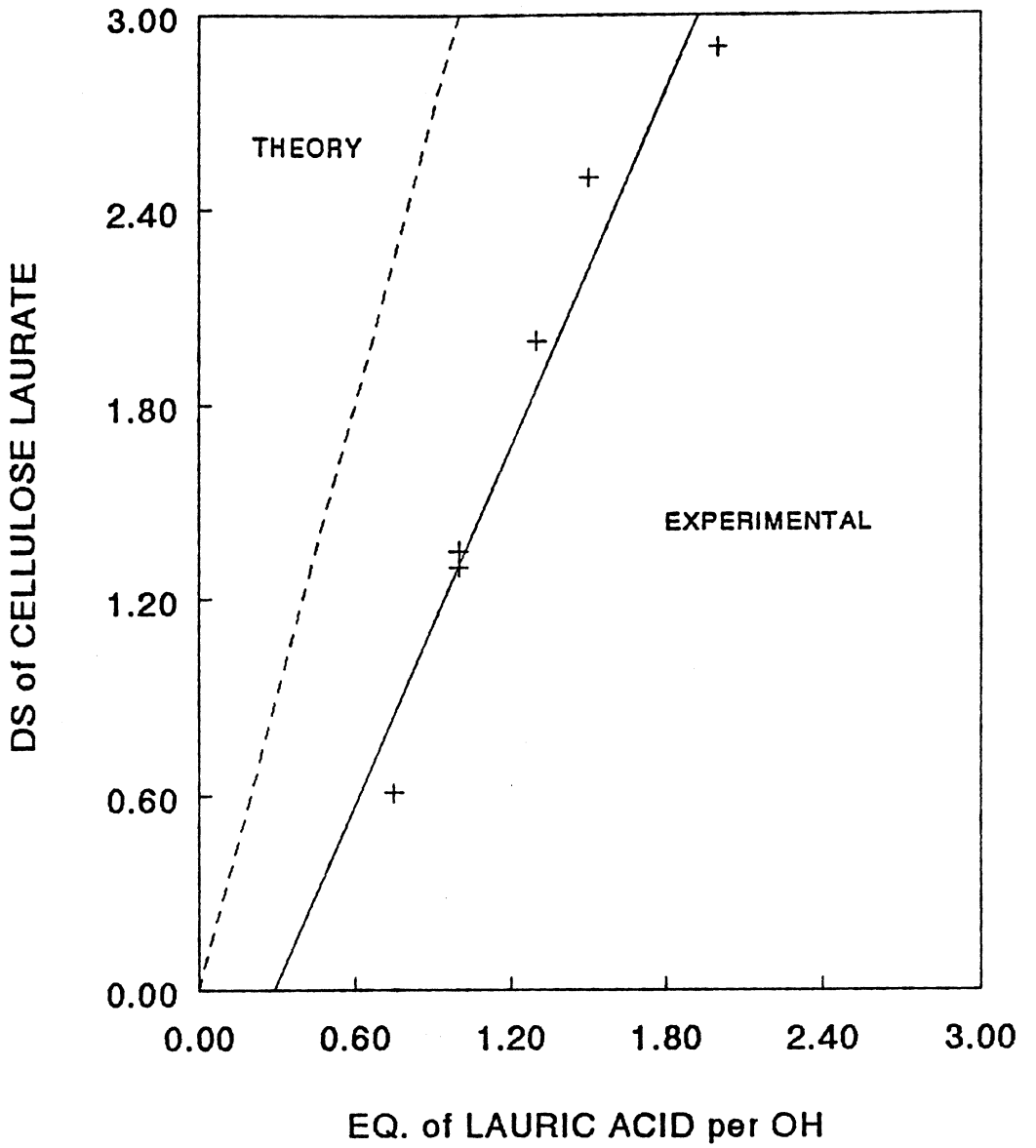

Figure 33. Relationship between DS of CL and amount of reagent used. The data supports shoichiometric control.

8.3 RESULTS AND DISCUSSION

8.3.1 CHEMICAL ANALYSIS

The NMR of the CL derivatives were very similar to the bulky esters except for increasing breadth of the cellulose backbone peaks as the DS decreased. The FTIR spectra reveled increased absorbance in the hydroxyl range and a decrease in absorbance in the 1735 cm^{-1} ester region. The DS calculations for the range of CL derivatives by NMR and GC method compared within $\pm$ 0.2 DS as reported in the literature (Samaranayake, Glasser 1993b).

The reaction conditions, molecular determination and DS calculations for the CAL derivatives were the same to very similar to the mixed esters in section 6.0. The DS determination by GC analysis was not performed because of the lack of a single column that was capable of analyzing both laurate and acetate substituent.

8.3.2 THERMAL ANALYSIS

Thermal analysis was performed by DMTA, TMA and DSC. DMTA data, which were used to determine side chain and main chain T_g, showed a β-transition at about -50°C for DS 1.3 and higher and a decreasing α-transition temperature for the same DS range (Figure 34). The films for DS below 1.3 were too brittle to test in the DMTA because the films cracked after tightening the clamps. However, the DS of

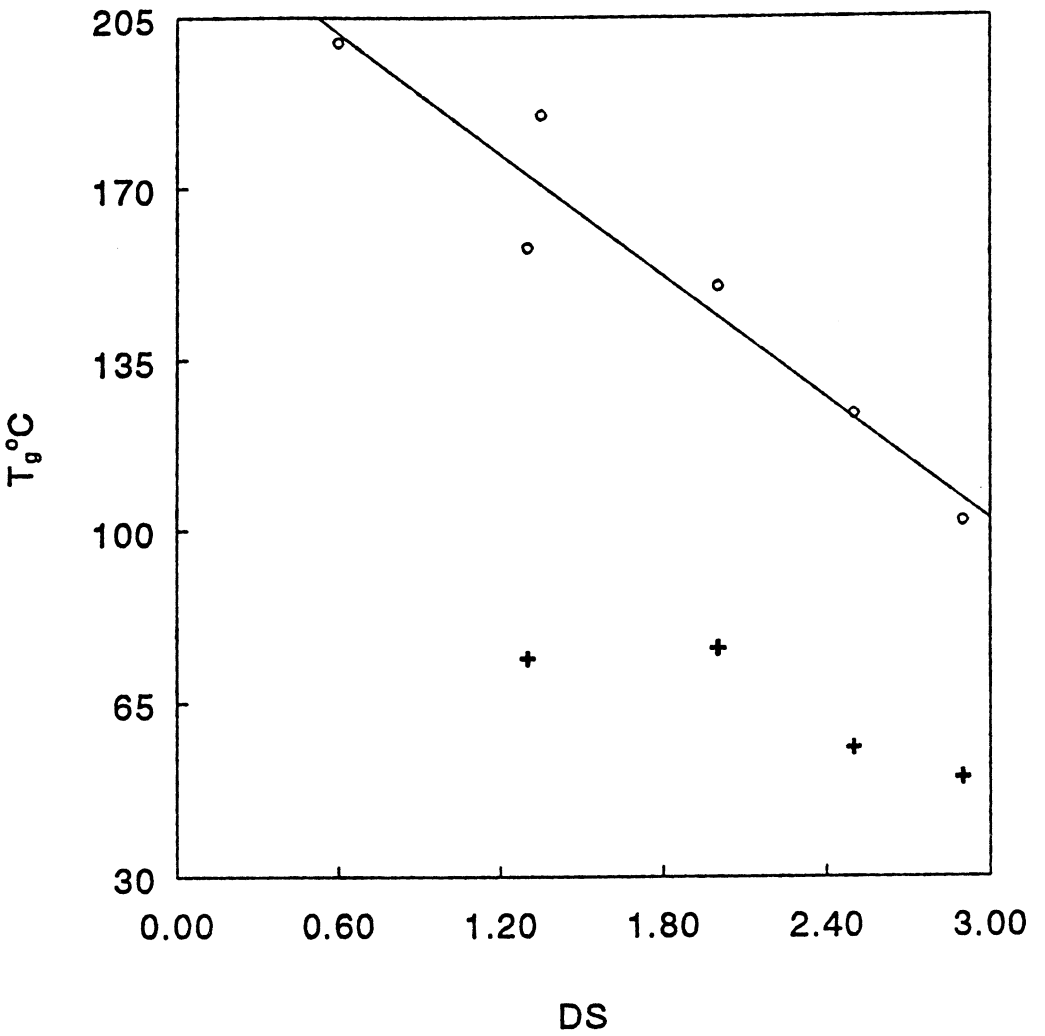

Figure 34. DMTA (+) and TMA (O) (expansion mode) transition temperatures of CL. Both techniques detected a trend of decreasing T_g with increasing DS of lauric acid.

1.3-3.0 samples were easily tested and surprisingly devoid of large moisture transitions. This could be due to the long hydrophobic side chains forming a water repelling coating over the cellulose backbone causing low moisture adsorption for lower substituted derivative.

The TMA in expansion mode detected T_g's of the main chain, determined by the onset of expansion. The CL derivatives had a linear relationship between DS and transition temperature for the entire DS range (Figure 34). The T_g of the side chain was also reported to remain constant at -50°C over the entire DS range (Table 8 in section 7.2.3). The DS test range was larger for the TMA because no clamping was required. The α- transition temperatures were about 40°C higher for TMA than for DMTA, but since these techniques detect different characteristics of the T_g, TMA thermal expansion and DMTA damping factor, both were detecting the same transition.

DSC analysis proved to be complex for most of the DS range. Moisture transitions were detected for DS derivatives as high as 2.5, but distinct T_m's were isolated for DS derivatives as low as 1.3 (Table 8 in section 7.3.2). Two samples with DS above 1.3 revealed no T_m even after several annealing studies. This could be caused by induced differences in morphology from sample work-up or thermal histories. Since each derivative with DS 1.3 and higher flowed without discoloration, the T_m's must be below the degradation temperature. The products that didn't reveal a T_m must be highly amorphous. If the T_c could be determined, T_m should be able to be

induced and isolated. The presence of low temperature T_ms (-50°C) was seen for almost all CL and CAL derivatives.

Thermal analysis on CAL derivatives was performed by DSC and TMA (Tables 9 in section 7.3.2). DMTA was not performed because of the lack of sufficient quantity of sample to make films. The DSC analysis was performed by several heating and cooling scans (Figure 35). Typically, a single sharp T_m was seen on the heat, and a very sharp T_c was seen on the cool. No T_g could be detected. The samples were then quench-cooled, and the next heat still revealed a T_m at the same temperature with no T_g except for the lowest DS of laurate sample (DSL 0.6). This sample revealed a T_g after quench-cooling with a small T_m. Apparently the T_g's and T_m's were within a few degrees of one another, and the highly crystalline CAL derivatives cause the T_g to disappear due to the small percentage of amorphous region in the material. This problem was seen for the cellulose acetate hexanoate derivatives, but T_g could be found because the crystallization was very slow and only the T_g was observed in the second heating scan. Heating scans without annealing revealed T_g's with little to no T_m's (Glasser et al. pending). The relationship between the T_m and the DS_L of cellulose acetate laurate was linear for DS_L of 0.6 to 3.0 (Figure 36). This trend agreed with the linear relationship between T_m and DS_H (hexanoate) between 0.8 to 3.0 (Figure 37).

The TMA data, which was performed in expansion mode, detected no expansion. This agrees with the DSC data which also detected no T_g. The only

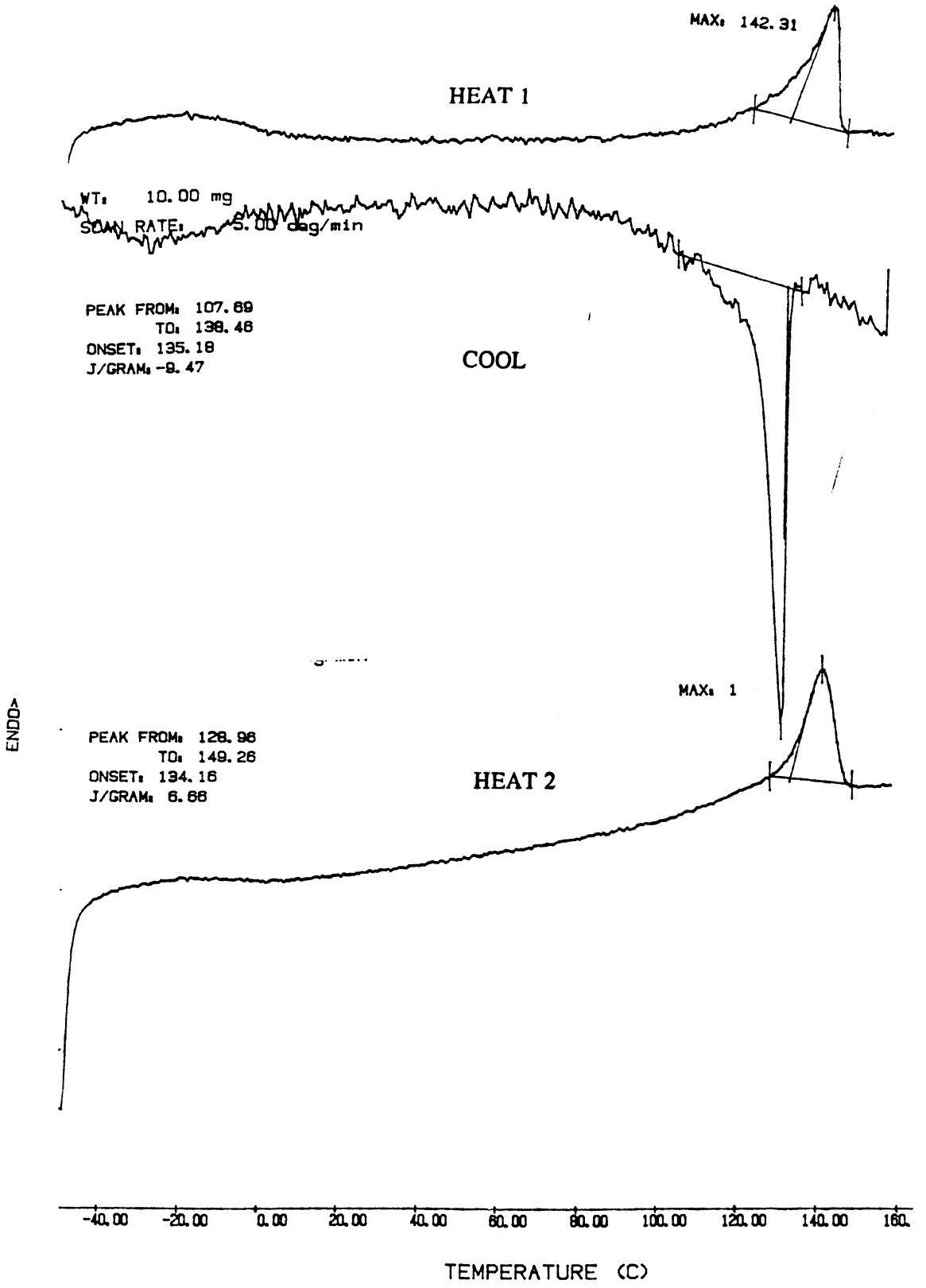

Figure 35. DSC scans of CAL derivatives. Sharp crystallization responses were detected for even quench cooling scans. The T_m detected on the heating scan remained constant regardless of cooling rate.

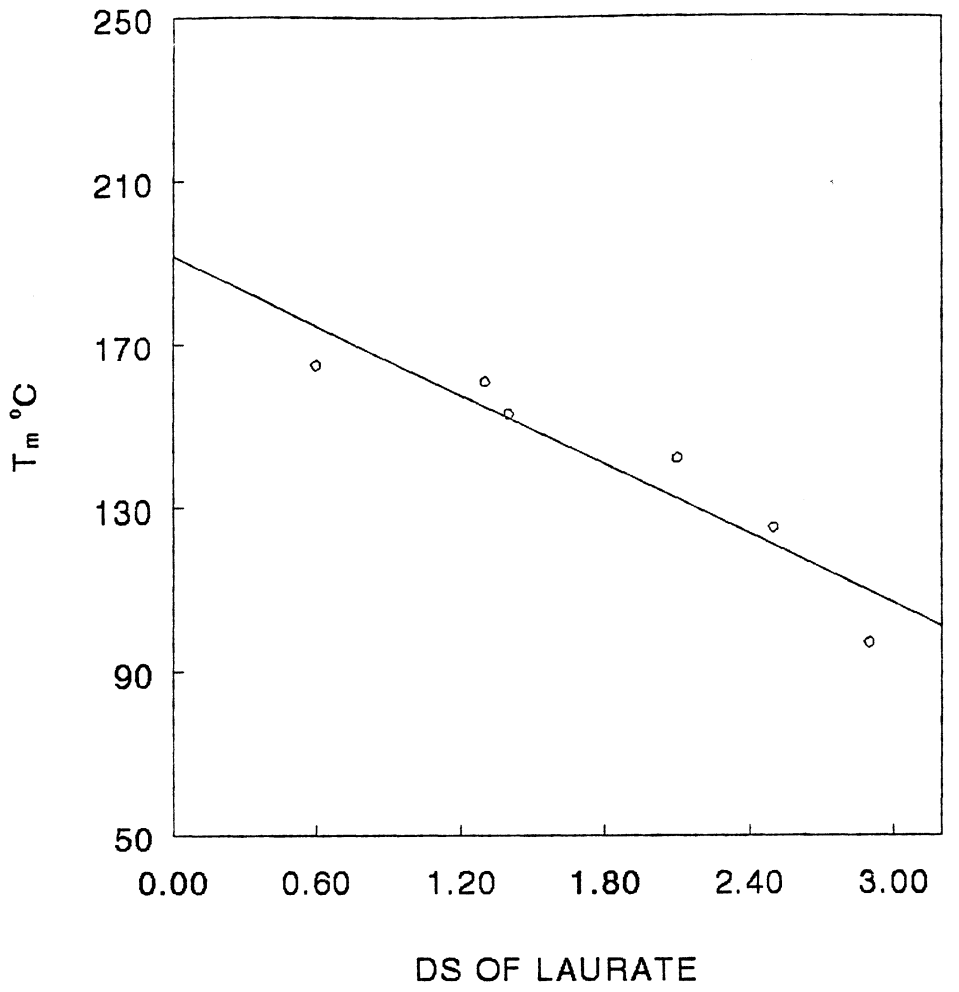

Figure 36. T_m vs DS_L for CAL derivatives. A linear decrease in T_m was detected with increasing DS_l between DS_l 0.6 and 2.9.

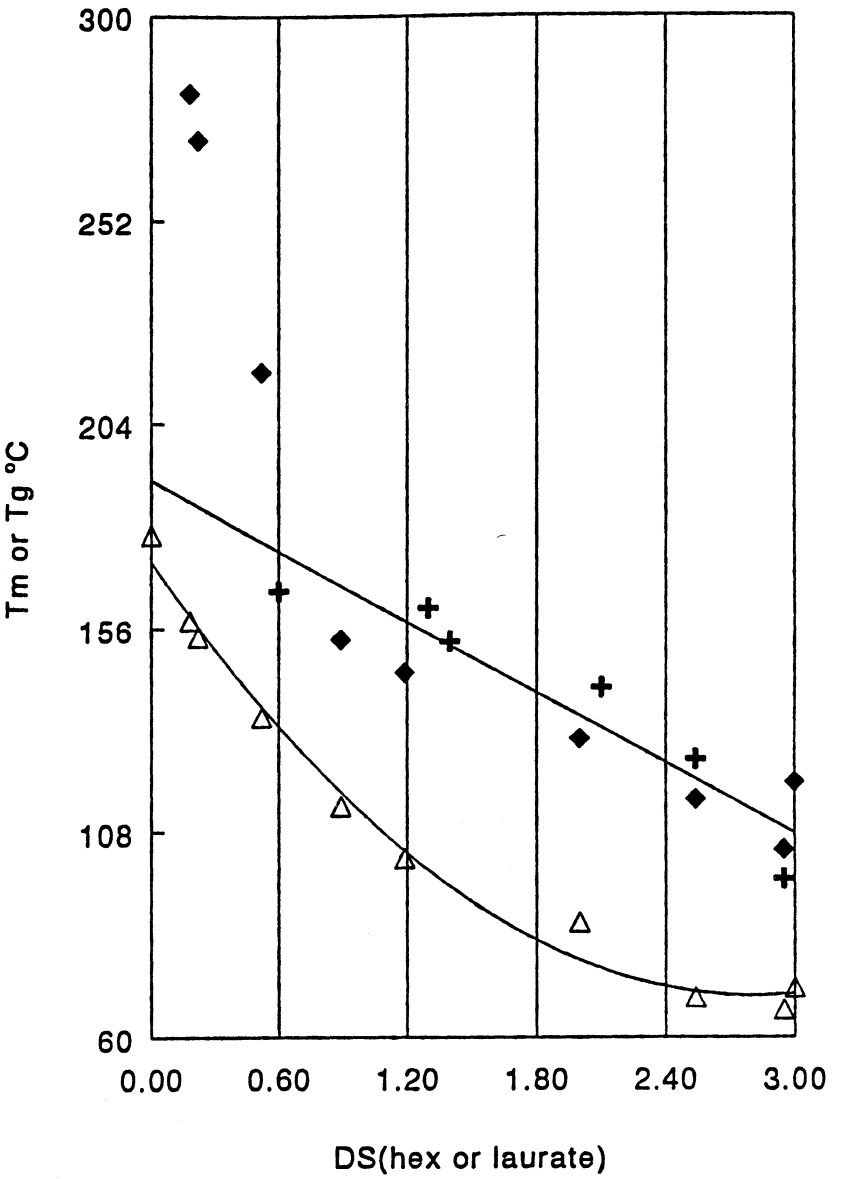

Figure 37. T_m vs DS_H and DS_L for CAH and CAL derivatives (♦) T_m CAH (+) T_m CAL (△) T_g CAH. The CAL T_ms compare closely with the CAH T_ms.

transition seen was the onset of flow (Table 9) which was represented by penetration of the probe. No clear trend was observed with a flow temperature range of 113 to 141°C.

The T_gs of the CL derivatives were within 10 to 20°C of the CAL T_m temperatures. If we assume that the T_g's are nearly unaffected by the presence of free hydroxyls as they were for the CT derivatives, this would again suggest very close proximity of the T_g and T_m for the CAL derivatives.

8.4 CONCLUSION

Cellulose laurates with free hydroxyls have significant moisture effects that complicate thermal analysis, but DMTA analysis could detect T_g temperatures for DS 1.3 and above. TMA analysis in expansion mode was useful in isolating T_g temperatures for the entire range 0.6 to 2.9 DS. While the DSC analysis for the cellulose laurates with free hydroxyls were complex, T_g's ranged from 87 to 180°C for DS 2.9 to 1.3.

Cellulose acetate laurate derivatives revealed sharp T_m's on the heat and sharp T_c's on the cooling curve. The T_c's ranged from 10 to 20°C lower than the T_m's. Only one T_m was clearly observed between the -50 to 200°C test range, but the presence of side chain crystals was evident at -50°C. If we assume that the T_g-temperatures were not significantly effected by acetylating the free hydroxyls, which was observed for fluorinated cellulose esters, the $\Delta(T_m-T_g)$ was only a few degrees.

Since the data was consistent with the conclusion that CAL derivatives have fast crystallization rates, the small $\Delta(T_m-T_g)$ was surprising because the polymers with small $\Delta(T_m-T_g)$ usually have very slow crystallization rates. The CAH and the CAL derivatives revealed small difference in their thermal transition temperatures since they both had linear relationships between T_m and $DS_{H\ OR\ L}$ for DS 0.6 to 2.9 with T_m's within 10 to 20°C.

REFERENCES

Astheimer, Hans-Joachim, Encyclopedia of chemical technology 3rd edition, vol A5 p447-448 (1988).

Balser, Klaus, Encyclopedia of chemical technology 3rd edition, vol A5 p419-437 (1988).

Beacham Research Laboratories (no author), patent Brit. 873,244. Penicillins stable in the presence of water (1960).

Blackwell, J., Marchessault, R.H., INFRARED SPECTROSCOPY, Chapter 13, p1-37, (1970).

Buchanan, C.M., Hyatt, J.A., Lawman, D.W., Macromolecules, 20,p2750 (1987).

Buchanan, C.M., Edgar, K.J.,Wilson, A.K., Macromolecules, 24, p3060,(1991).

Bogan, R.T., Kuo, C.M., Brewer, R.J., Ullmann's encyclopedia of industrial chemistry, Vol. 5 p118-143,(1990).

Cowie, J.M.G., Ranson, R.J., Macromolecules, 143, p110, (1971).

Daly, W.H., Negulescu, I.I., Russo, P.S., Poche, D.S., ASC Symposium series 493; chapter 23(1992).

Daly, W.H., Poche, D., Polymer Preprints, 30(1),p107,(1989).

Eastman, presentation at the Brooks research center, 1992.

Eicher, T.S., Encyclopedia of chemical technology 3rd edition, vol A5 p 438-444 (1988).

Frazier, C., Synthesis and Characterization of Fluorinated Cellulose Derivatives, dissertation VPI&SU, 1992.

Glasser, W.G., Samaranayake, G., Dave, V., III Manuscript in prep.

Hsu, W.P., Levon, K., Ho K.S., Myerson, A.S., Kwei, TK., Manuscript in prep.

Hassner, A., Alaxanian, V., Tetrahedron Letters, 23, p667-670, (1978).

Kamide, K.,Saito, M., Polymer, vol 11,p285 (1979).

Kent, P.W.,FLUORINATED CARBOHYDRATES ACS.,ch1,p1-12 1990.

Kimura, M., Hatakeyama, H., Usuda, M., Nakano, K., Journal of applied polymer science, vol 16, p1749-1759 (1972).

Klason, C., Kubat, J., Svensk Papparstidn, 15,p494-500 (1976).

Krassig, H., Ullmann's encyclopedia of Industrial Chemistry, vol 5,p89-95 (1990).

Malm, C.J., Barkey, K.T., Salo, M., May, D.C., Industrial and Engineering Chemistry, 49(1) p79-83, (1957).

Mandelkera, L.,Flory, P.S., J. of American Chemical Society, 73,3206 (1951).

Manley, R.J., Encyclopedia of Industial Chemistry, vol 5 p95-117 (1990).

Mansson, P., Samuelsson, B., Svensk Papperstidn, 84(3), p15 (1981).

Matsui, H., Shiraishi, N., Mokuzai Gakkaishi, vol 39,no10,p1194-1200 (1993a).

Matsui, H., Shiraishi, N., Mokuzai Gakkaishi, vol 39,no10,p1188-1193 (1993b).

McCormick, C.L., Dawsey, T.R., Macromolecules, vol 23, no15 (1990).

McCormick, C.L., Callais, P.A., Polymer, vol 28, p2317-2323, Dec. (1987).

Morooka, T., Norimoto, M., Yamada, T., Journal of Applied Polymer Science, vol 29, p3981-3990 (1984).

Morooka, T., Norimoto, M., Yamada, J., Journal of Applied Polymer Science, vol 35, p717-726 (1988).

Nakamura, S., Shindo, S., Matsuka, K., Journal of Polymer Science part b,9,p591 (1971).

Olabisi, O., Encylopedia of Chemical Technology 3rd edition, vol 18, p443-478 (1988).

Ott, E., Spurlin, H., Grafflin, M., CELLULOSE AND CELLULOSE DERIVATIVES, p673-815 (1954).

Paul, D.R., Barlow, J.W., Bernstein, R.E., Wahrmund, D.C., Polymer Engineering and Science, vol 16, Dec. p1225-1234 (1978).

Poche, D., Daly, W.H., Russo, P.S., Polymer Preprints, 31(2), p418 (1990).

Sakamoto, R.,Osawa, A., Mol. Cryst. Liq. Cryst, 154,p305 (1987).

Salman, N.L., Back, E.L., Tappi, vol 60, no 12,p137-140, Dec. (1977).

Samaranayake, G., Glasser, W.G., Carbohydrate Polymers 22(1993) p1-7 (a).

Samaranayake, G., Glasser, W.G.,Carbohydrates Polymer 22(1993) p79-86 (b).

Sarmadi, A.,Kwon, Y.,Young, R., Ind. Eng. Chem. Res. 32 p279-287 (1993).

Scandola, M.,Ceccorulli, G., Polymer, 26,p1953 (1985).

Schranwen, C.,Pakulu T., Wegner, G., Makromol. Chem., 193,p11-30 (1992).

Serad, G.A., Sander, J.R., Encylopedia of Chemical Techology 3rd edition, vol 5,p109-117 (1988).

Seymour, R.B., Johnson, E.L., Journal of Polymer Science, 16,p 1 (1978).

Shimizu, Y., Hayashi, J., Cell. Chem. Technol., 23, p667-670 (1989).

Stuttgart, T.E., Encyclopedia of Chemical Technology 3rd edition,vol A5, p438-446 (1988).

Furniss, VOGEL'S PRACTICAL ORGANIC CHEMISTRY, 5th ed. 1989.

Watanabe, J.,Ono, H., Uematsu, I., Macromolecules, 18, p2141 (1987).

Watanabe, J.,Goto, M.,Negase, T.,Macromolecules, 20,p298 (1987).

Wandel, M., Bayer, A.G., Encyclopedia of Chemical Technology 3rd edition, vol A5,p446-457 (1988).

The two page vita has been removed from the scanned document. Page 1 of 2

The two page vita has been removed from the scanned document. Page 2 of 2